TRAVELING WAVE ENDFIRE ANTENNAS

On page 100 we discussed the endfire array of two isotropic antennas and on page 105 the general N element linear array. One of the special cases of this array is an endfire array. From page 105 the electric field for an N element linear array is given by

$$E = E_o \frac{\text{Sin}(N\psi/2)}{\text{Sin}(\psi/2)}$$

where $\psi = \beta$ d Cos $\theta + \delta$, d is the distance between elements, θ the angle from the axis of the array, and δ is the equal phase shift between elements. If we have the restriction $\delta = -\beta$ d, then the array will have no back-lobe (endfire). A wave traveling on a transmission line with the free space velocity will just fit this criterion.

Also discussed on page 107 was the increased directivity endfire array of Hansen and Woodyard. This required that the phase shift between elements be increased by a factor π/N radians. There is an extra half wavelength phase shift over and above the free space shift. We can get increased phase shift over a given length by using slow wave structures (like waves in a dielectric). We want to discuss the general antennas of this type in this section.

The antennas fall into two categories. The first can be considered an array of N elements all having equal structure and radiation pattern. In almost all cases the elements will also have equal amplitude. These cases are covered by the analysis given on page 105. Once we know the phase shift between the elements, δ , we can calculate the radiation patterns. The polarization of the wave is determined by the radiation from the single periodic element, such as the single loop of a helical antenna. The second type of antenna is a continuous array where the individual elements of the array cannot be distinquished. We have already discussed one of these types on page 164 when we covered traveling wave currents on long wires. It will be helpful to solve the problem of a continuous array of isotropic elements excited by a traveling wave. Using the notation given on page 164, we can say the excitation voltage or electric field is given by

$$E = E_o e^{-j\beta p z}$$

where p is the relative propagation constant of the wave. From page 117, the pattern of a continuous array on the Z axis is given by the integral:

$$E = \int_{-L/2}^{L/2} E_o e^{-j\beta z(p - \cos\theta)} dz$$

The solution to this integral is found on page 117; after normalizing we get

$$E = \frac{\sin(\psi/2)}{\psi/2}$$

where $\psi = \beta$ L(P - Cos θ). We can use this to find approximate patterns even for periodic surface wave structures where the repeat length is small in wavelengths. The traveling wave current is one of the types of endfire

antennas. In this case the element pattern is an incremental dipole which has a null in the direction of the axis of the array. Patterns for this antenna are given on pages 165 and 166. We can generate a similiar set of patterns for various lengths of the antenna which are given on pages 350 and 351. In all cases the beamwidth narrows for increased length of the antenna in wavelengths. Note too that the first sidelobe level on all the patterns is identical (13.3 dB). We can get these patterns from the curve on page 119 for the uniform continuous array which also has the general shape Sin (X)/X by a change of variable on the abscissa to $\psi/2$, $\psi = \beta L(P - \text{Cos } \theta)$.

Using the patterns, we can generate a plot of directivity versus the length for a continuous array of various lengths. The curve is given on page 352. Similiarly a curve of the 3 dB beamwidth has been plotted on page 353 and on page 354 is a curve of the location of the first sidelobe. On all these curves is plotted also the Hansen and Woodyard array.

If we want the Hansen and Woodyard array, the relative propagation constant must be adjusted to the length of the array. The condition is that there must be an extra half wavelength phase shift through the length of the array. The extra phase shift is achieved by using a slow wave structure which corresponds to a relative propagation constant given by

$$P = \frac{1 + 2L}{2L}$$

The directivity of a continuous Hansen and Woodyard array is given on page 352 along with the free space velocity case. The Hansen & Woodyard design has considerable more directivity than the free space velocity case. When the length of the antenna is increased by 2, the directivity increases by approximately 3 dB (exact for the free space velocity case). The practical antenna is limited in gain to that obtained with about 10 or 20 wavelengths. This falls off even quicker when the aperture distribution decreases along the surface wave device which happens if the transverse dimensions of the structure are varied or are caused by the end effects of the antenna.

On pages 355 and 356 are patterns for uniform amplitude aperture distribution line sources which satisfy the Hansen and Woodyard criterion. Notice that the relative propagation constant must be adjusted to match the length of the antenna in each case. The patterns no longer have zero backlobe. This is similiar to the Yagi antenna which did not give maximum gain at the dimensions of minimum backlobe. The Yagi antenna can be analyzed as an endfire traveling wave antenna. Notice that the first sidelobe level has increased to 9.3 dB. The beamwidth and location of the first sidelobe were plotted along with the free space velocity cases. The magnitude of the first sidelobe can be calculated from the following formula.

$$\text{Sidelobe} = 13.26 + 20 \text{ Log } \left(\frac{\text{Sin}(\pi L(P - 1))}{\pi L(P - 1)} \right)$$

This is valid until the sidelobe level is greater than zero; then the pattern has bificated and the first sidelobes are the main beams.

TRAVELING WAVE ENDFIRE LENGTH = 1, P = 1

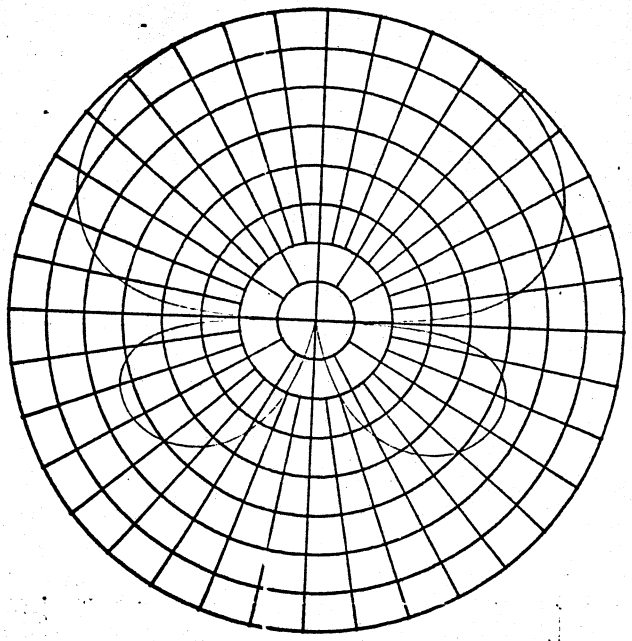

TRAVELING WAVE ENDFIRE LENGTH = 2, P = 1

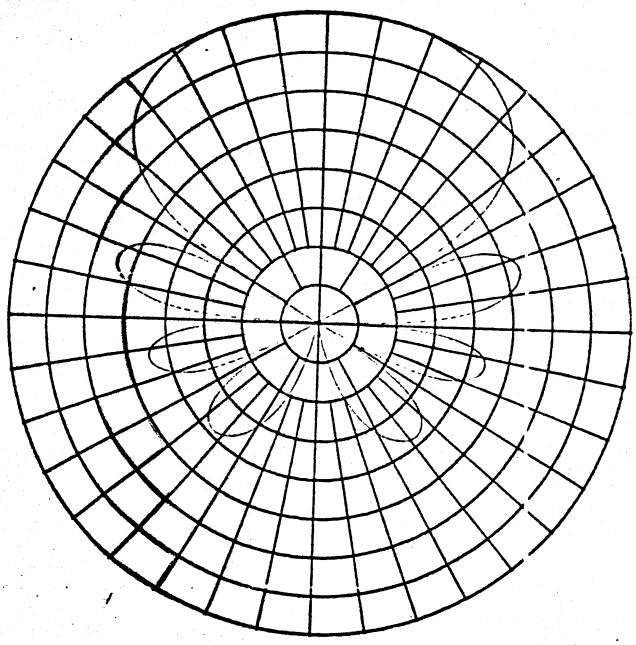

TRAVELING WAVE ENDFIRE LENGTH = 3, P = 1

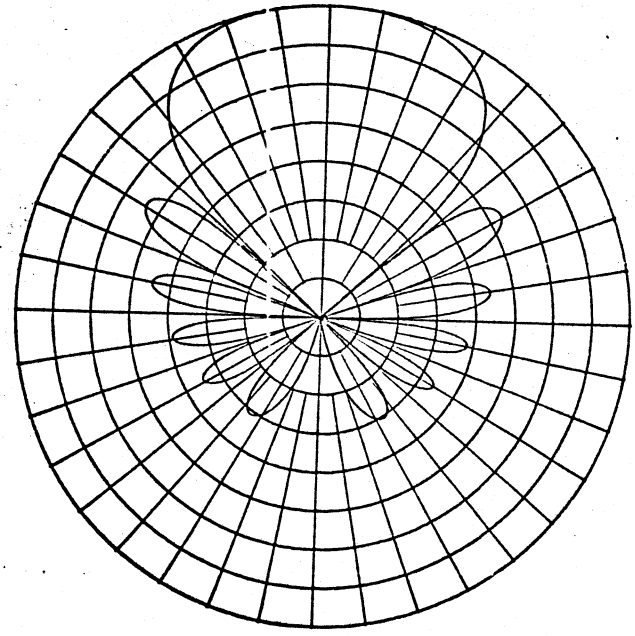

TRAVELING WAVE ENDFIRE PATTERN LENGTH = 4, P = 1

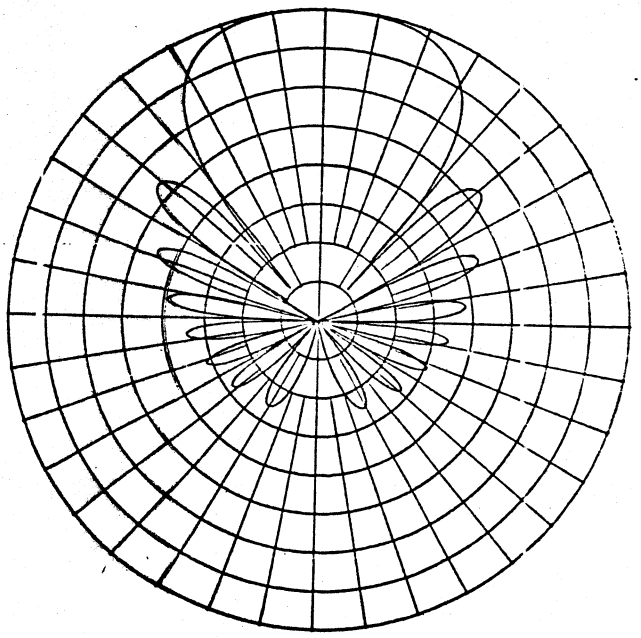

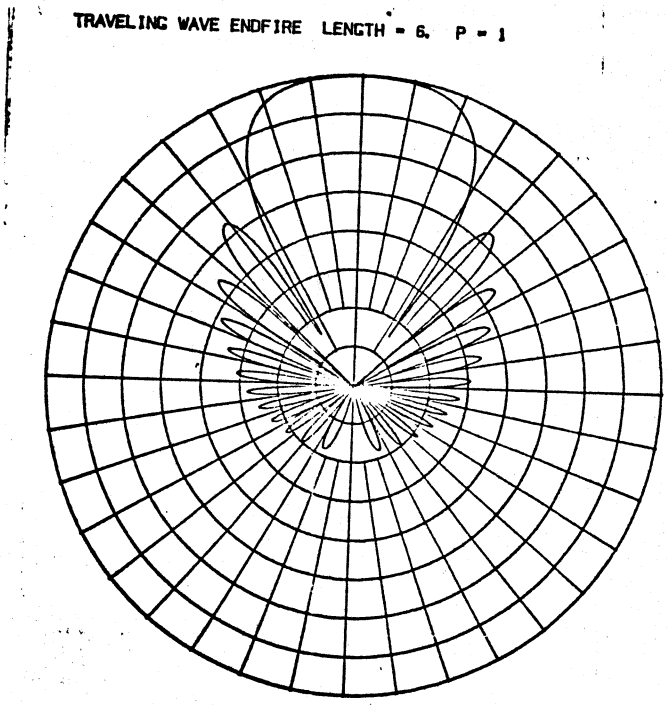

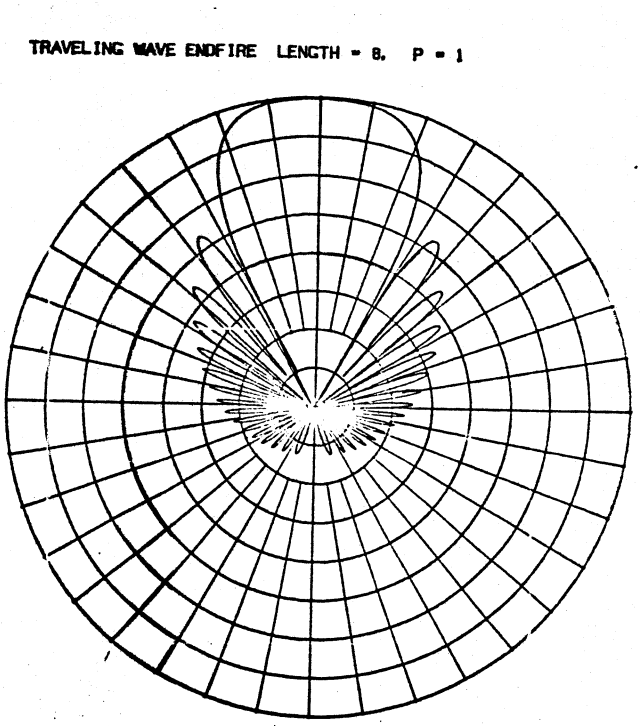

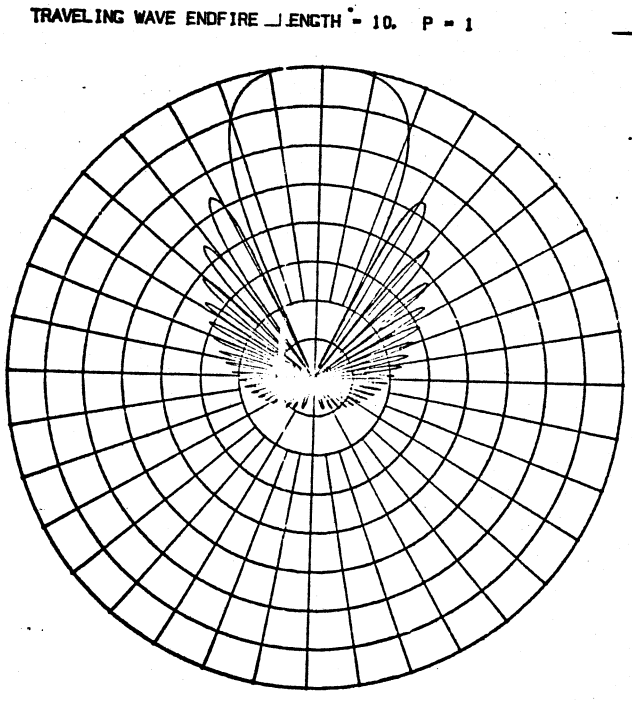

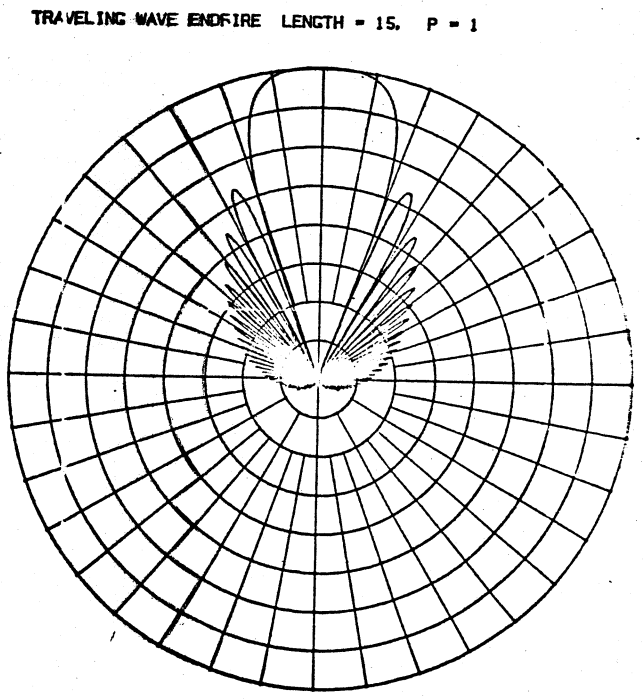

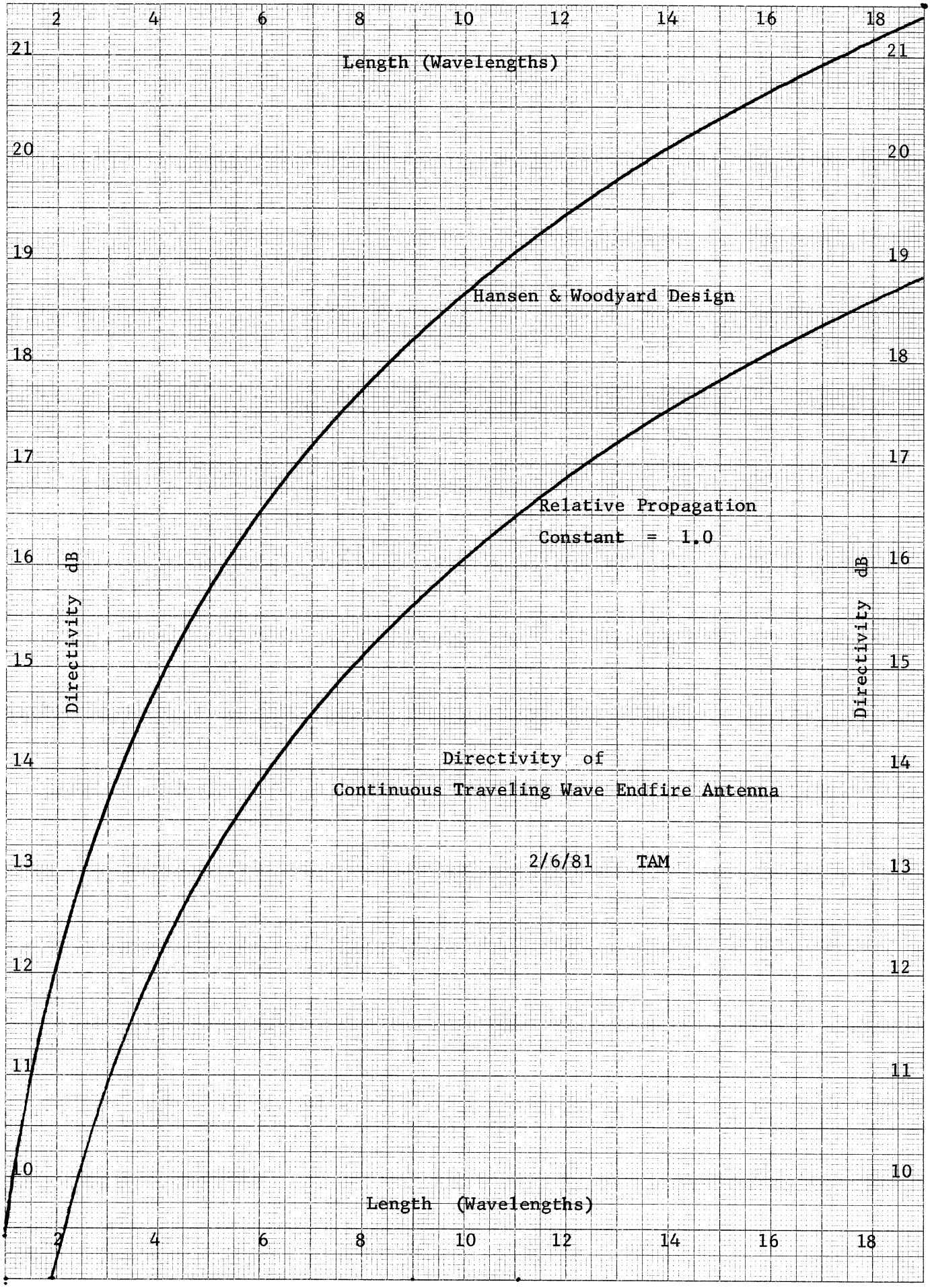

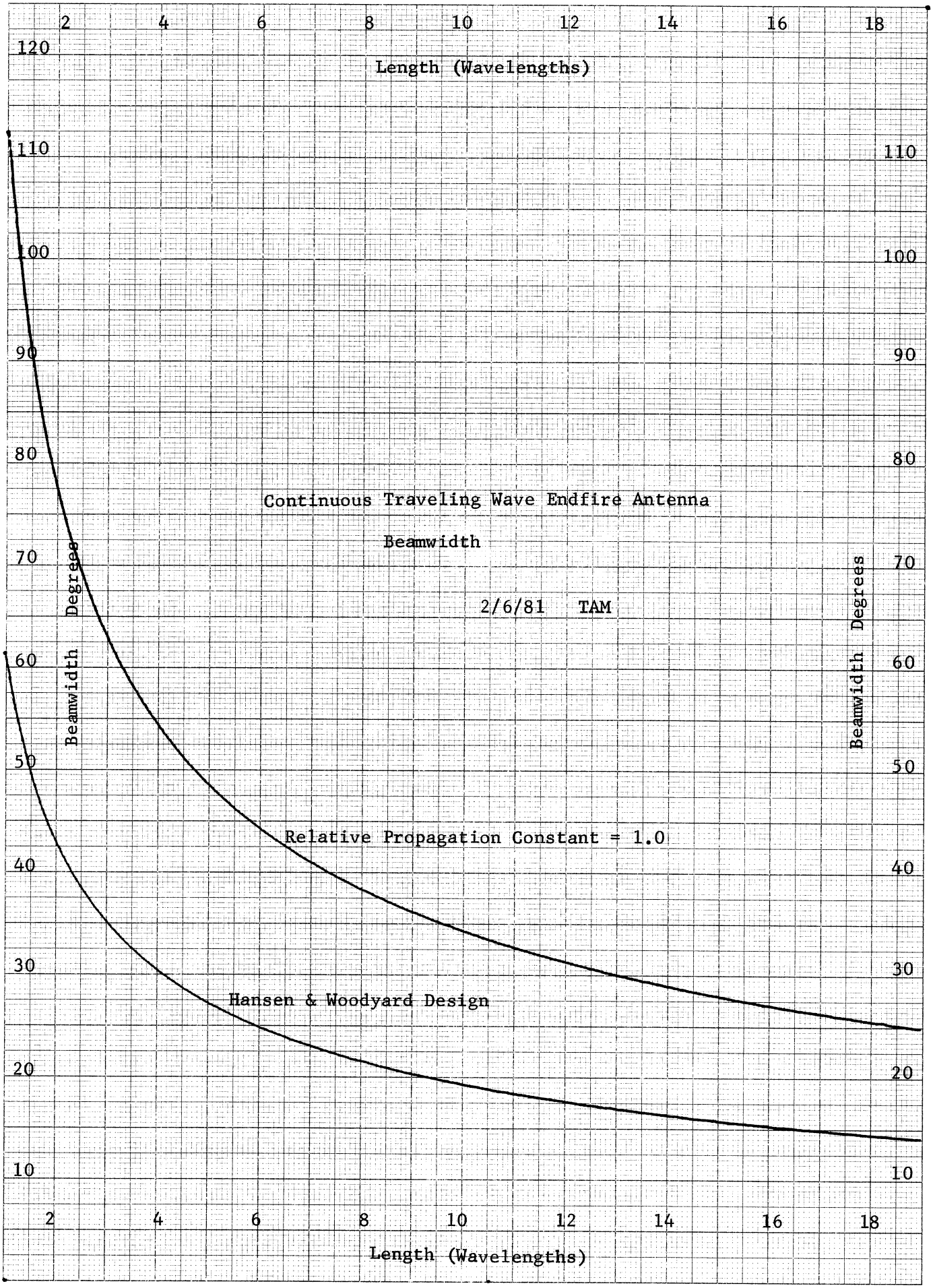

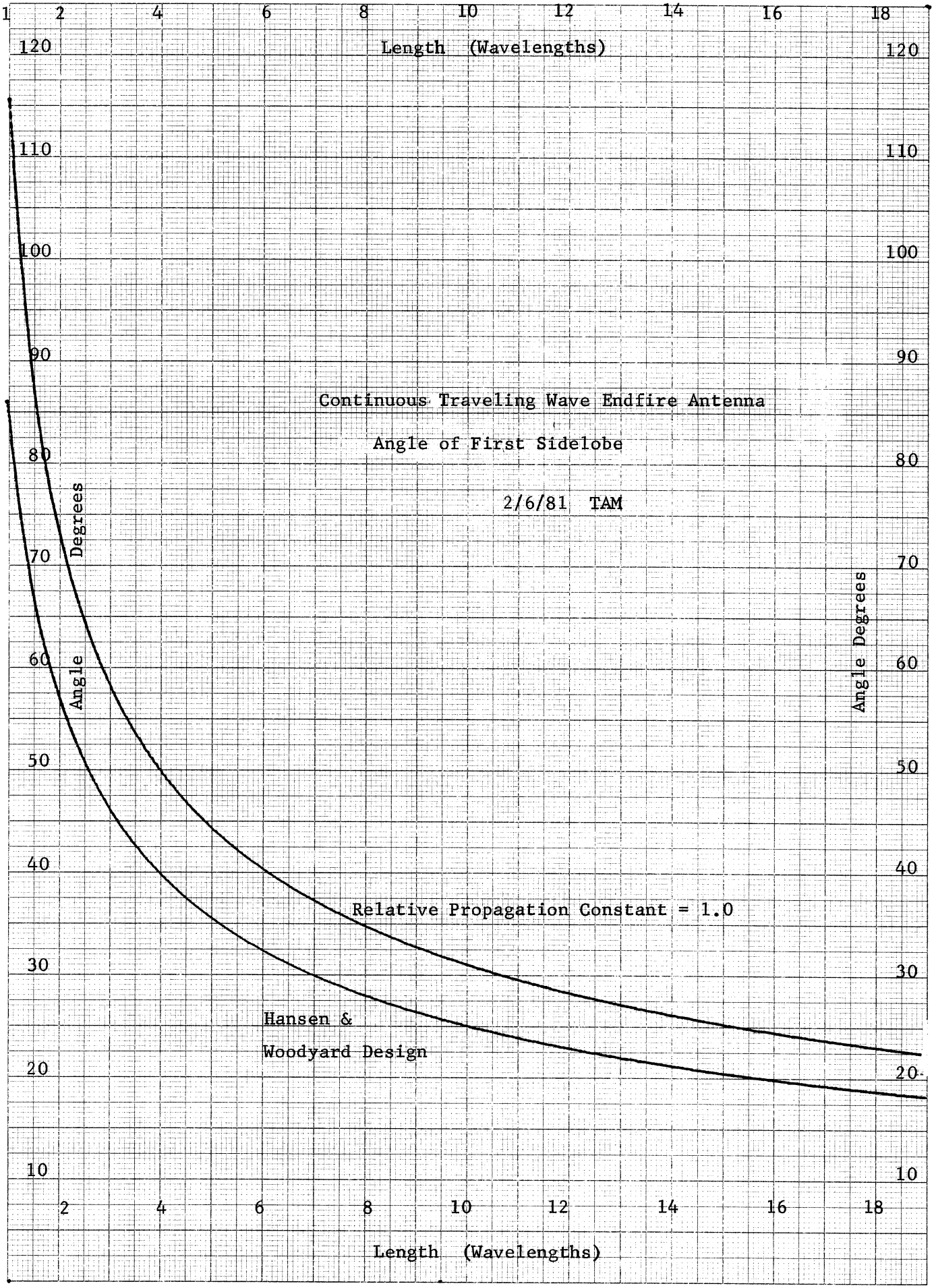

TRAVELING WAVE ENDFIRE LENGTH = 1. P = 1.5

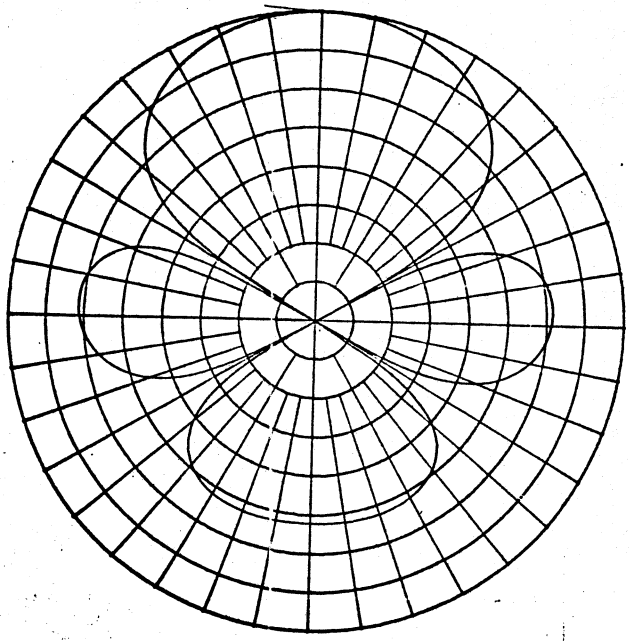

TRAVELING WAVE ENDFIRE LENGTH = 2. P = 1.25

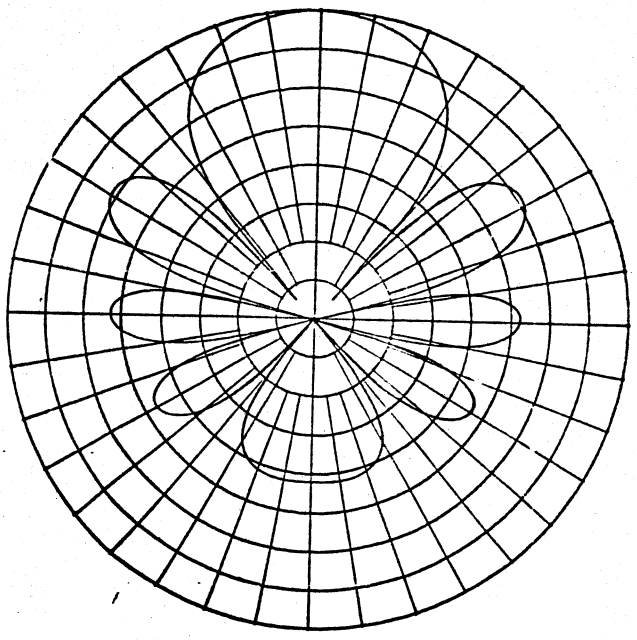

TRAVELING WAVE ENDFIRE LENGTH = 3. P = 1.167

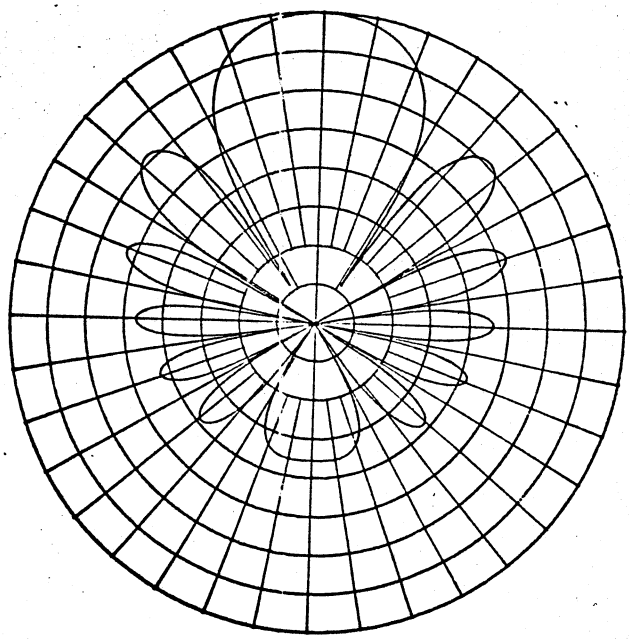

TRAVELING WAVE ENDFIRE LENGTH = 4. P = 1.125

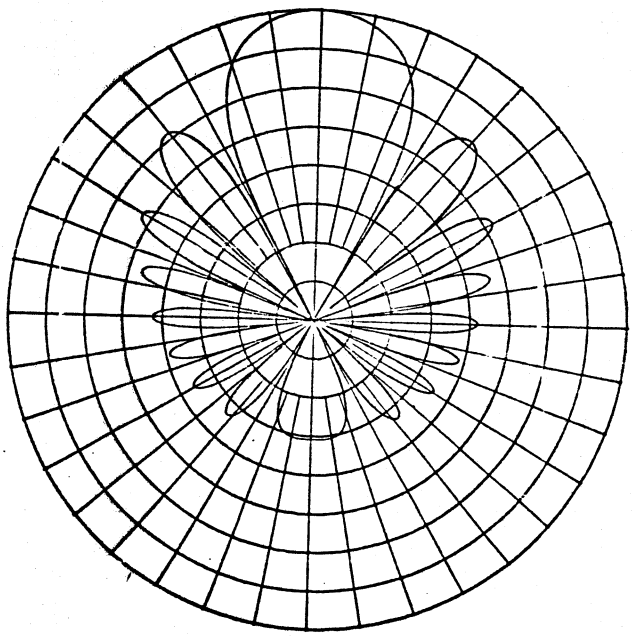

TRAVELING WAVE ENDFIRE LENGTH = 6. P = 1.0833

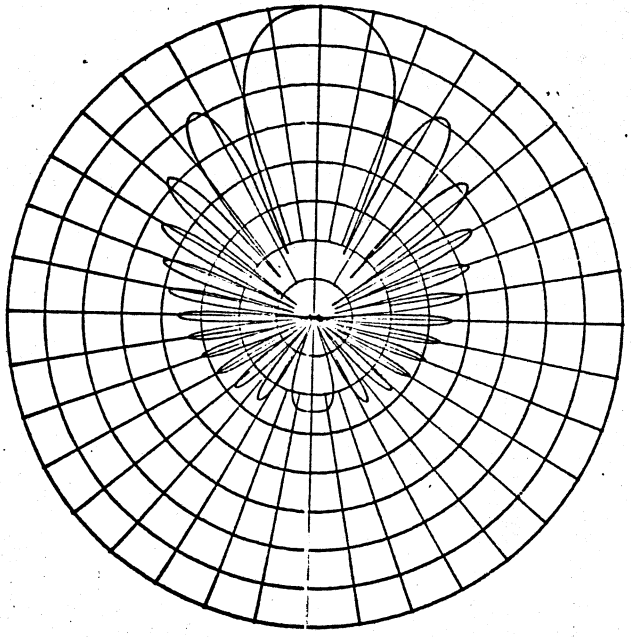

TRAVELING WAVE ENDFIRE LENGTH = 8. P = 1.0625

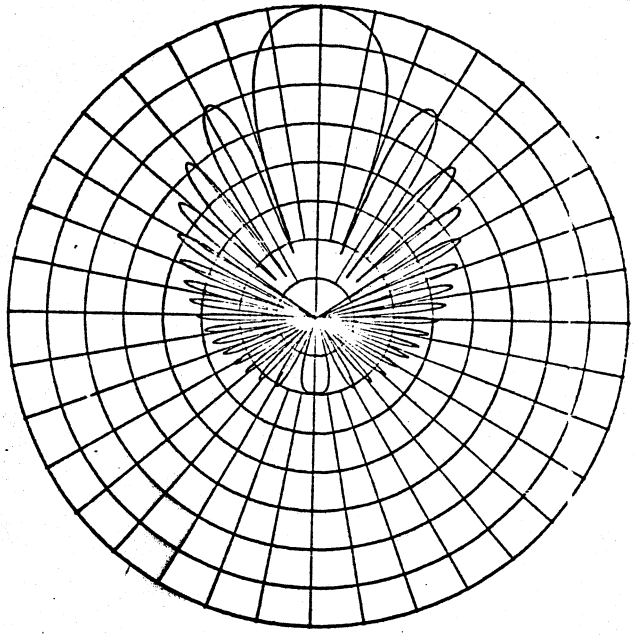

TRAVELING WAVE ENDFIRE LENGTH = 10. P = 1.05

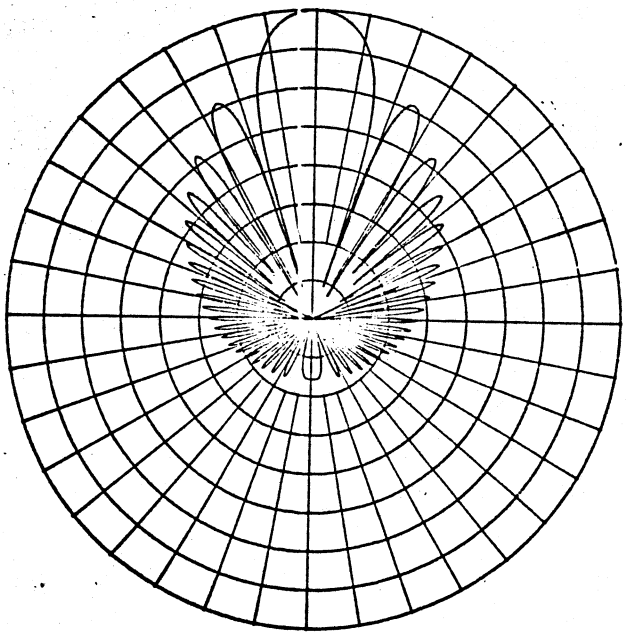

TRAVELING WAVE ENDFIRE LENGTH = 15. P = 1.03333

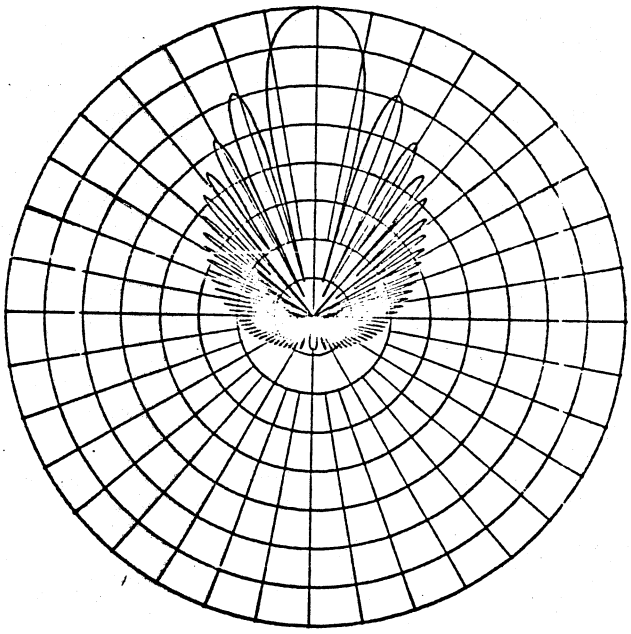

In order to understand the role of the relative propagation constant, a curve of the directivity versus P has been plotted on page 358 for various lengths of the antenna. The directivity rises until the Hansen and Woodyard criterion is reached and then falls rapidly afterward. Not shown directly is that the levels of the sidelobes are rising with increasing P and the beamwidth is decreasing. On pages 359 and 360 are a series of patterns showing the effect of increasing the relative propagation constant beyond the Hansen and Woodyard criterion for an antenna 4 wavelengths long. The main beam starts disappearing for P through 1.22 and 1.24 and is gone for P = 1.25. At P = 1.3 the two sidelobes have joined into a main beam and the pattern looks normal at P = 1.35 except that the sidelobe levels are quite high.

GENERATION OF TRAVELING WAVES

We can analyze the dipole as two traveling waves going in opposite directions on the element. The traveling wave antenna on page 164 was achieved by loading the end of the antenna so that the mode would not be reflected and give a standing wave pattern on the antenna. The problem with all traveling wave endfire antennas is to prevent the reflection of the radiation mode at the end of the antenna. In some cases the radiation mode is not bound strongly to the structure. When the end of the antenna is reached, the radiation mode is only slightly reflected. The energy is coupled into other modes which satisfy the boundary conditions. Away from the end these modes die away. The end is tapered sometimes to reduce the reflections of the radiation mode.

We can also think of the antenna setting up modes on the transmission line and then tapering the end of the line so that the mode is no longer attached and it flies off into space. This is similiar to the argument given on page 24 for the biconical horn. This idea has given rise to a method of analysis which is equivalent to the aperture field method. The traveling slow wave antenna must have a discontinuity at the beginning of the antenna to set up the mode as well as at the end where the mode ends. Between the discontinuities the slow wave structure is a transmission line which does not radiate. The antenna is analyzed as a two element array (or more if there are many discontinuities). There is some difficulty finding the proper element pattern for the discontinuity, but once it is found, the patterns will be the same as the other analysis.

The second method of considering the radiation from discontinuities is more satisfying because the structures of the antennas are transmission line modes which have zero radiation fields. Modes are set up on dielectric shapes or on corrugated surfaces (artifical dielectrics) which are open transmission line modes, but the fields reduce exponentially when moving away from the surface and do not radiate. From this point of view, the antenna can only radiate from discontinuities; it also explains the problem of traveling waves in both directions on the transmission line. The end of the surface wave structure is like the mouth of a large horn; there is little reflection.

We have curves for uniform amplitude and equal velocity traveling waves, but real antennas are not so nice. The amplitude is usually quite high at the beginning of the slow wave structure and varies throughout the length.

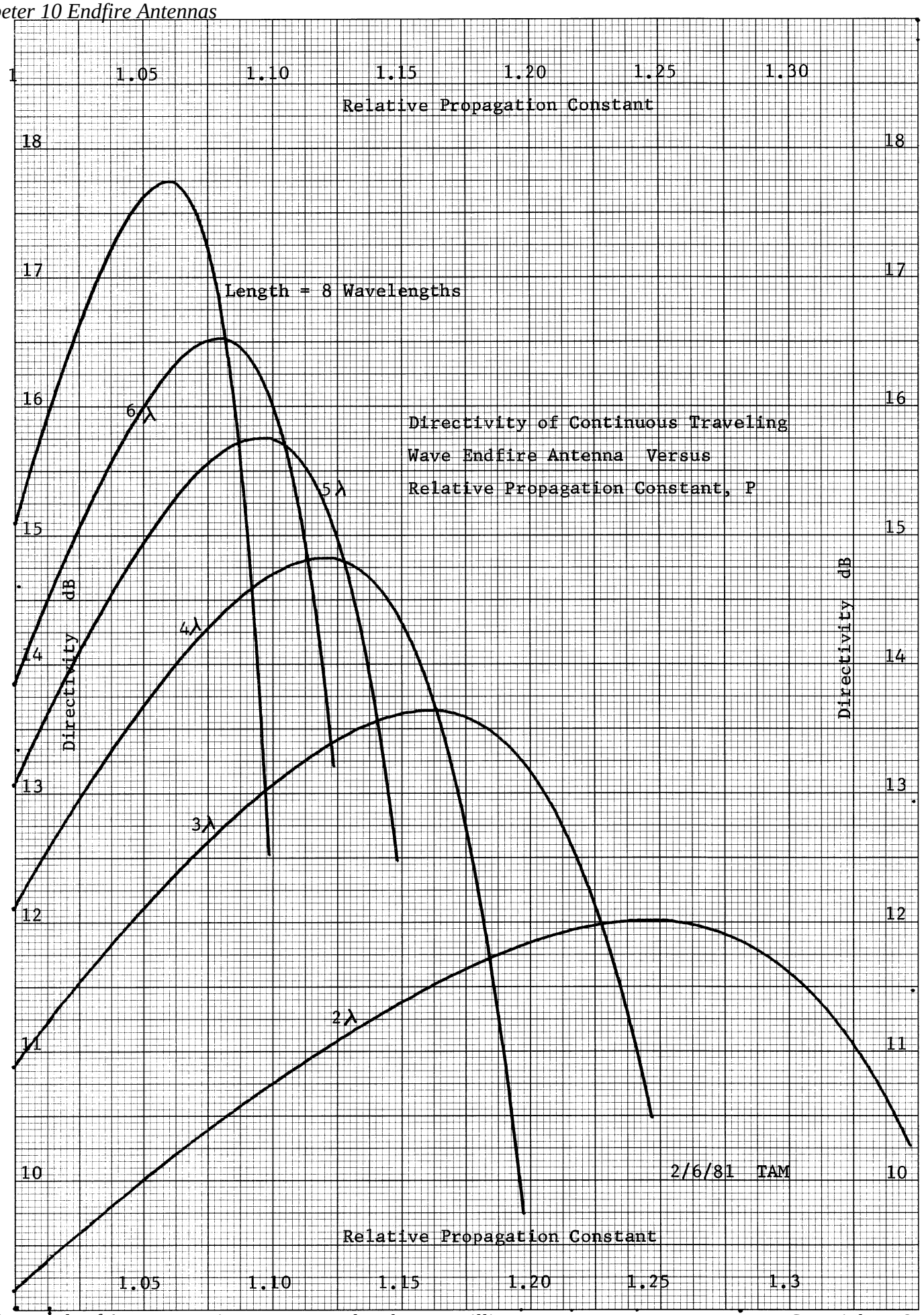

46 1320

10 X 10 TO ½ INCH 7 X 10 INCHES
KEUFFEL & ESSER CO. MADE IN U.S.A.

TRAVELING WAVE ENDFIRE LENGTH = 4. P = 1.125

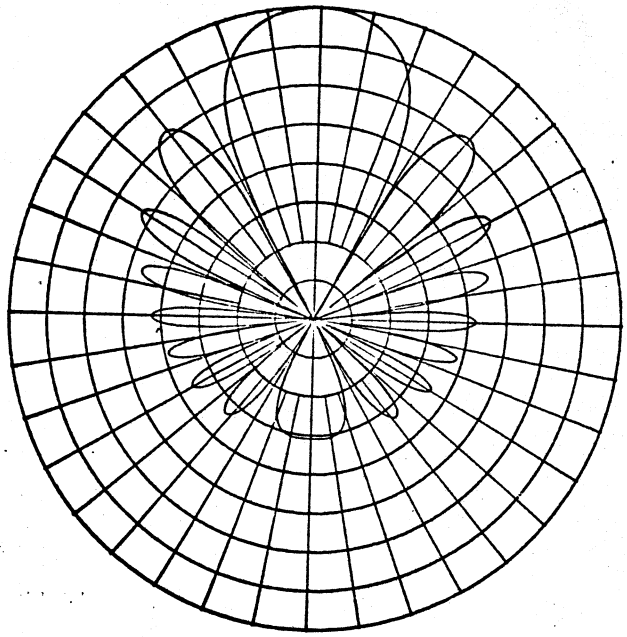

TRAVELING WAVE ENDFIRE LENGTH = 4 P = 1.15

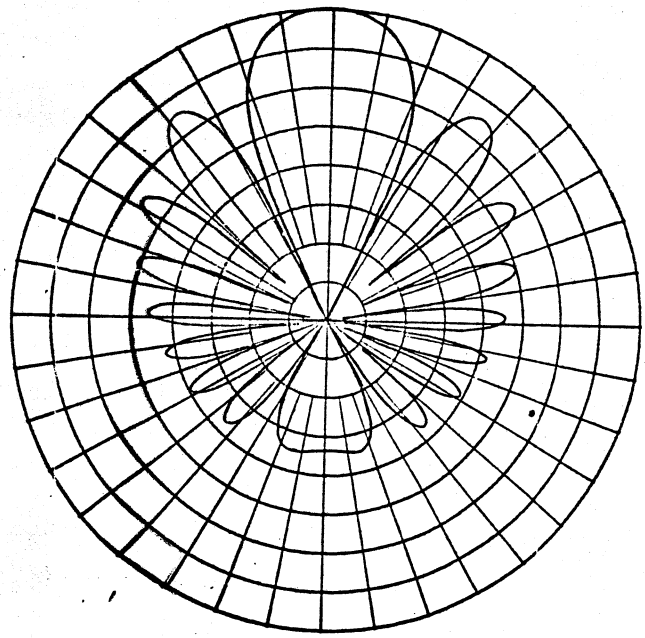

TRAVELING WAVE ENDFIRE LENGTH = 4 P =1.2

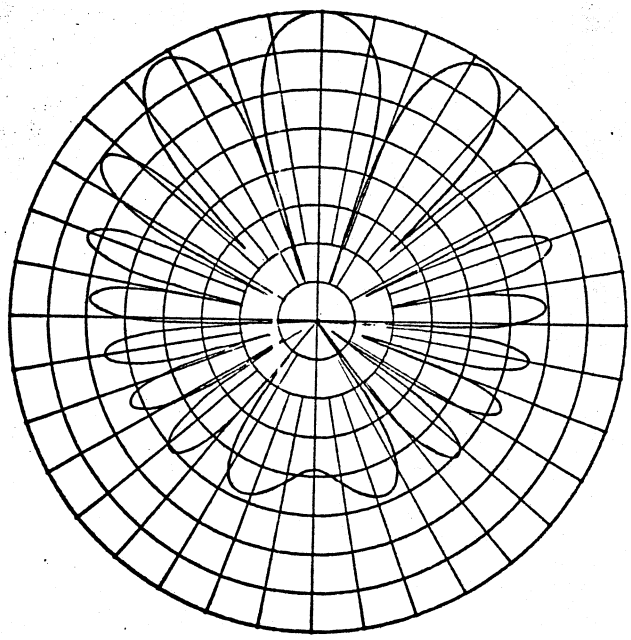

TRAVELING WAVE ENDFIRE LENGTH = 4 P = 1.22

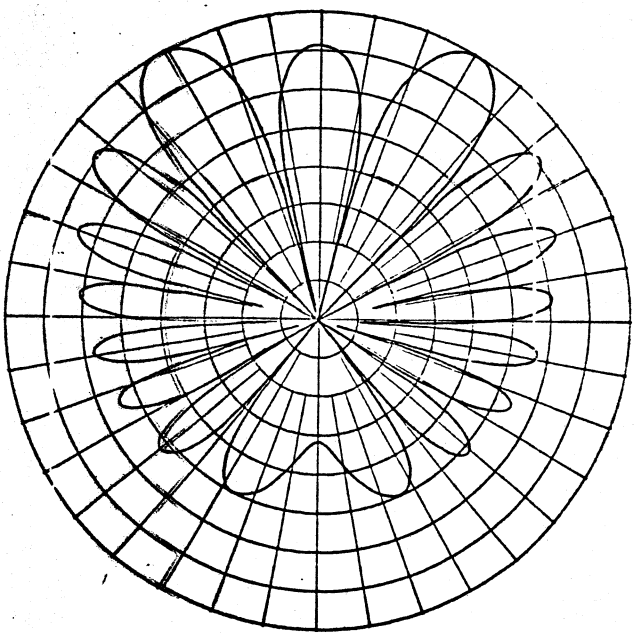

TRAVELING WAVE ENDFIRE LENGTH = 4 P =1.24

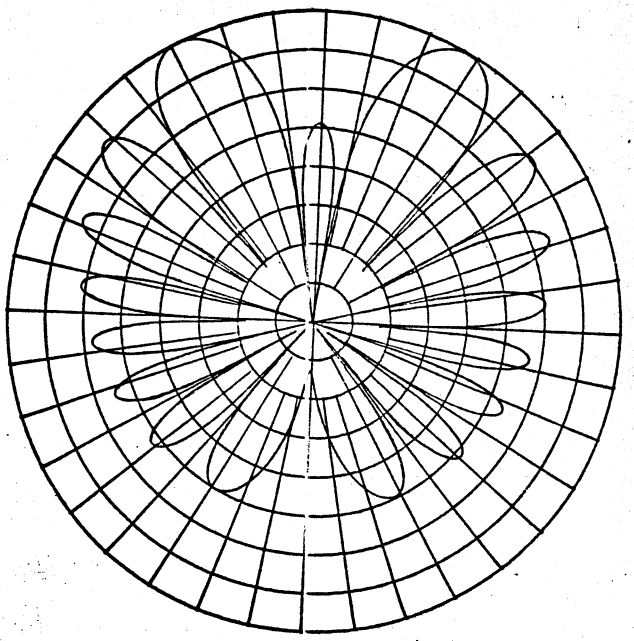

TRAVELING WAVE ENDFIRE LENGTH = 4 P = 1.25

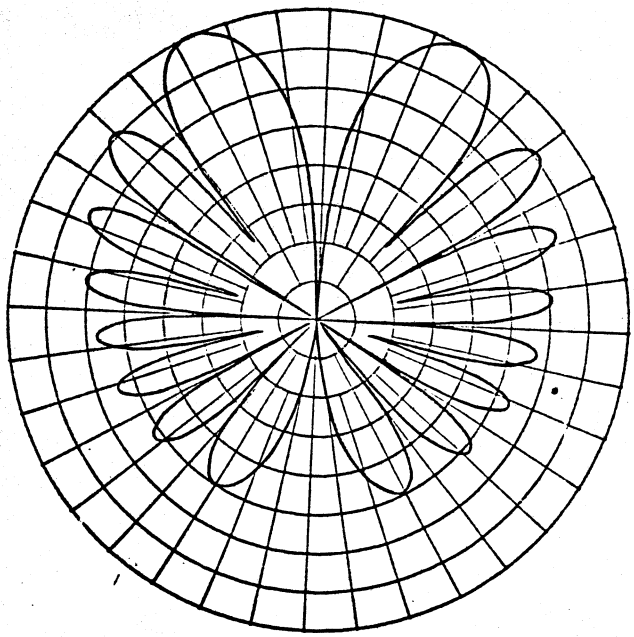

TRAVELING WAVE ENDFIRE LENGTH = 4 P = 1.3

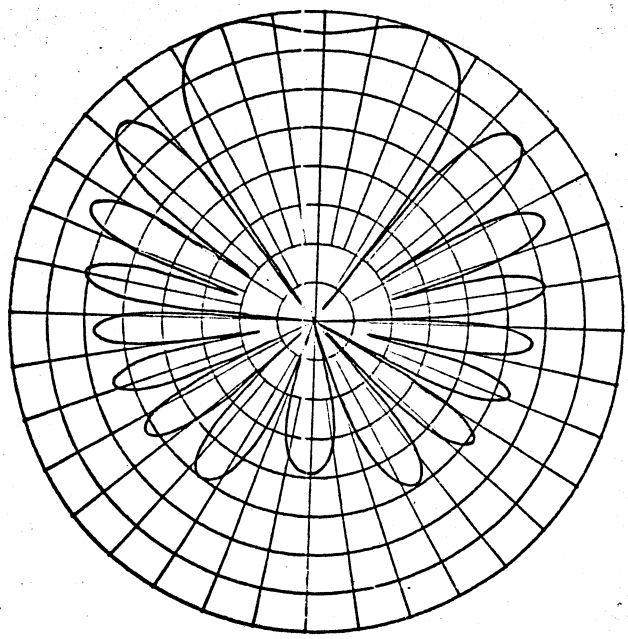

TRAVELING WAVE ENDFIRE LENGTH = 4 P = 1.35

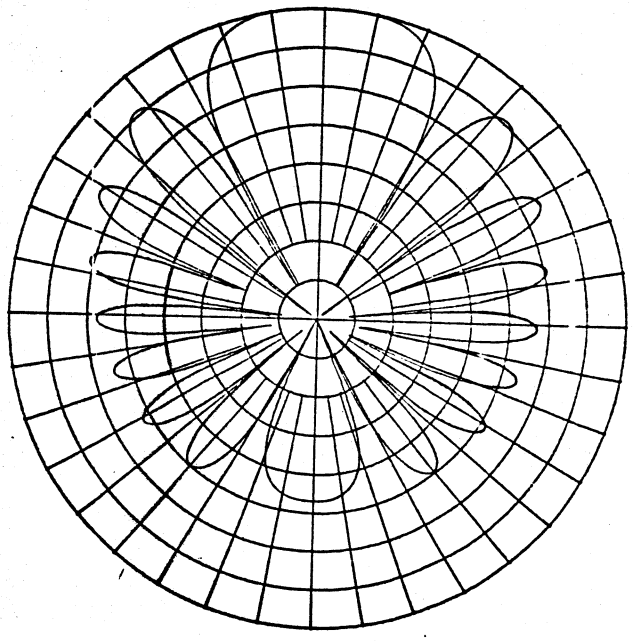

Many of these antennas have varying dimensions along the length which will in itself change the amplitude of the fields on the antenna. There will always be some sort of end effect and reflected wave, but many times this involves a change of mode which dies out rapidly and has little effect on the radiation pattern. The uniform distribution along the length will still give us an approximate pattern and results about these antennas.

GENERAL SURFACE WAVE DEVICE

There are two types of surface wave transmission lines we will discuss. The first is a two dimensional structure in rectangular coordinates where there is no dependence on one of the coordinates (Y for example). When we solved the Helmholtz equation in circular coordinates on page 256, we found that the propagation constant is only a function of the radial coordinate, ρ , separation constant and not on the separation constant of ϕ. We will still pick Z as the direction of propagation which establishes the function set as the harmonic functions:

$$e^{-j\beta_z z} \quad , \quad e^{j\beta_z z}$$

which are traveling waves in the plus and minus Z directions. We have the following two cases

where there is a surface wave device on the Y-Z plane or a circularly symmetric structure centered on the Z axis. The propagation constants are found from pages 240 and 260 as:

$$\beta_z^2 = \beta^2 - \beta_x^2 \quad \text{OR} \quad \beta_z^2 = \beta^2 - \beta_\rho^2$$

In the case of the rectangular coordinates the choice of harmonic functions are given from the set

$$\sin\beta_x x \ , \ \cos\beta_x x \ , \ e^{j\beta_x x} \ , \ e^{-j\beta_x x}$$

None of these functions are suitable because there is bound on X and it would require infinite energy if we used the standing wave solutions. If we used the traveling wave solutions, we cannot say that the structure is guiding the energy, but merely an obstacle in the path of a passing plane wave. The only solution is to use the functions:

$$e^{-\alpha x} \quad \text{OR} \quad e^{\alpha x}$$

We will have to restrict solution to $e^{-\alpha x}$ or the waves will grow to infinity as X increases. We will have this solution if

$$\alpha = j\beta_x$$

This changes the separation constant equation to

$$\beta_z^2 = \beta^2 + \alpha^2$$

Since α is positive, the propagation constant in the Z direction on the structure is always greater than the free space propagation constant, β . This is a slow wave structure

$$\beta_z = \frac{2\pi}{\lambda_z} = \frac{2\pi F}{V_z}$$

where V_z is the velocity of the wave in the Z direction. For a given frequency, F, the velocity, V_z, decreases for an increase in β_z.

In circular coordinates we have the same problem as in rectangular coordinates. The fields must decay exponentially in the radial direction. Neither the Bessel function, $J_n(\beta_\rho \rho)$, or the Neumann function, $Y_n(\beta_\rho \rho)$, is a suitable function because they are standing waves and require infinite energy on an open structure. A field decribed by the Hankel functions, $H_1(\beta_\rho \rho)$ and $H_2(\beta_\rho \rho)$ are traveling waves or unbounded waves of a plane wave described in circular coordinates. We must use modified Bessel functions which are similiar to $e^{\alpha r}$ AND $e^{-\alpha r}$

This leads us to solutions which have complex β_ρ. The equation for the propagation constant becomes

$$\beta_z^2 = \beta^2 + \alpha^2 \qquad \alpha = j\beta_\rho$$

This is the same equation as for the two dimensional rectangular coordinate case.

Once we know the exponential rate of decrease of the fields away from the surface wave structure, we can find the relative propagation constant, P.

$$\beta_z^2 = \beta^2 P^2 = \beta^2\left(1 + \frac{\alpha^2}{\beta^2}\right)$$

$$P = \sqrt{1 + \frac{\alpha^2}{\beta^2}} = \sqrt{1 + \left(\frac{\lambda\alpha}{2\pi}\right)^2}$$

Solving for α we get

$$\alpha = \frac{2\pi}{\lambda}\sqrt{P^2 - 1}$$

Once we have found the relationship between the dimensions of a structure and the constant α , we can design the antenna to a given relative propagation constant P. P is a measure of the boundness of the wave to the structure. For large α the fields are concentrated near the slow wave structure. This corresponds to large values of P. As P approaches one, the wave is only lightly bound to the structure. On page 363 is a plot of distances from the slow wave structure for given field levels versus the relative propagation constant. We can see from the plot that the fields fall off very rapidly from the slow wave structure and are definitely not radiating.

We will need to investigate some unconventional transmission line structures all which will be open structures and have exponentially decaying fields surrounding them.

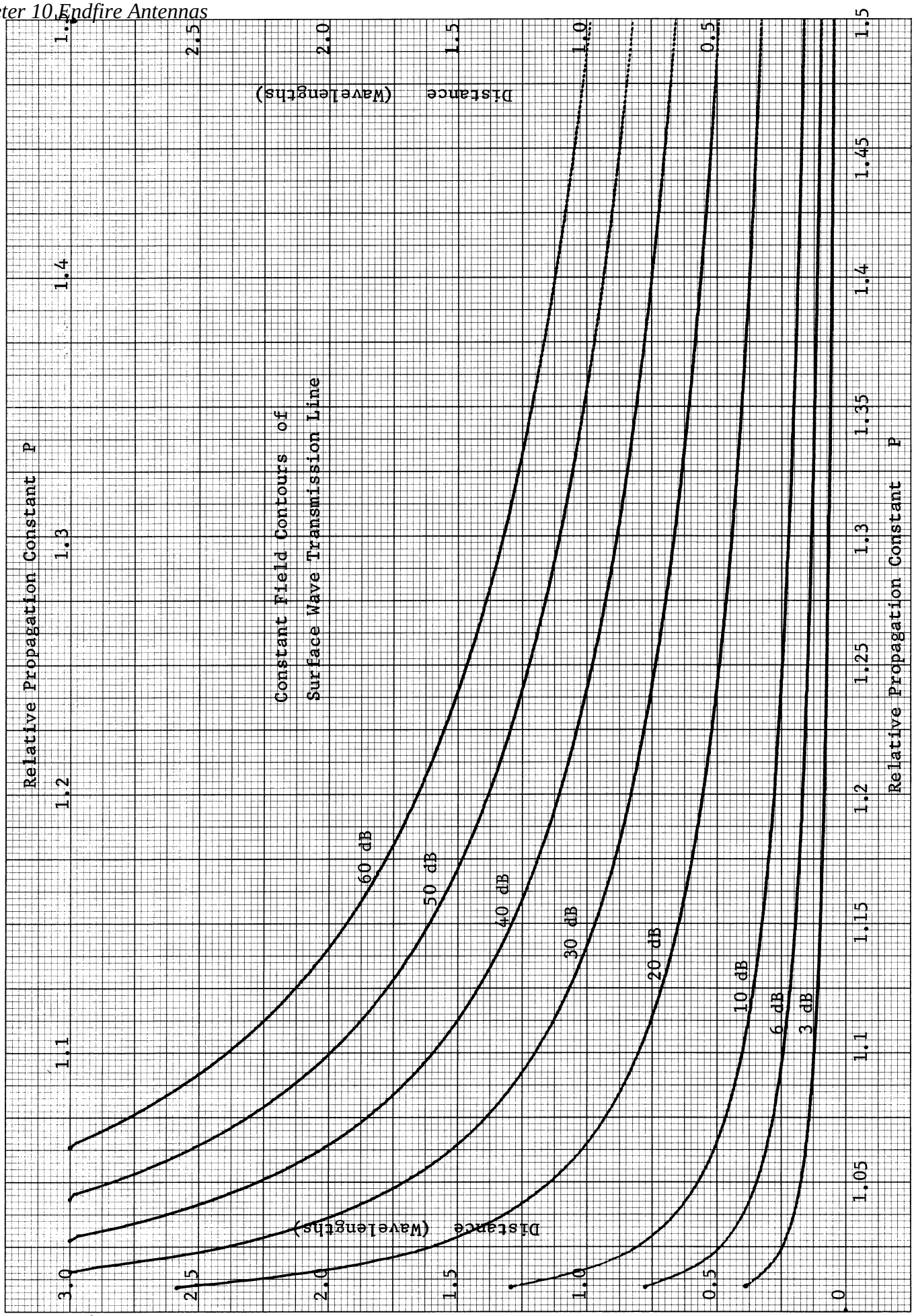

LEAKY WAVES

There are transmission structures whose relative propagation constants, P, are less than one. If we assume a uniform amplitude along the structure, then we can use the same pattern function as on page 348.

$$E = \frac{\sin(\psi/2)}{\psi/2} \qquad \psi = \beta L (P - \cos\theta)$$

The leaky wave structure continuously leaks energy along its length. The propagation constant includes an attenuation constant due to the energy leakage.

$$\beta_z - j\alpha_z$$

α_z is the attenuation. If the attenuation is small, which it must be on a long structure, then we can ignore it. The maximum radiation occurs when $\psi = 0$.

$$\theta_{max} = \cos^{-1} P$$

In order to have a wave with a relative propagation constant less than one, we must have a structure which will support fast waves. That is, ones whose phase velocities are greater than the free space speed of light. Waveguide modes have phase velocities which are fast waves (see page 205). If the guide is openned up, then the energy will leak out and radiate.

We can use the uniform amplitude distribution to find an upper bound on the gain of a cylindrical structure versus length. A pattern of such an antenna which is four wavelengths long and scanned to an angle of 45° is given on page 363b. The first sidelobe is down 13.3 dB as for a unifrom amplitude. The relative propagation constant is 0.707 (P = Cos 45°). We can find the directivity by integrating the pattern. If we fix the length and vary the velocity to scan the beam, then we find that the directivity is constant until the two beams are joined into a single endfire beam. We can calculate the directivity when P = 0, broadside radiation, and use it for the scanned beam. This has been done and is plotted on page 363c. The beamwidth increases as the beam is scanned toward endfire, which is plotted on page 363d.

Consider a continuous traveling wave antenna as it scans toward endfire. If we pick a particular length, then we can see that there is a considerable difference between the directivity given on page 352 and on page 363c. The directivity drops because there is a cone beam instead of a single endfire beam. A length of 10 wavelengths was picked and scanned from near endfire into endfire (P = 1) and beyond to super directive (Hansen and Woodyard criterion). On page 363e is a plot of directivity versus P. For lower values on the curve, the directivity is constant. The directivity rises rapidly as the beams join together. Beyond the super directive point the directivity drops rapidly as the sidelobes become about the same level as the main beam. The same result was seen on page 358.

The relative propagation constant of a waveguide is a function of the ratio of the cutoff frequency to the operating frequency.

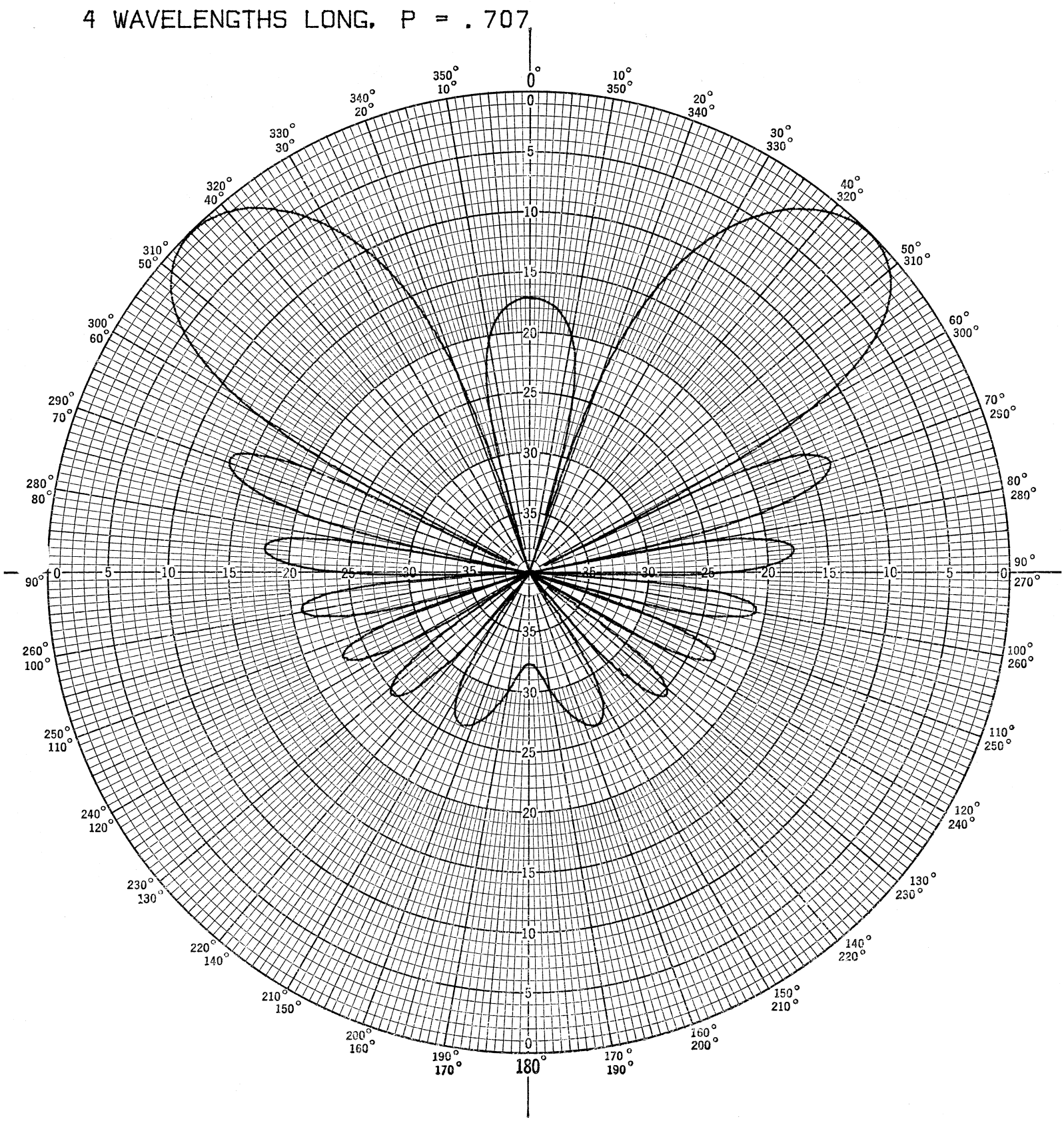

Polar Chart No. 127D
SCIENTIFIC-ATLANTA, INC.
ATLANTA, GEORGIA

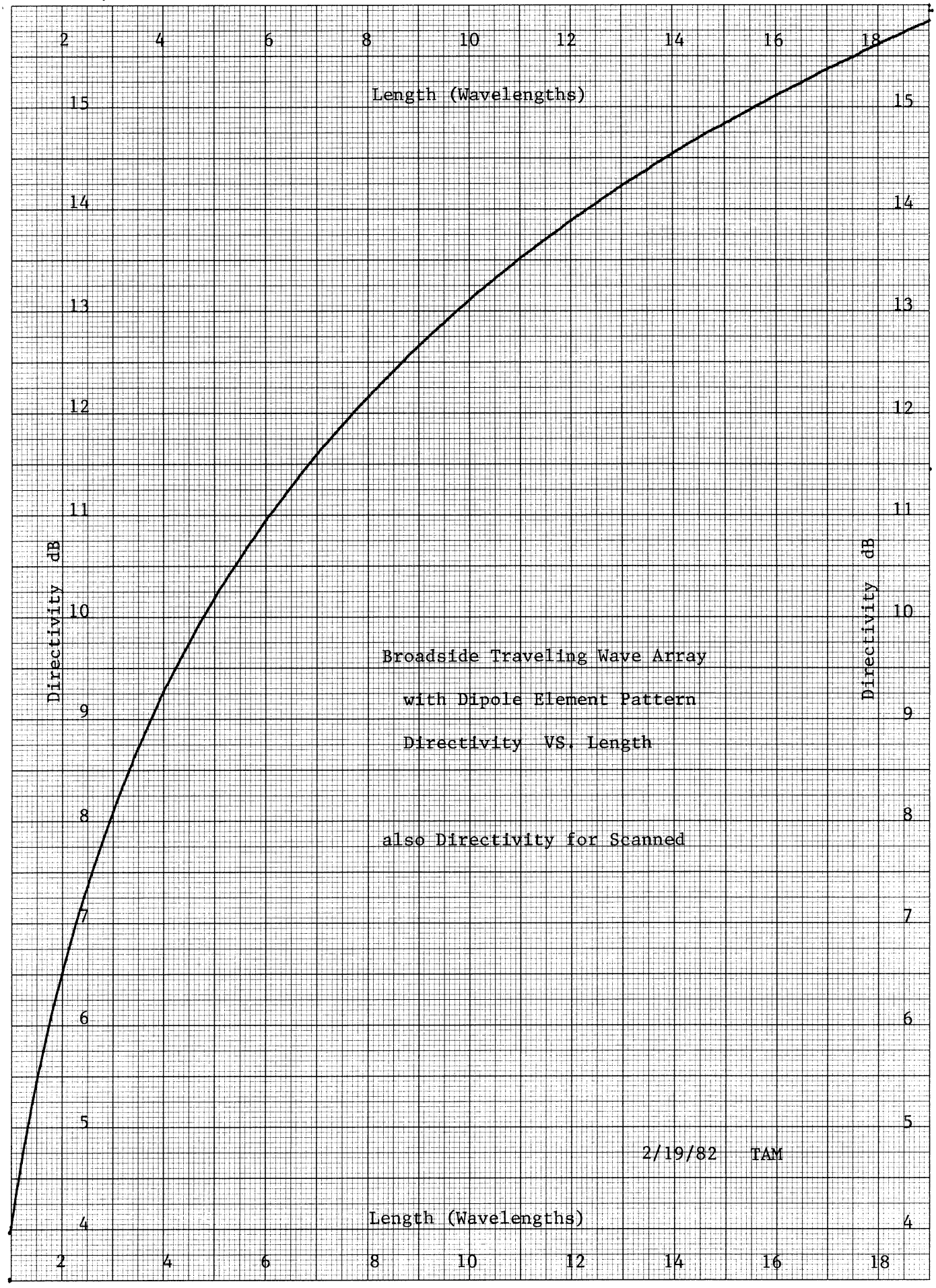

461510

10 X 10 TO THE CENTIMETER 18 X 25 CM.
KEUFFEL & ESSER CO. MADE IN U.S.A.

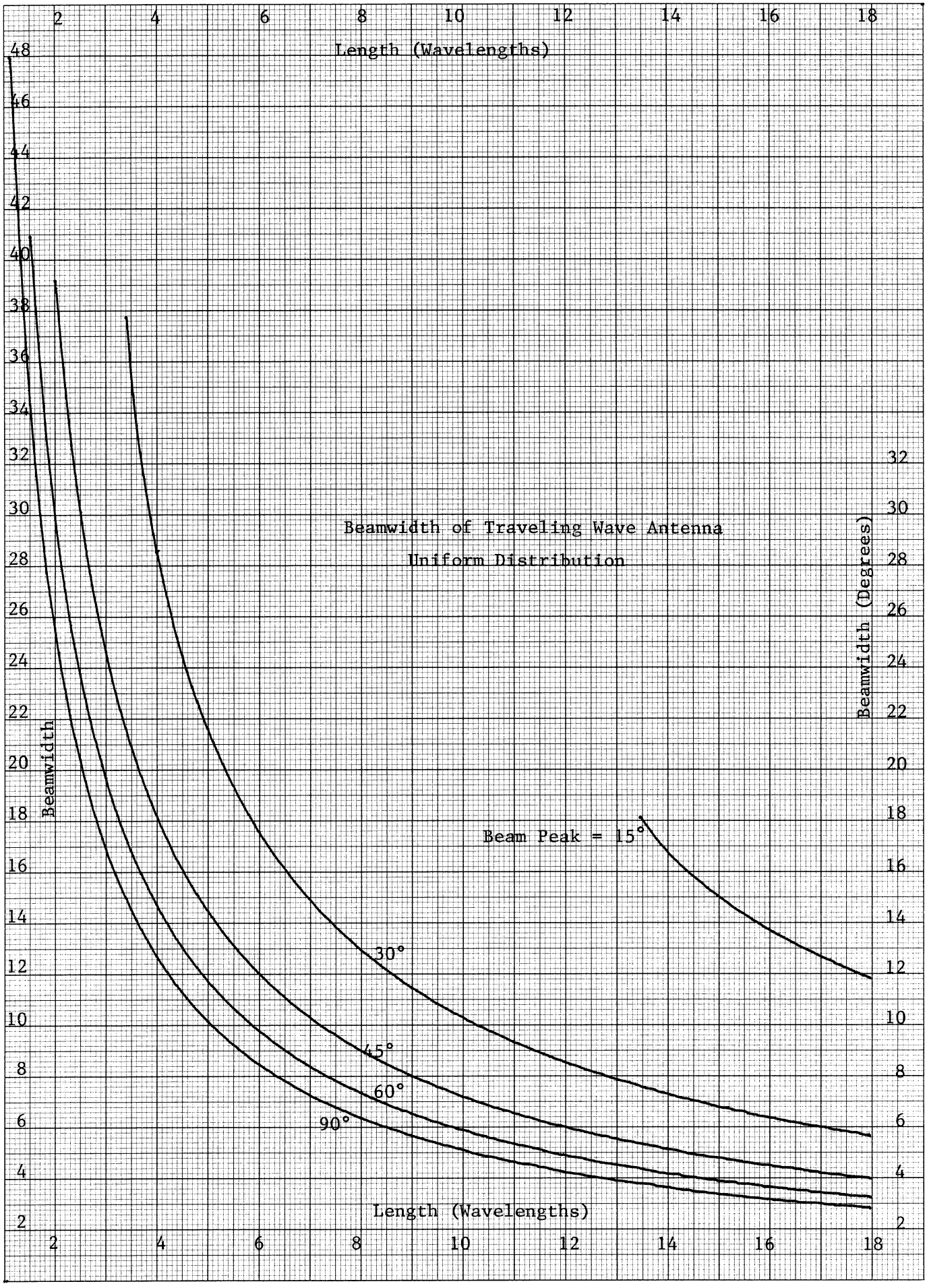

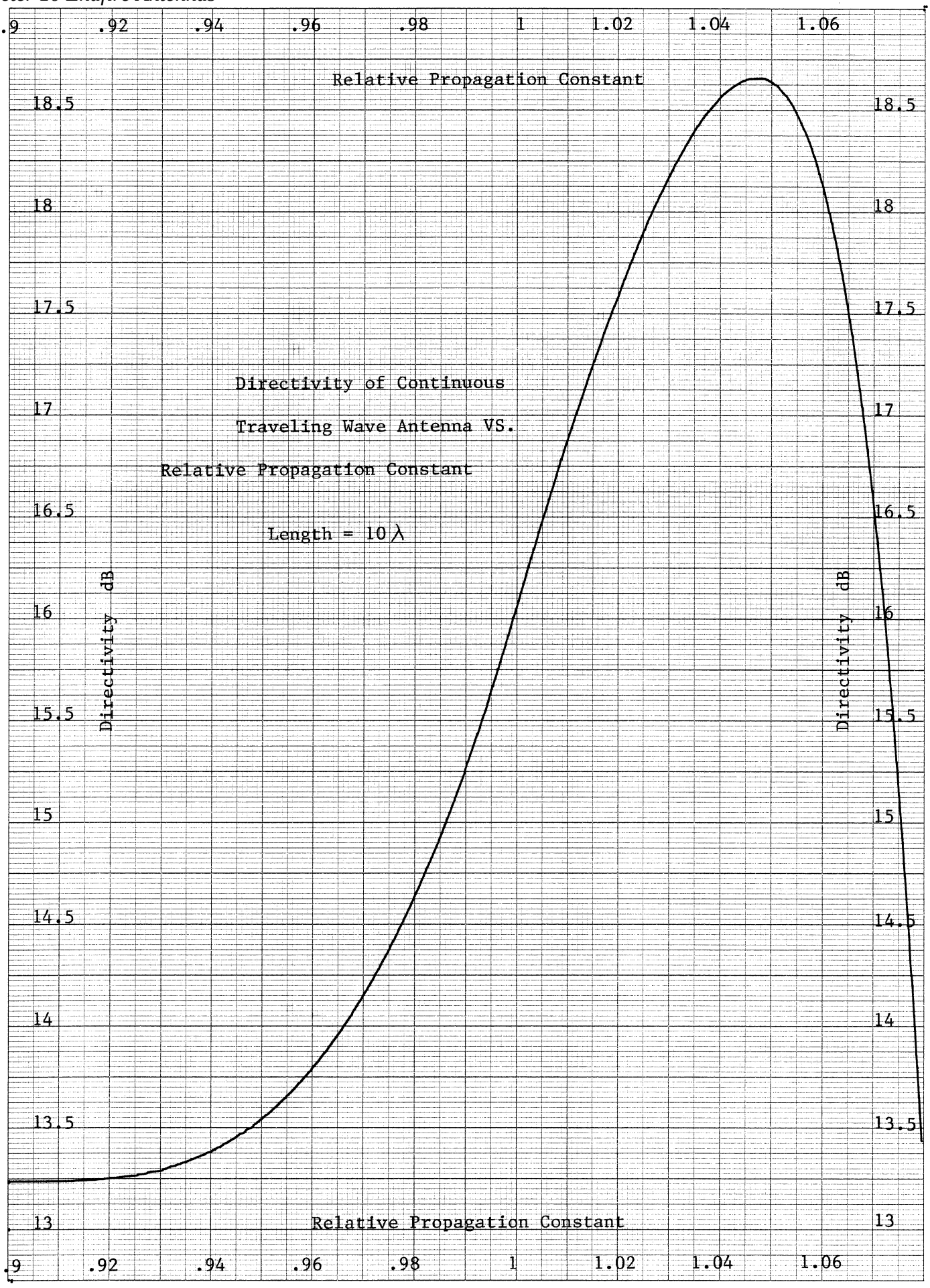

46 1510

10 X 10 TO THE CENTIMETER 18 X 25 CM.
KEUFFEL & ESSER CO. MADE IN U.S.A.

10 WAVELENGTHS LONG. P = 0.9

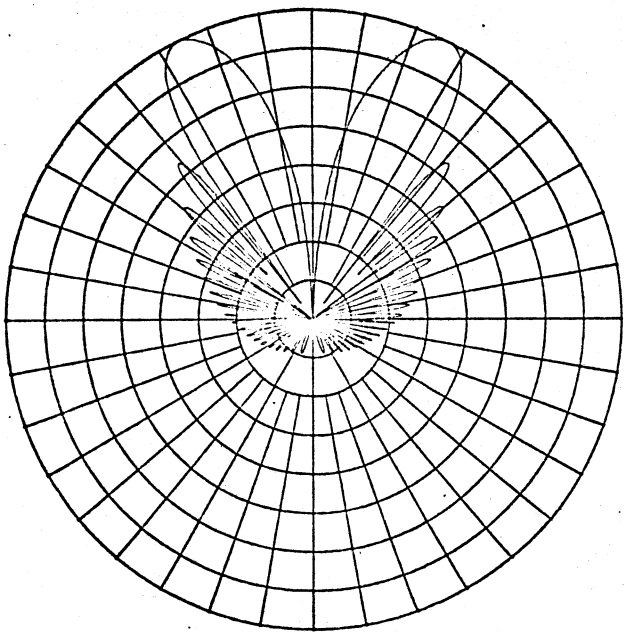

10 WAVELENGTHS LONG P = 0.929

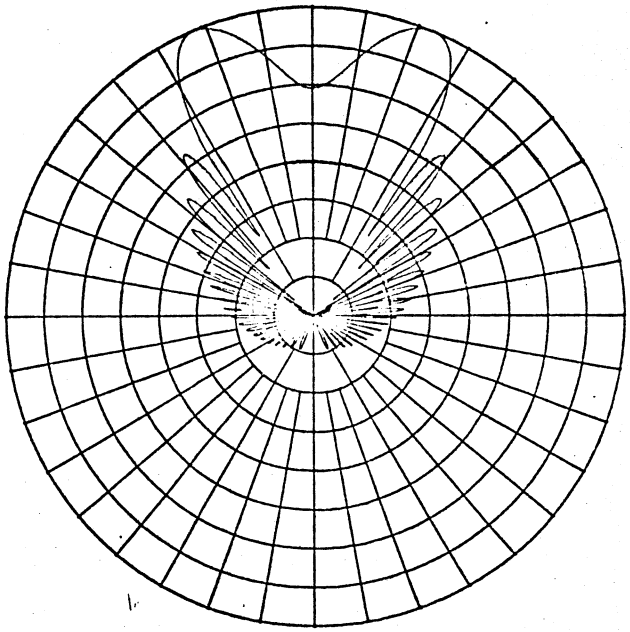

10 WAVELENGTHS LONG. P = .95

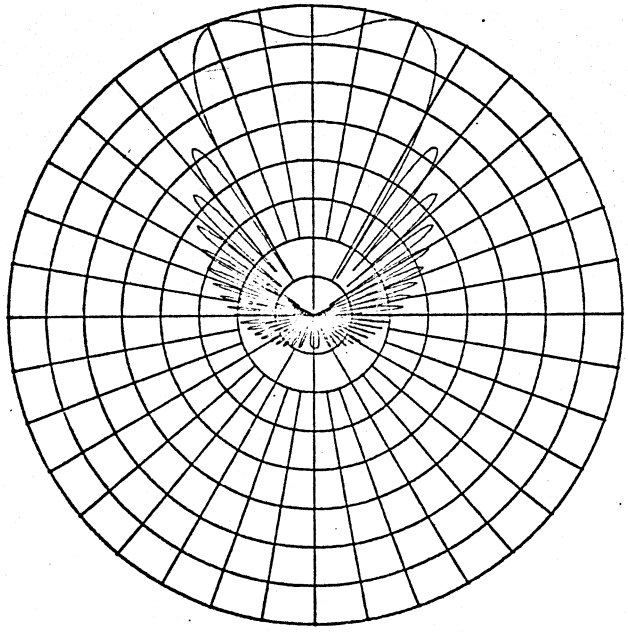

10 WAVELENGTHS LONG P = 0.975

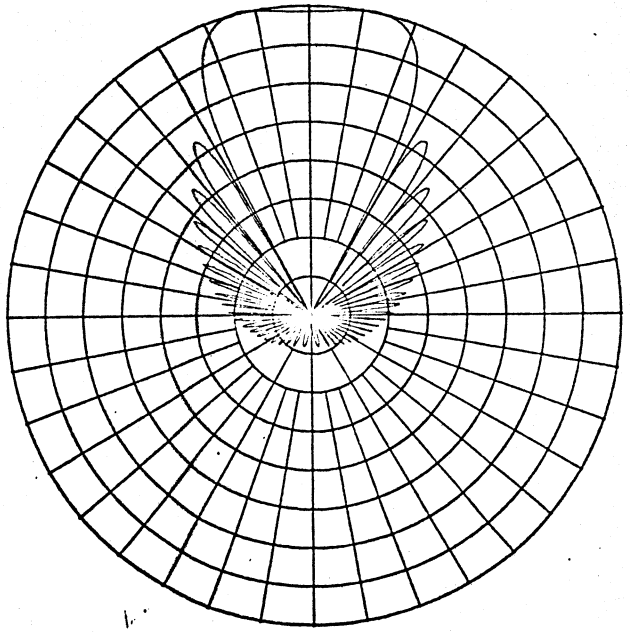

363f

$$P = \sqrt{1 - (f_c/f)^2} = \sqrt{1 - (\lambda/\lambda_c)^2}$$

The beam approaches endfire as the frequency increases and approaches broadside as the cutoff frequency is approached. Because the leaky wave antenna is an internal field device, unlike the slow wave antenna, it is necessary to load the end. Without it, the wave will be reflected and radiate another beam in the backfire direction. The backfire beam will be attenuated because the internal wave is reduced as the wave leaks energy into radiation.

The waveguide can be made into a leaky wave antenna by cutting a slot in the wall such as the top and varying the distance from the center line to control the leakage. Another method is to cut a series of closely spaced slots and control the leakage by the placement or length of each slot. We can include waveguide slots arrays with large spacings as leaky wave devices except that the slots appear as finite loads and cannot be analyzed as a continuous structure. The restriction on directivity for a given length plotted above will also hold for these antennas.

As the wave propagates along the waveguide, it continuously losses energy. It is necessary for the wave slots to leak more and more of the remaining energy to obtain a uniform distribution. For closely spaced wall slots, it is necessary to continuously increase the loading on the waveguide when moving down the guide toward the termination. Suppose the attenuation is given by $\alpha(z)$. The power at any point in the guide is given by

$$P(Z) = E_o^2 \exp\left(-2\int_o^z \alpha(z)\, dz \right)$$

E_o is the initial field. The attenuation is expressed in nepers/ length. Suppose we have a desired amplitude variation: A(z).

$$P_{in} = \int_o^L |A(z)|^2\, dz + P_{load}$$

We assume that a ratio of the input power will be lost in the load.

$$P_{load} = R\, P_{in}$$

$$P_{in} = \frac{1}{1 - R} \int_o^L |A(z)|^2\, dz$$

The power anywhere along the leaky wave antenna is given by

$$P(z) = P_{in} - \int_o^L |A(z)|^2\, dz$$

If we differentiate this, we get the expression

$$\frac{dP}{dz} = - |A(z)|^2$$

The attenuation equation gives us the usual logarithm differential equation.

$$\frac{1}{P(z)} \frac{dP}{dz} = -2\alpha(z)$$

Using these equations, $\alpha(z)$, the attenuation, can be found as a function of the desired aperture distribution.

$$\alpha(z) = \frac{\frac{1}{2}|A(z)|^2}{\frac{1}{1-R}\int_0^L |A(z)|^2 dz - \int_0^z |A(z)|^2 dz}$$

BRILLOUIN DIAGRAM

The various mode velocities of a transmission line structure can be described by a k_o vs. β_z diagram. k_o is the free space propagation constant, $2\pi/\lambda_o$. β_z is the mode propagation constant for a wave assumed to be traveling in the Z direction. A free space wave has the following diagram.

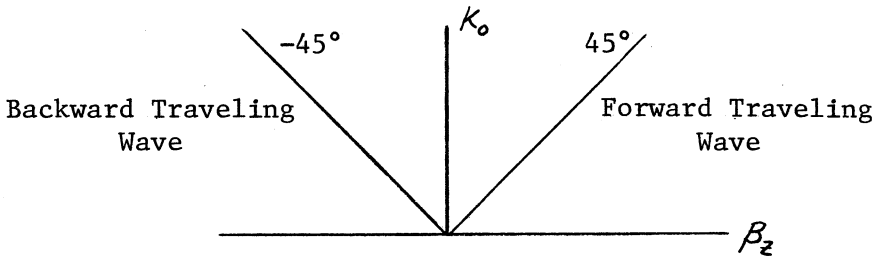

A TEM mode on a transmission line has the following diagram when dielectric loaded.

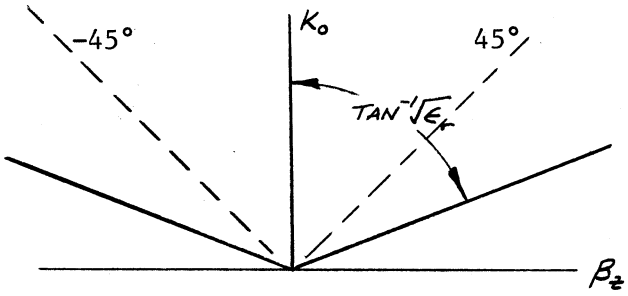

This is a slow wave because the curve lies below the ±45° lines.

A waveguide will not propagate until the frequency is higher than the cutoff frequency. As the frequency becomes higher and higher the waveguide propagation constant will approach the free space value.

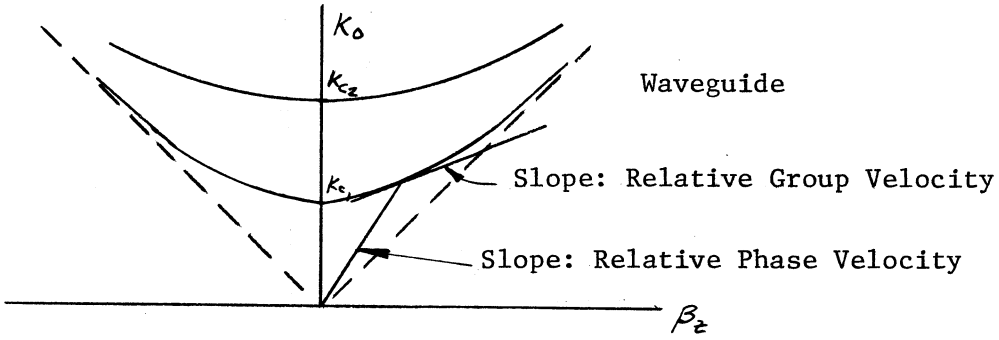

In this example we can identify the relative phase velocity as the slope of the line drawn from the origin to a point on the curve. The slope is always greater than one which means that the wave is fast in a waveguide. The slope of the line which is tangent to the curve is the relative group velocity. Since this is the velocity of energy transfer, it cannot be greater than one. The second curve is the next higher order mode.

We can divide the Brillouin diagram into various regions.

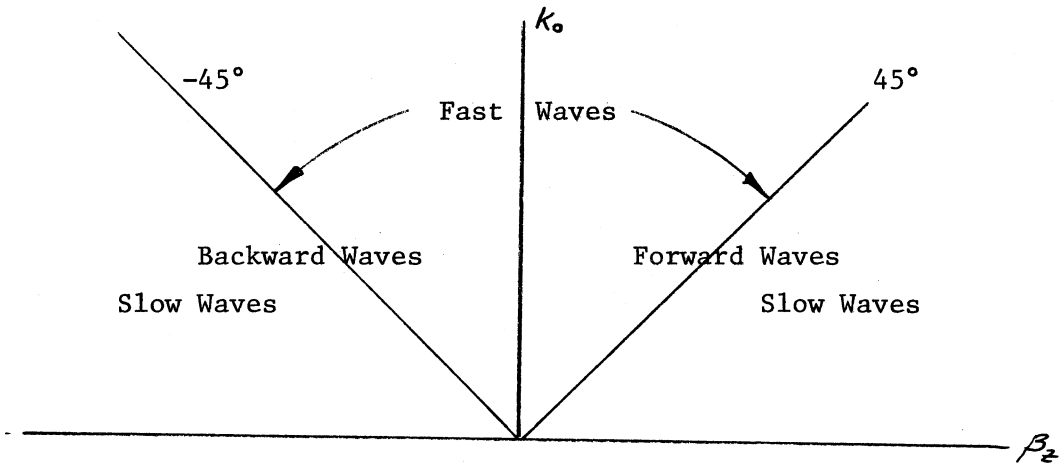

If the β_z curve lies below the ±45° lines, it is a slow wave structure. Slow waves are bound to the surface of an open structure and can only radiate at discontinuities or by coupling to radiating fast wave modes. All the open structures we will discuss are slow wave structures. Open structures cannot support fast waves since the energy is quickly radiated. Fast waves must be contained inside waveguide structures to be non-radiating. When fast waves are allowed to be coupled to free space, they radiate readily.

Although slow wave and fast wave (leaky wave) radiating structures can be analyzed with similiar mathematics, it is important to realize that they are describing different types of radiation. The slow wave structure radiates at discontinuities. The leaky wave antenna radiates everywhere that it can couple to free space. The only similiarity is that both structures are traveling wave radiators. When properly designed, the slow wave antenna is an endfire antenna. But of course, it is possible to get an antenna which is not endfire such as the example on page 360 because of an improper design and still a slow wave structure. A fast wave antenna has its radiation peak between broadside and endfire but not at either.

For a given structure the type of wave can be measured by using a near field probe. A method of measuring phase is required as the probe is moved along the axis. By comparing the change of phase relative to what would be measured in a free space wave, the type of operation determined and the value of the relative propagation constant, P, measured.

DIELECTRIC SLAB

Consider a dielectric slab in the Y-Z plane as shown below.

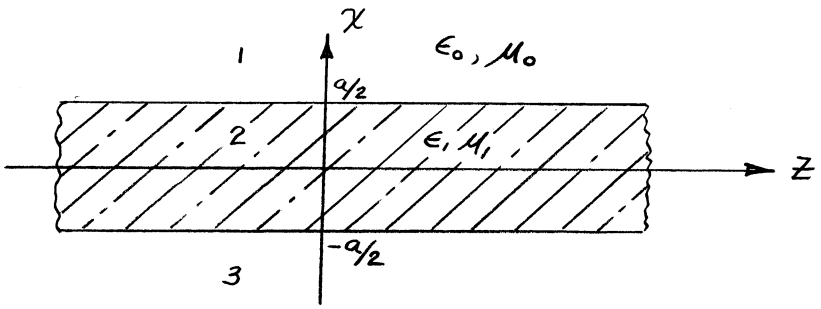

From our solution of the Helmholtz equation in rectangular coordinates, we know the potential function in the two regions.

$$\psi_1 = A_1 e^{-\frac{2\pi b}{\lambda}x} e^{-j\beta_z z} \qquad \text{Region 1}$$

$$\psi_2 = A_2 \left\{ \begin{matrix} \sin\left(\frac{2\pi p_x x}{\lambda}\right) \\ \cos\left(\frac{2\pi p_x x}{\lambda}\right) \end{matrix} \right\} e^{-j\beta_z z} \qquad \text{Region 2}$$

Where $2\pi b/\lambda$ was substituted for α and $2\pi p_x/\lambda$ was substituted for β_x. These substitutions make it easier to identify the solution on a per wavelength basis. We can pick a scalar potential in region 2 which is either an odd function (sine) or even function (cosine) of the X coordinate. The scalar potential in region 3 will depend on the choice.

$$\psi_3 = (\pm) A_1 e^{\frac{2\pi b}{\lambda}x} e^{-j\beta_z z} \qquad \text{Region 3}$$

Where the (+) sign corresponds to the odd mode function in region 2 and the (-) sign corresponds to the even mode function in region 2 (cosine). We have only assumed a wave traveling in the positive Z direction. The constants p_x and b will be found by satisfying the boundary conditions at $x = a/2$ and $x = -a/2$ and restrictions on the propagation constant.

First the propagation constant must be equal in both regions.

$$\beta_z^2 = \beta_0^2 + \left(\frac{2\pi b}{\lambda}\right)^2 = \omega^2 \epsilon_0 \mu_0 + \left(\frac{2\pi b}{\lambda}\right)^2 \qquad \text{Region 1 and 3}$$

$$\beta_z^2 = \beta_1^2 - \left(\frac{2\pi p_x}{\lambda}\right)^2 = \omega^2 \epsilon_1 \mu_1 - \left(\frac{2\pi p_x}{\lambda}\right)^2 \qquad \text{Region 2}$$

Equating these equations gives us the first equation.

$$\omega^2 \epsilon_0 \mu_0 + \left(\frac{2\pi b}{\lambda}\right)^2 = \omega^2 \epsilon_1 \mu_1 - \left(\frac{2\pi p_x}{\lambda}\right)^2$$

We can find a second equation by matching the tangential fields across the boundary at $X = a/2$. We will assume that there is no Y variation ($\partial\psi/\partial y = 0$).

TE Fields

From the equations on page 237 we can find the fields for TE modes with no Y variation.

$$E_x = 0 \qquad H_x = \frac{1}{j\omega\mu}\frac{\partial^2\psi}{\partial x \partial z}$$

$$E_y = \frac{\partial\psi}{\partial x} \qquad H_y = 0$$

$$E_z = 0 \qquad H_z = \frac{1}{j\omega\mu}\left(\frac{\partial^2}{\partial z^2} + \beta^2\right)\psi = \frac{1}{j\omega\mu}\left(\beta^2 - \beta_z^2\right)\psi$$

$$\beta^2 - \beta_z^2 = \left(\frac{2\pi p_x}{\lambda}\right)^2 = -\left(\frac{2\pi b}{\lambda}\right)^2$$

This is a horizontally polarized field with respect to the dielectric and free space boundary. Performing the indicated operations, we get the following tangential fields.

$$E_{y_1} = -A_1\frac{2\pi b}{\lambda}\, e^{-\frac{2\pi b}{\lambda}x}\, e^{-j\beta_z z} \qquad \text{Region 1}$$

$$E_{y_2} = (\pm) A_2\frac{2\pi p_x}{\lambda}\left\{\begin{matrix}\cos\left(\frac{2\pi p_x}{\lambda}x\right)\\ \sin\left(\frac{2\pi p_x}{\lambda}x\right)\end{matrix}\right\} e^{-j\beta_z z} \qquad \text{Region 2}$$

$$H_{z_1} = -\left(\frac{2\pi b}{\lambda}\right)^2\frac{A_1}{j\omega\mu_0}\, e^{-\frac{2\pi b}{\lambda}x}\, e^{-j\beta_z z} \qquad \text{Region 1}$$

$$H_{z_2} = \left(\frac{2\pi p_x}{\lambda}\right)^2\frac{A_2}{j\omega\mu_1}\left\{\begin{matrix}\sin\left(\frac{2\pi p_x}{\lambda}x\right)\\ \cos\left(\frac{2\pi p_x}{\lambda}x\right)\end{matrix}\right\} e^{-j\beta_z z} \qquad \text{Region 2}$$

These fields must be continuous across the boundary X = a/2. We equate the fields and obtain the following equations.

$$-A_1\frac{2\pi b}{\lambda}\, e^{-\frac{2\pi b}{\lambda}\frac{a}{2}} = (\pm) A_2\left(\frac{2\pi p_x}{\lambda}\right)\left\{\begin{matrix}\cos\left(\frac{2\pi p_x}{\lambda}\frac{a}{2}\right)\\ \sin\left(\frac{2\pi p_x}{\lambda}\frac{a}{2}\right)\end{matrix}\right\} \qquad E_y \text{ Field}$$

$$\frac{-A_1}{\mu_0}\left(\frac{2\pi b}{\lambda}\right)^2 e^{-\frac{2\pi b}{\lambda}\frac{a}{2}} = \left(\frac{2\pi p_x}{\lambda}\right)^2\frac{A_2}{\mu_1}\left\{\begin{matrix}\sin\left(\frac{2\pi p_x}{\lambda}\frac{a}{2}\right)\\ \cos\left(\frac{2\pi p_x}{\lambda}\frac{a}{2}\right)\end{matrix}\right\} \qquad H_z \text{ Field}$$

If we take the ratio of these equations, we can eliminate the constants A_1 and A_2, and get the following equations in the propagation constants.

$$\frac{\pi b}{\lambda \mu_0} = (\pm)\frac{\pi P_x}{\lambda \mu_1}\begin{Bmatrix} TAN\left(\frac{\pi P_x}{\lambda} a\right) \\ COT\left(\frac{\pi P_x}{\lambda} a\right) \end{Bmatrix}$$

This is the second equation in the set of two simultaneous equations. The upper portion corresponds to an odd mode solution of ψ (sine) in X and the lower portion to the even mode solution (cosine). Before proceeding to the solution of these equations, let us consider the TM modes.

TM Fields

From the equations on page 238 we can find the fields for TM modes with no Y variation.

$$E_x = \frac{1}{j\omega\epsilon}\frac{\partial^2\psi}{\partial x \partial z} \qquad H_x = 0$$

$$E_y = 0 \qquad H_y = -\frac{\partial \psi}{\partial x}$$

$$E_z = \frac{1}{j\omega\epsilon}(\beta^2 - \beta_z^2)\psi \qquad H_z = 0$$

This is a vertically polarized field with respect to the dielectric and free space boundary. Performing the indicated operations, we get the following tangential fields.

$$E_{z_1} = -\left(\frac{2\pi b}{\lambda}\right)^2 \frac{A_1}{j\omega\epsilon_0} e^{-\frac{2\pi b}{\lambda}x} e^{-j\beta_z z} \qquad \text{Region 1}$$

$$E_{z_2} = \left(\frac{2\pi P_x}{\lambda}\right)^2 \frac{A_2}{j\omega\epsilon_1}\begin{Bmatrix} SIN\left(\frac{2\pi P_x}{\lambda}x\right) \\ \cos\left(\frac{2\pi P_x}{\lambda}x\right) \end{Bmatrix} e^{-j\beta_z z} \qquad \text{Region 2}$$

$$H_{y_1} = \frac{2\pi b}{\lambda} A_1 e^{-\frac{2\pi b}{\lambda}x} e^{-j\beta_z z} \qquad \text{Region 1}$$

$$H_{y_2} = (\pm)\frac{2\pi P_x}{\lambda} A_2 \begin{Bmatrix} \cos\left(\frac{2\pi P_x}{\lambda}x\right) \\ SIN\left(\frac{2\pi P_x}{\lambda}x\right) \end{Bmatrix} e^{-j\beta_z z} \qquad \text{Region 2}$$

These tangential fields must be equal at the boundary X = a/2.

$$-\left(\frac{2\pi b}{\lambda}\right)^2 \frac{A_1}{\epsilon_0} e^{-\frac{2\pi b}{\lambda}\frac{a}{2}} = \left(\frac{2\pi P_x}{\lambda}\right)^2 \frac{A_2}{\epsilon_1}\begin{Bmatrix} SIN\left(\frac{2\pi P_x}{\lambda}\frac{a}{2}\right) \\ \cos\left(\frac{2\pi P_x}{\lambda}\frac{a}{2}\right) \end{Bmatrix} \qquad E_z \text{ Field}$$

$$\frac{2\pi b}{\lambda} A_1 e^{-\frac{2\pi b}{\lambda}\frac{a}{2}} = (\pm)\frac{2\pi P_x}{\lambda} A_2 \begin{Bmatrix} \cos\left(\frac{2\pi P_x}{\lambda}\frac{a}{2}\right) \\ SIN\left(\frac{2\pi P_x}{\lambda}\frac{a}{2}\right) \end{Bmatrix} \qquad H_y \text{ Field}$$

If we take the ratio of these equations, we get the following equations.

$$\frac{\pi b}{\lambda \epsilon_0} = (\pm)\frac{\pi p_x}{\lambda \epsilon_1}\begin{Bmatrix} TAN\left(\frac{\pi p_x a}{\lambda}\right) \\ COT\left(\frac{\pi p_x a}{\lambda}\right)\end{Bmatrix}$$

Except for an interchange of ϵ and μ, this is the same equation as for the TE mode case.

We are left with the problem of solving a simultaneous set of equations for the propagation constant. Take the second equation and multiply through by a, so that we get a dimensionless equation.

$$\frac{\mu_1}{\mu_0}\left(\frac{\pi b}{\lambda} a\right) = (\pm)\frac{\pi p_x}{\lambda} a \begin{Bmatrix} TAN\left(\frac{\pi p_x}{\lambda} a\right) \\ COT\left(\frac{\pi p_x}{\lambda} a\right)\end{Bmatrix} \qquad \text{TE Modes}$$

$$\frac{\epsilon_1}{\epsilon_0}\left(\frac{\pi b}{\lambda} a\right) = (\pm)\frac{\pi p_x}{\lambda} a \begin{Bmatrix} TAN\left(\frac{\pi p_x}{\lambda} a\right) \\ COT\left(\frac{\pi p_x}{\lambda} a\right)\end{Bmatrix} \qquad \text{TM Modes}$$

We get the following result from the propagation constant equation.

$$\left(\frac{2\pi b}{\lambda}\right)^2 = \omega^2(\epsilon_1\mu_1 - \epsilon_0\mu_0) - \left(\frac{2\pi p_x}{\lambda}\right)^2$$

Multiply through by $(a/2)^2$ and take the square root to obtain:

$$\frac{\pi b}{\lambda} a = \sqrt{\left(\frac{\omega a}{2}\right)^2(\epsilon_1\mu_1 - \epsilon_0\mu_0) - \left(\frac{\pi p_x}{\lambda}\right)^2}$$

When we substitute this in the set of equations above, we get a single equation in the separation constant.

$$\sqrt{\left(\frac{\omega a}{2}\right)^2(\epsilon_1\mu_1 - \epsilon_0\mu_0) - \left(\frac{\pi p_x}{\lambda} a\right)^2} = (\pm)\frac{\mu_0}{\mu_1}\left(\frac{\pi p_x}{\lambda} a\right)\begin{Bmatrix} TAN\left(\frac{\pi p_x}{\lambda} a\right) \\ COT\left(\frac{\pi p_x}{\lambda} a\right)\end{Bmatrix} \qquad \text{TE}$$

$$\sqrt{\left(\frac{\omega a}{2}\right)^2(\epsilon_1\mu_1 - \epsilon_0\mu_0) - \left(\frac{\pi p_x}{\lambda} a\right)^2} = (\pm)\frac{\epsilon_0}{\epsilon_1}\left(\frac{\pi p_x}{\lambda} a\right)\begin{Bmatrix} TAN\left(\frac{\pi p_x}{\lambda} a\right) \\ COT\left(\frac{\pi p_x}{\lambda} a\right)\end{Bmatrix} \qquad \text{TM}$$

We can solve this equation graphically for the separation constant. Before we do this, we should consider the concept of the cutoff frequency. The wave is bound to the slab only if $\alpha > 0$; otherwise it is only a passing plane wave. We define cutoff as $\alpha = 0$. At this point the equation becomes

$$\frac{2\pi p_x}{\lambda_c} = \omega\sqrt{\epsilon_1\mu_1 - \epsilon_0\mu_0} = \omega\sqrt{\epsilon_0\mu_0}\sqrt{\frac{\epsilon_1\mu_1}{\epsilon_0\mu_0} - 1}$$

The expression $\omega\sqrt{\epsilon_0\mu_0}$ equals $\beta = \frac{2\pi}{\lambda_c}$

$$\frac{2\pi P_x}{\lambda_c} = \frac{2\pi}{\lambda_c}\sqrt{\frac{\epsilon_1\mu_1}{\epsilon_0\mu_0} - 1} \qquad P_{x_c} = \sqrt{\frac{\epsilon_1\mu_1}{\epsilon_0\mu_0} - 1}$$

This gives us an equation for P_x at cutoff. We must also satisfy the propagation constant equation from equating the fields on the boundary.

$$TAN\left(\frac{\pi P_{x_c}}{\lambda_c}a\right) = COT\left(\frac{\pi P_x}{\lambda_c}a\right) = 0$$

These equations are satisfied if

$$\frac{\pi P_x}{\lambda_c}a = \frac{n\pi}{2}$$

n = 0, 2, 4,... for Tan( ): Odd ψ

n = 1, 3, 5,... for Cot( ): Even ψ

Using these equations, we can solve for the cutoff wavelength.

$$\lambda_c = \frac{2a}{n}\sqrt{\frac{\epsilon_1\mu_1}{\epsilon_0\mu_0} - 1}$$

For odd ψ the cutoff frequency will be zero. Remember that the cutoff frequency is that point where the fields become bound to the dielectric slab.

The usual method of finding the separation constant, $\pi p_x a/\lambda$, is to use a graphical solution. We plot both sides of the expression in the separation constant as a function of $\pi P_x\ a/\lambda$ and find the solution as the intersection of the curves. The function

$$\sqrt{\left(\frac{\pi a}{\lambda}\right)^2\left(\frac{\epsilon_1\mu_1}{\epsilon_0\mu_0} - 1\right) - \left(\frac{\pi P_x a}{\lambda}\right)^2}$$

is the equation of a circle with valid solutions in the first quadrant. The maximum value is given by

$$\frac{\pi a}{\lambda}\sqrt{\frac{\epsilon_1\mu_1}{\epsilon_0\mu_0} - 1}$$

The above expression intersects with the curve

$$(\pm)\frac{\mu_0}{\mu_1}\left(\frac{\pi P_x a}{\lambda}\right)\left\{\begin{matrix} TAN\left(\frac{\pi P_x a}{\lambda}\right) \\ COT\left(\frac{\pi P_x a}{\lambda}\right)\end{matrix}\right\} \qquad \text{TE Modes}$$

$$(\pm)\frac{\epsilon_0}{\epsilon_1}\left(\frac{\pi P_x a}{\lambda}\right)\left\{\begin{matrix} TAN\left(\frac{\pi P_x a}{\lambda}\right) \\ COT\left(\frac{\pi P_x a}{\lambda}\right)\end{matrix}\right\} \qquad \text{TM Modes}$$

For a given value of μ_0/μ_1 or ϵ_0/ϵ_1, we can plot both of these curves as a function of ($\pi P_x\ a/\lambda$) and find intersections. As the frequency

increases or the thickness increases, the circle diameter will grow and the separation constant (πP_x a/λ) will increase.

On page 370 is a mode chart for the dielectric slab guide for TE modes where $\mu_o = \mu_1$. This is a graphical solution of the transcendental equation of the separation constant. Two circles have been drawn on the plot which correspond to the cases:

1) Thickness = .25λ , Dielectric Constant = 2.55

2) Thickness = 1/2λ , Dielectric Constant = 2.55

The first circle only intersects one of the vertical curves while the second case intersects two vertical curves. There is only one possible mode in case one. We can read the value of the separation constant at the intersection of the two curves as 0.73 . The vertical coordinate on the graph corresponds to πb (a/λ) or the attenuation constant times the thickness of the slab. We read this value as 0.67 . The second case has two intersections.

n	πP_x a/λ	πb (a/λ)	b	P
0	1.02	1.68	1.070	1.44
1	1.88	0.60	.382	1.07

There are two possible TE modes for this thickness and dielectric constant.

We can find the relative propagation constant from a formula on page 362.

$$P = \sqrt{1 + \left(\frac{\lambda\alpha}{2\pi}\right)^2} \qquad \alpha = \frac{2\pi b}{\lambda}$$

$$P = \sqrt{1 + b^2}$$

Hence in the first case above

$$\pi b\ (a/\lambda) = 0.67 \qquad b = 0.85 \qquad P = 1.31$$

The mode chart for TM modes is plotted on page 371. In this case we must use a different curve for each dielectric constant; shown on the plot are three typical dielectric constants. The lower circle is drawn for a thickness of a quarter wavelength for a dielectric constant of 2.5. In this case the value of πb (a/λ) is .44 which converts to a value for b = .56 and a relative propagation constant, P, equal to 1.15 . If we draw the circles for the dielectric constants of 5 and 10, we get calculated values of P of 1.57 and 2.52, respectively. The surface wave is more strongly bound to the higher dielectric constant slabs.

By solving the transcendental equation, a set of curves of the relative propagation constant can be drawn for various dielectric constants versus the thickness. Curves for the two lowest order modes are drawn on pages 372 through 375. These curves enable us to be able to design the dielectric slab guide to a particular velocity.

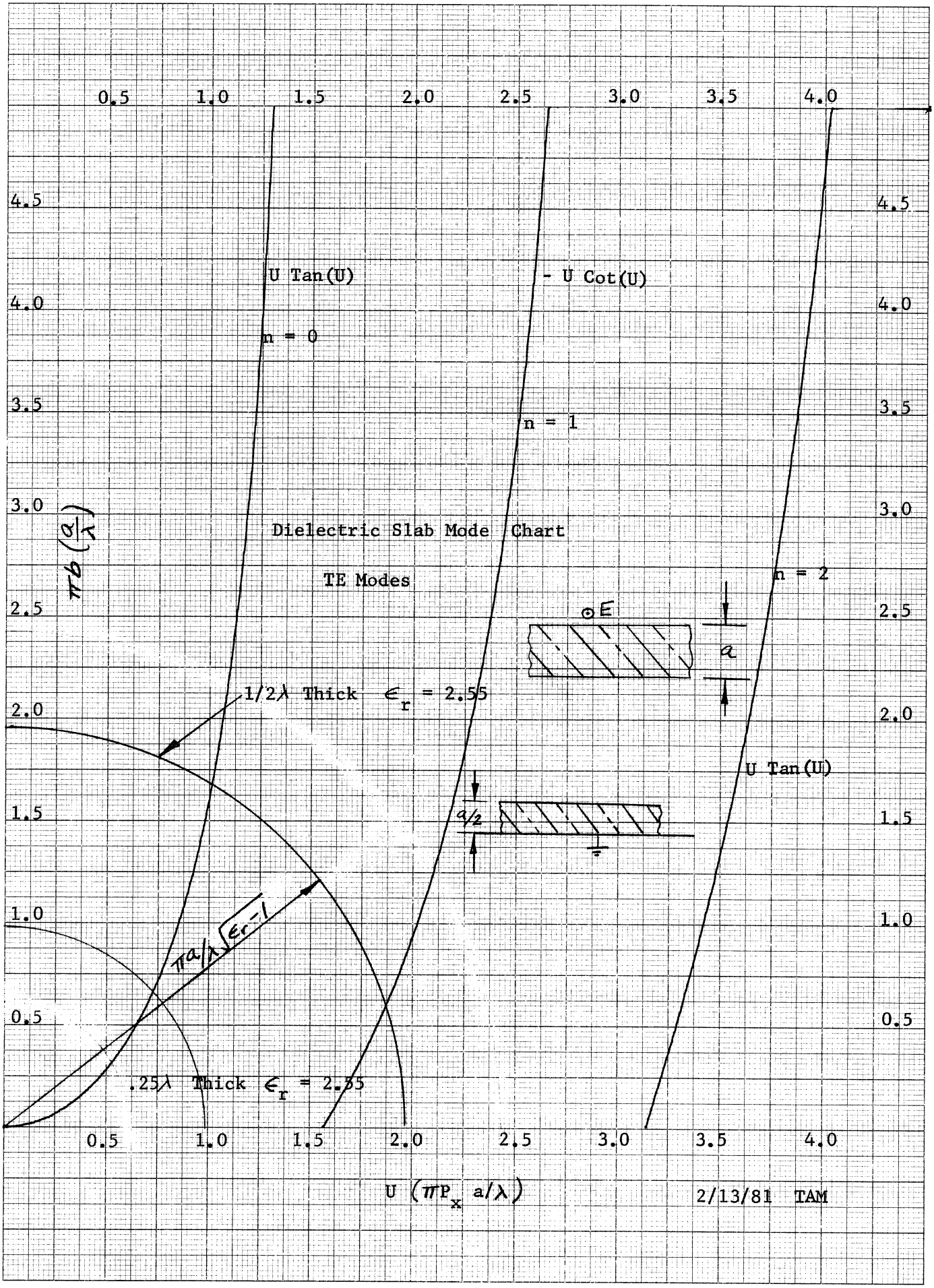

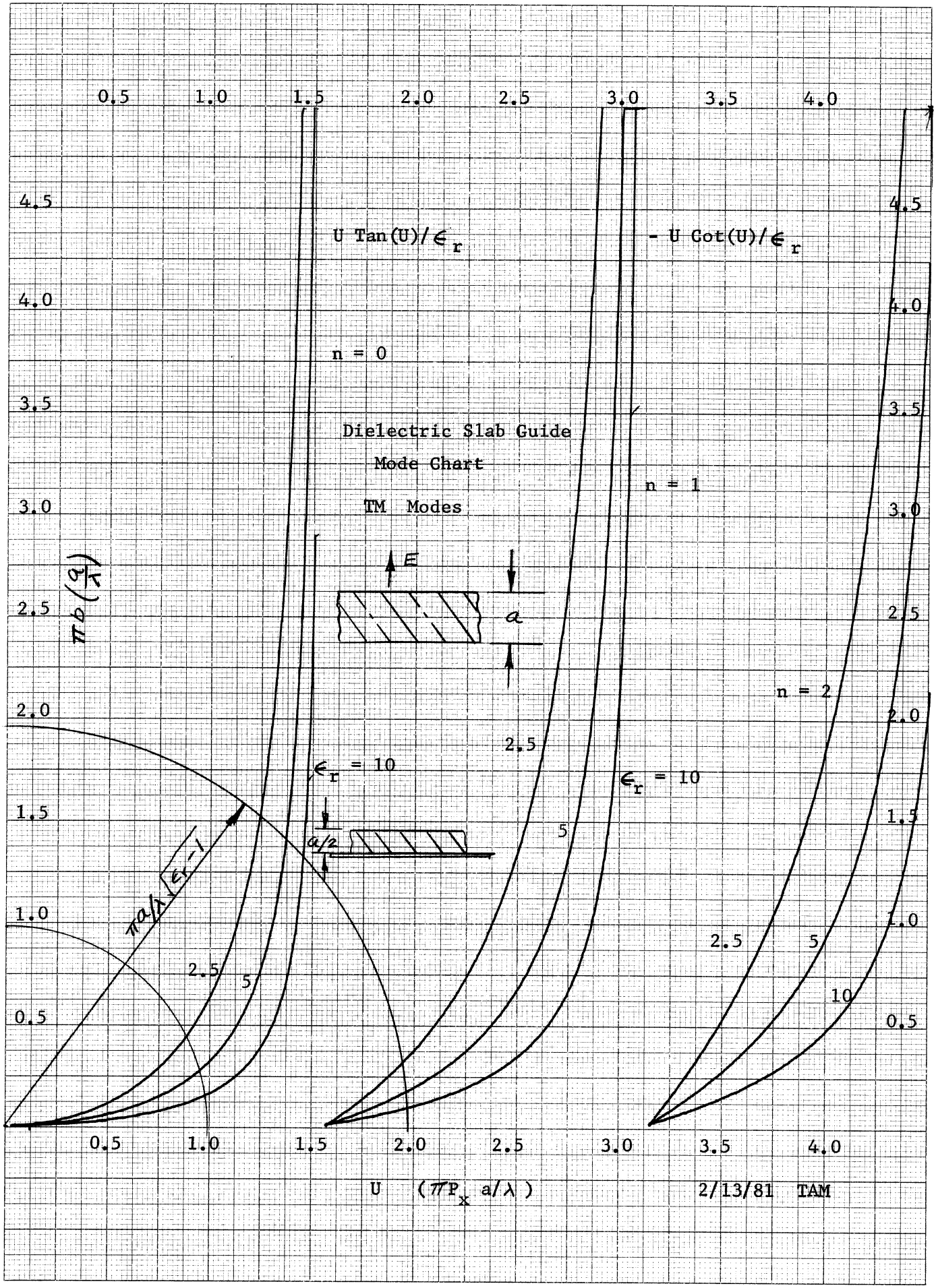

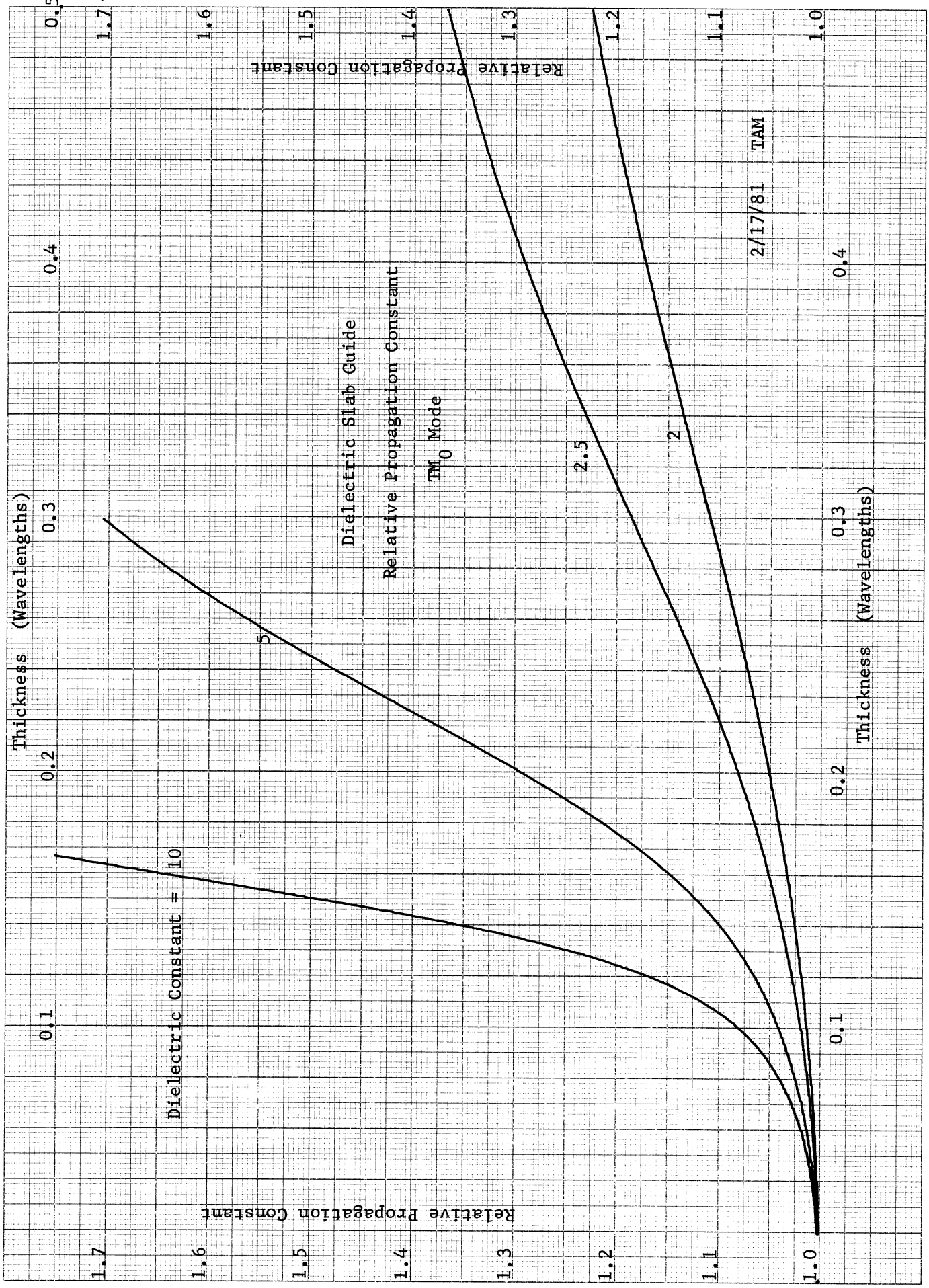

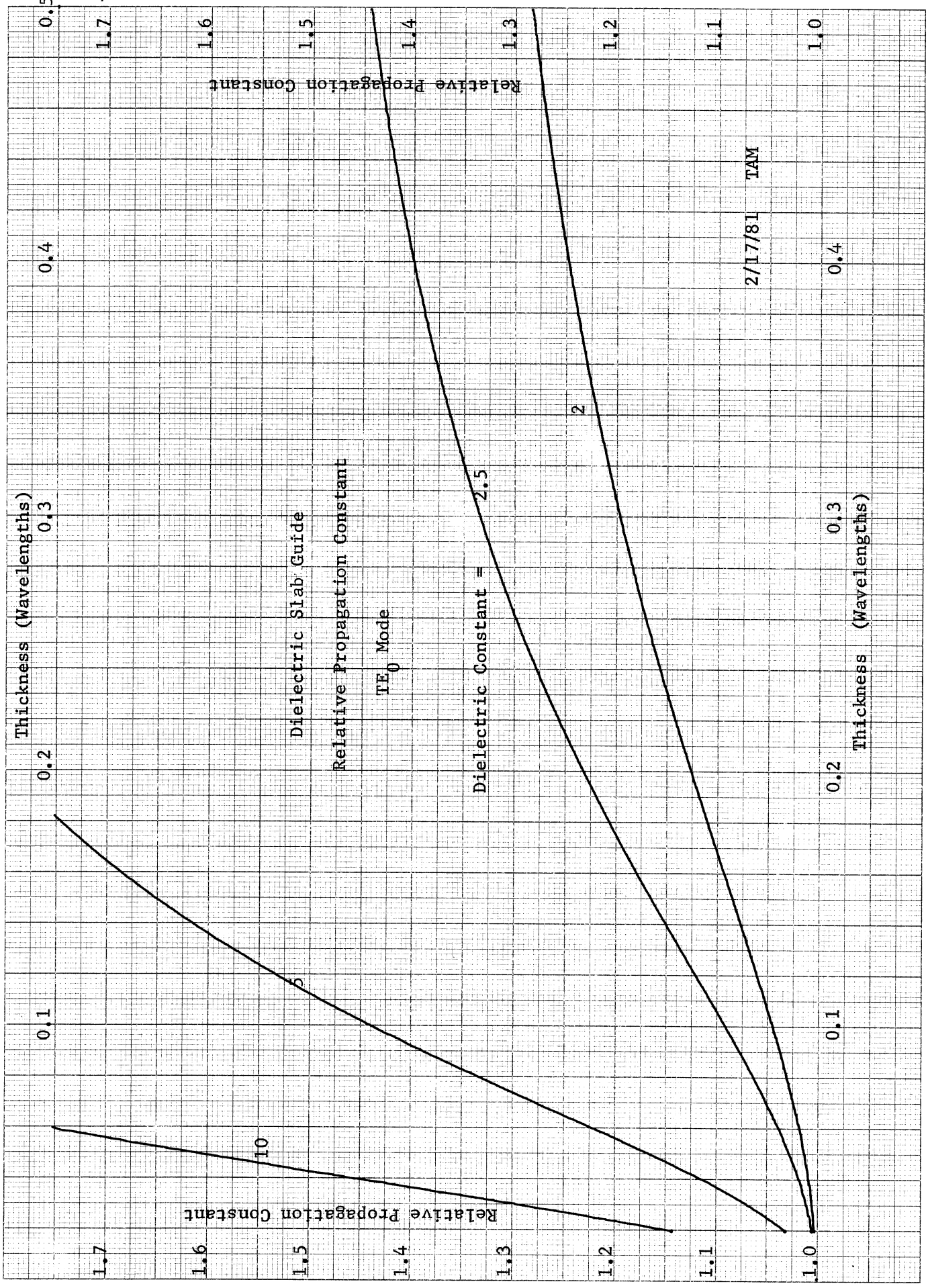

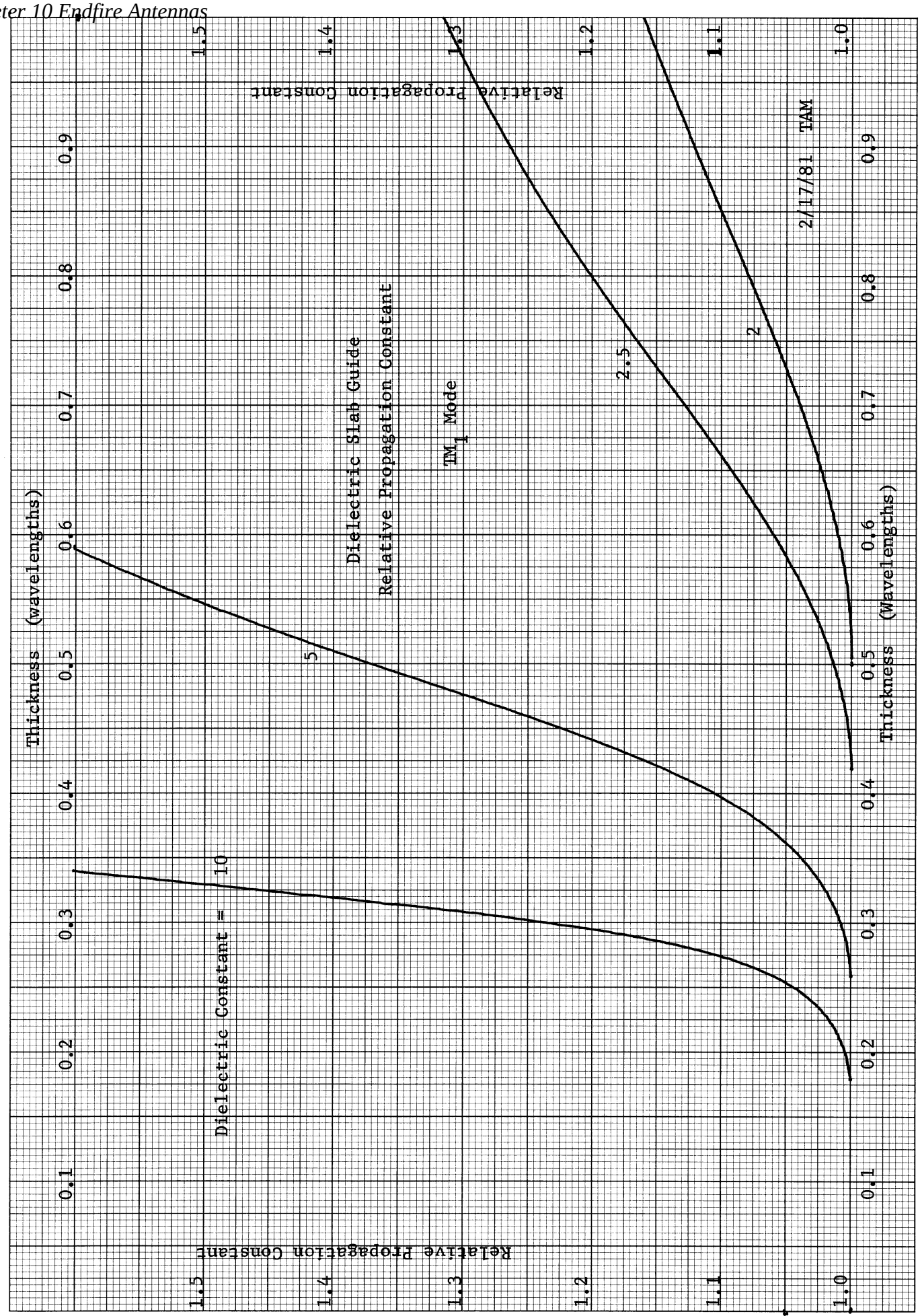

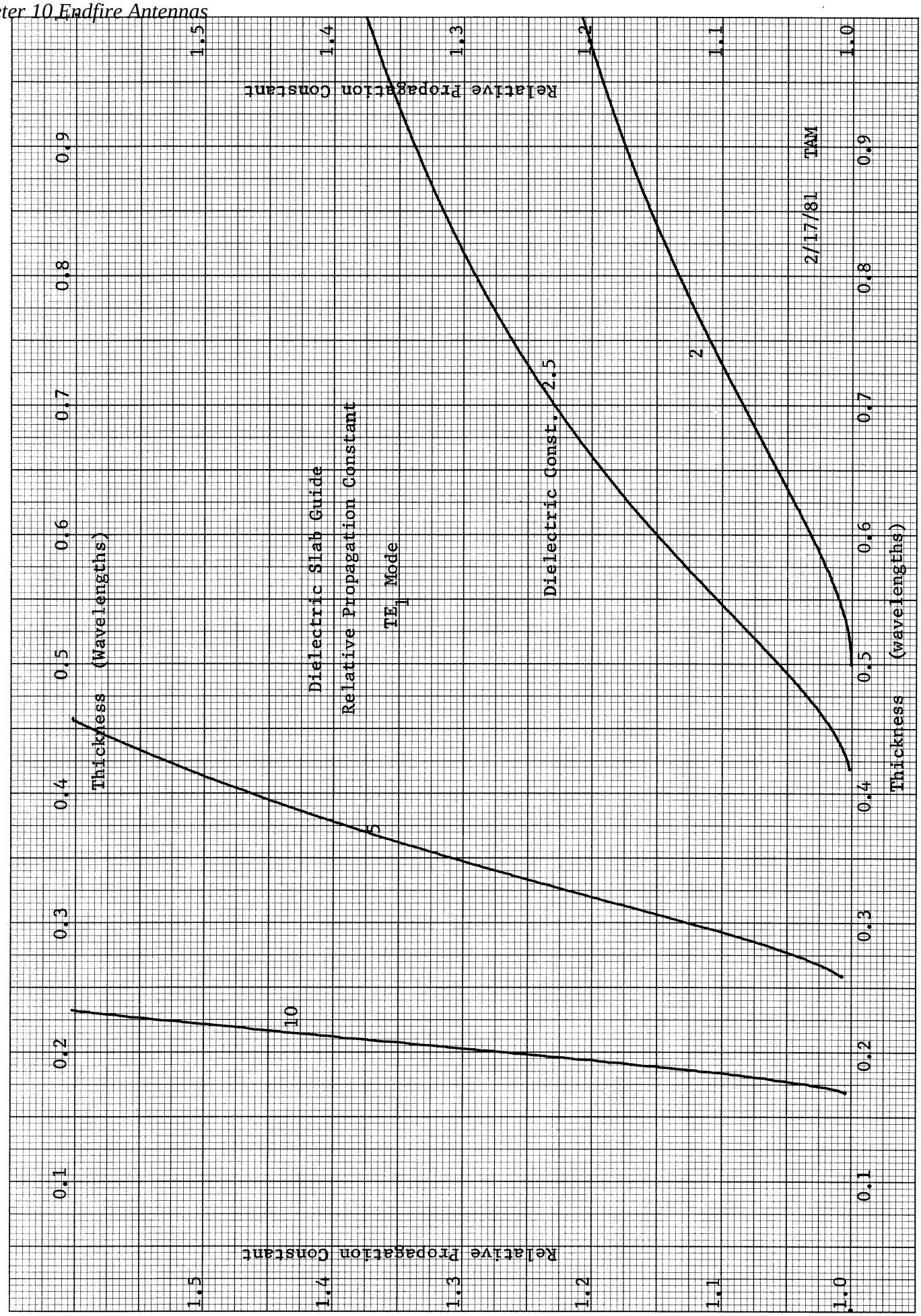

DIELECTRIC SLAB ON A GROUND PLANE

Suppose we have a dielectric slab on a ground plane whose thickness is a/2.

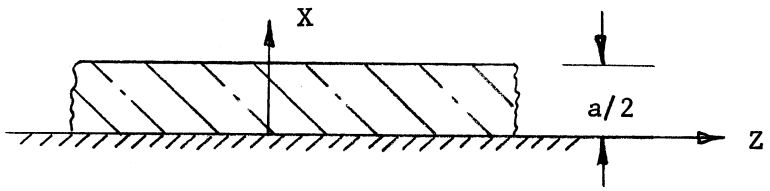

The thickness was picked to be a/2 so that the results of the full slab may be applied to this case. We have the requirement that the tangential electric field must be zero on the ground plane.

TE Solution

From page 365 the tangential electric field is the Y component. In the slab the fields are given by

$$E_{y_2} = \left(\pm\right) A_2 \frac{2\pi P_x}{\lambda} \left\{ \begin{matrix} \cos\left(\frac{2\pi P_x}{\lambda} x\right) \\ \sin\left(\frac{2\pi P_x}{\lambda} x\right) \end{matrix} \right\} e^{-j\beta_z z}$$

The requirement is that $E_y = 0$ at $X = 0$; hence we can only use the even solution for the scalar potential. The equation for the separation constant, (πP_x a/λ) becomes

$$\sqrt{\left(\frac{\pi a}{\lambda}\right)^2 \left(\frac{\epsilon_1 \mu_1}{\epsilon_0 \mu_0} - 1\right) - \left(\frac{\pi P_x a}{\lambda}\right)^2} = -\frac{\mu_0}{\mu_1} \left(\frac{\pi P_x a}{\lambda}\right) \cot\left(\frac{\pi P_x a}{\lambda}\right)$$

and the cutoff wavelengths are given by

$$\lambda_c = \frac{2a}{n} \sqrt{\frac{\epsilon_1 \mu_1}{\epsilon_0 \mu_0} - 1} \qquad n = 1, 3, 5, 7, \ldots$$

The slab will only support a TE mode (horizontally polarized) if the slab is thick enough.

TM Solution

The tangential electric field in the dielectric slab is the Z component which is given on page 366.

$$E_{z_2} = \left(\frac{2\pi P_x}{\lambda}\right)^2 \frac{A_2}{j\omega\epsilon_1} \left\{ \begin{matrix} \sin\left(\frac{2\pi P_x}{\lambda} x\right) \\ \cos\left(\frac{2\pi P_x}{\lambda} x\right) \end{matrix} \right\} e^{-j\beta_z z}$$

This electric field is zero at X = 0 which restricts the scalar potential to an odd function. The equation for the separation constant, (πP_x a/λ) becomes

$$\sqrt{\left(\frac{\pi a}{\lambda}\right)^2 \left(\frac{\epsilon_1 \mu_1}{\epsilon_0 \mu_0} - 1\right) - \left(\frac{\pi P_x a}{\lambda}\right)^2} = \frac{\epsilon_0}{\epsilon_1} \left(\frac{\pi P_x a}{\lambda}\right) \tan\left(\frac{\pi P_x a}{\lambda}\right)$$

and the cutoff wavelengths are given by $\lambda_c = \frac{2a}{n} \sqrt{\frac{\epsilon_1 \mu_1}{\epsilon_0 \mu_0} - 1} \qquad n = 0, 2, 4, \ldots$

The slab will support a TM mode (vertically polarized) to zero frequency.

The dielectric slab cases can be summarized.

1) A free standing slab will support TE modes (horizontally polarized) and TM modes (vertically polarized) to zero frequency.

2) A slab backed by a ground plane will support a TM (vertically polarized) solution to zero frequency, but a TE (horizontally polarized) solution has a finite cutoff wavelength.

EXCITATION OF DIELECTRIC SLAB GUIDES

The dielectric slab guide may be excited by a passing wave. The possible mode that will be excited depends on the incident fields. We need to expand the fields on both sides of the slab guide to determine the requirements of the excitation wave. The scalar potential function for the solutions are given on page 364.

$$\psi_1 = A_1 e^{-\frac{2\pi b}{\lambda}x} e^{-j\beta_3 z}$$

$$\psi_2 = A_2 \left\{ \begin{matrix} \sin\left(\frac{2\pi p_x x}{\lambda}\right) \\ \cos\left(\frac{2\pi p_x x}{\lambda}\right) \end{matrix} \right\} e^{-j\beta_z z}$$

$$\psi_3 = (\pm) A_1 e^{\frac{2\pi b}{\lambda}x} e^{-j\beta_z z}$$

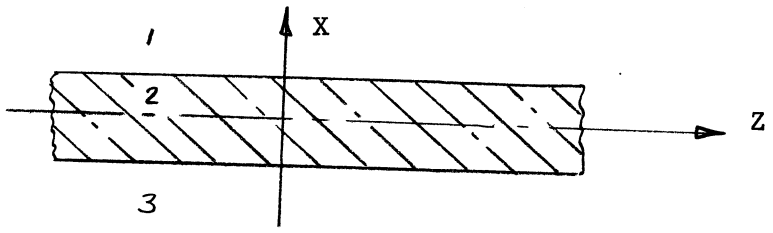

TE Fields: These fields are horizontally polarized to the plane of the slab and are given by

$$E_y = \frac{\partial \psi}{\partial x}$$

$$E_{y1} = -\frac{2\pi b}{\lambda} A_1 e^{-\frac{2\pi b}{\lambda}x} e^{-j\beta_z z}$$

$$E_{y3} = (\pm)\frac{2\pi b}{\lambda} A_1 e^{\frac{2\pi b}{\lambda}x} e^{-j\beta_z z}$$

The odd mode solution requires that the excitation fields be 180° out of phase on different sides of the slab. The possible n of the mode comes from the

set (0, 2, 4,...). This includes the zero order mode which has no low frequency cutoff. The mode may be fed out a waveguide in the TE_{20} mode.

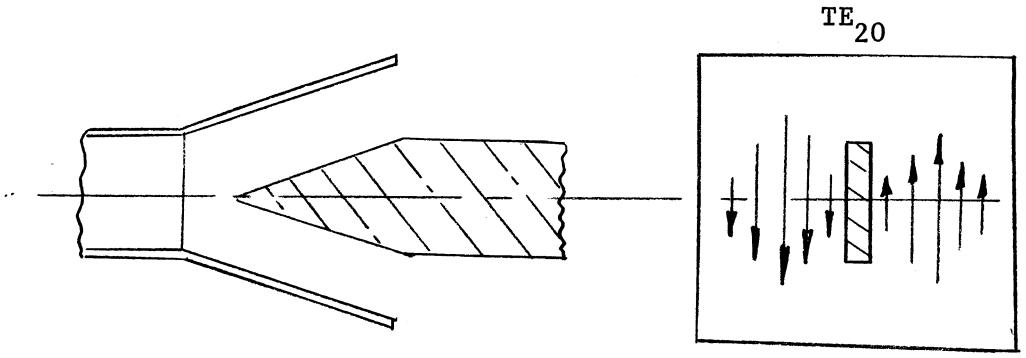

TE_n Mode in Dielectric n = 0, 2, 4, ...

The pattern of the traveling wave antenna will have a null on axis like the traveling wave current patterns on page 164 and like the TE_{20} mode given on page 244.

Consider the even mode solution. There are equal horizontally polarized fields on both sides of the slab. A waveguide may excite this mode with the TE_{10} mode.

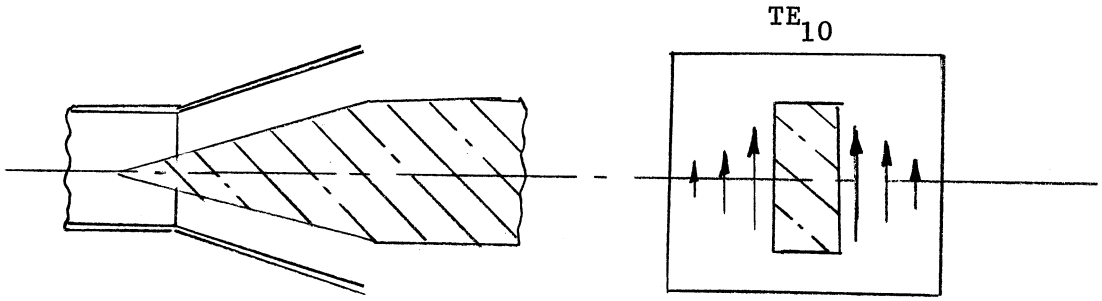

TE_n Mode in Dielectric n = 1, 3, 5, ...

The slab must be thick enough to support the TE_1 mode which is determined from the curves on page 375.

TM Fields: These fields are vertically polarized with respect to the plane of the slab. We can expand the electric fields in the upper and lower regions.

$$E_x = \frac{1}{j\omega\epsilon}\frac{\partial^2\psi}{\partial x \partial z}$$

$$E_{x_1} = \frac{\beta_z}{\omega\epsilon_0}\left(\frac{2\pi b}{\lambda}\right)A_1 e^{-\frac{2\pi b}{\lambda}x} e^{-j\beta_z z} \qquad \text{Region 1}$$

$$E_{x_3} = \left(\mp\right)\frac{\beta_z}{\omega\epsilon_0}\left(\frac{2\pi b}{\lambda}\right)A_1 e^{\frac{2\pi b}{\lambda}x} e^{-j\beta_z z} \qquad \text{Region 3}$$

The even mode solution requires that the electric field be in the same direction on both sides of the slab. We can achieve this by feeding with a waveguide in the TE_{10} mode.

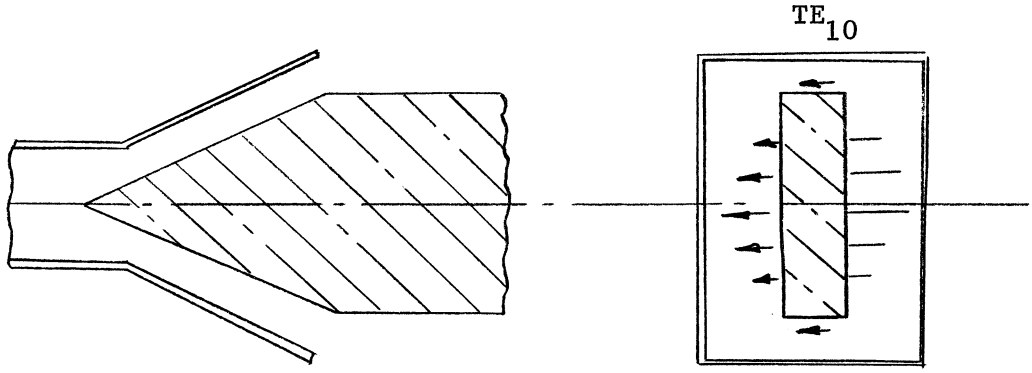

TM_n Mode in the Dielectric $n = 1, 3, 5, \ldots$

These correspond to the solutions given on page 374 and requires that the slab be thick enough to support the modes $n = 1, 3, 5, \ldots$.

The odd mode solutions can support waves without a cutoff frequency, but the fields are in opposite directions on the opposite sides of the slab. We can feed the slab with a waveguide in the TE_{02} mode which will give us a null on axis.

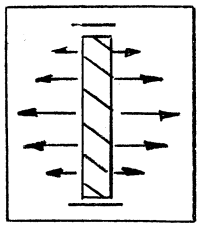

TE_{02} Mode in Waveguide

TM_n Mode in Dielectric $n = 0, 2, \ldots$

SLABS ON GROUND PLANES

We can also excite slabs on ground planes. The most common configuration is a TM_o solution because a thin dielectric can be excited on a ground plane by a vertically polarized wave since there is no low frequency cutoff for this wave. Remember that below cutoff, the wave is not bound to the dielectric. In a similiar manner we can excite TE modes on a grounded slab. The slab must be thick enough to support the wave.

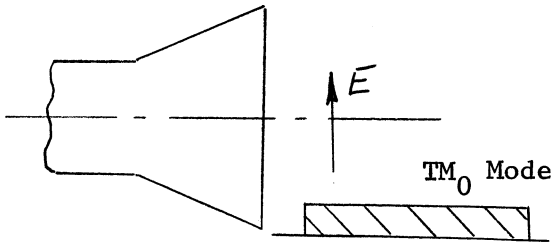

TM_0 Mode in the Dielectric

CORRUGATED CONDUCTOR

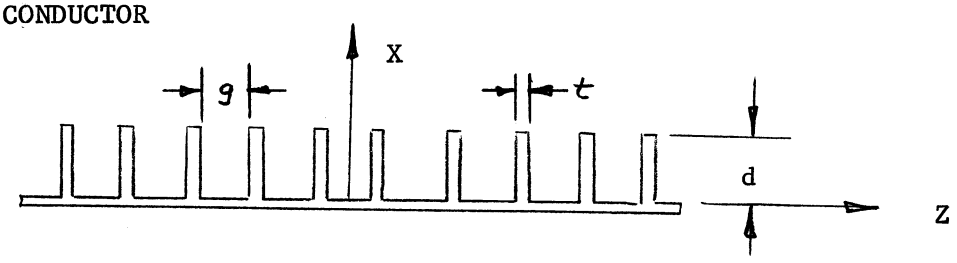

A corrugated surface can support TM surface waves if the depth, d, of the slots is less than $\lambda/4$. These fields are similiar to the TM fields on page 366 of the dielectric slab guide on a ground plane. They are vertically polarized with respect to the Y-Z plane.

$$E_x = \frac{1}{j\omega\epsilon}\frac{\partial^2\psi}{\partial x \partial z} \qquad H_x = 0$$

$$E_y = 0 \qquad H_y = -\frac{\partial\psi}{\partial x}$$

$$E_z = \frac{1}{j\omega\epsilon}(\beta^2 - \beta_z^2)\psi \qquad H_z = 0$$

This is a suitable solution since the corrugations will short out any E_y field at the corrugations. We have assumed that there are many corrugations per wavelength and that the corrugations are thin. We will use the same scalar potential function given on page 364.

$$\psi_1 = A_1 e^{-\frac{2\pi b}{\lambda}x} e^{-j\beta_z z} \qquad \text{Above Corrugations}$$

$$E_x = \frac{2\pi b}{\lambda}\frac{\beta_z A_1}{j\omega\epsilon} e^{-\frac{2\pi b}{\lambda}x} e^{-j\beta_z z}$$

$$E_z = -\left(\frac{2\pi b}{\lambda}\right)^2 \frac{A_1}{j\omega\epsilon} e^{-\frac{2\pi b}{\lambda}x} e^{-j\beta_z z}$$

$$H_y = \frac{2\pi b}{\lambda} A_1 e^{-\frac{2\pi b}{\lambda}x} e^{-j\beta_z z}$$

From these expressions we can find a -X directed wave impedance looking into the corrugated surface.

$$Z_{-x} = \frac{E_z}{H_y} = \frac{j\left(\frac{2\pi b}{\lambda}\right)}{\omega\epsilon_0} = j\frac{\left(\frac{2\pi b}{\lambda}\right)\sqrt{\mu_0}}{\omega\epsilon_0\sqrt{\mu_0}}$$

The surface must present this impedance to support the surface waves.

$$\beta = \omega\sqrt{\mu_0\epsilon_0} \qquad \eta = \sqrt{\frac{\mu_0}{\epsilon_0}} \qquad Z_{-x} = j\frac{\left(\frac{2\pi b}{\lambda}\right)\eta_0\lambda}{2\pi} = jb\eta_0$$

Looking into the corrugated surface, we see a series of parallel plate wave-

guides. The wave impedance per unit length of this structure is

$$Z_{-x} = j\eta_0 \tan \beta_0 d$$

When we equate these wave impedances, we get the result

$$b = \tan \beta_0 d$$

The relative propagation constant, P, is found from the equation on page 369.

$$P = \sqrt{1 + \tan^2 \beta_0 d}$$

As an approximation we can allow for the thickness of the corrugations. If the thickness of the corrugations is t and the gap is g, then we can assume that the impedance of the edge of the corrugations is zero and average the impedance of the edges and gaps. The impedance looking into the corrugated surface is then

$$Z_{-x} = j \frac{\eta_0 g}{(g+t)} \tan \beta_0 d$$

The relative propagation constant becomes

$$P = \sqrt{1 + \left(\frac{g}{g+t}\right)^2 \tan^2 \beta_0 d}$$

This function is plotted on page 382 for various thickness to gap ratios. As the height of the corrugations increases the waves become more and more bound to the surface. When $\beta_0 d$ approaches $\pi/2$, the attenuation constant of the external fields, α, approaches infinity and the fields will be zero a short distance from the corrugations. This is the case for corrugated horns; the fields were zero at the corrugated surface.

TE FIELDS ON A CORRUGATED SURFACE

Will a corrugated surface support a horizontally polarized wave? Consider the TE mode solution given on page 365 of the dielectric slab guide. It has a Y component which would be shorted out by the corrugations. This will not do. Let us try rotating the corrugated surface so that the corrugations run in the Z axis direction. Now the E_y is not shorted out by the corrugations but supported by a parallel plate waveguide system. The fields above the corrugated surface are given by:

$$E_y = -A_1 \frac{2\pi b}{\lambda} e^{-\frac{2\pi b}{\lambda} x} e^{-j\beta_z z}$$

$$H_z = -\left(\frac{2\pi b}{\lambda}\right)^2 \frac{A_1}{j\omega\mu_0} e^{-\frac{2\pi b}{\lambda} x} e^{-j\beta_z z}$$

The wave impedance looking into the corrugated surface is given as

$$Z_{-x} = \frac{-E_y}{H_z} = -j\omega\mu_0 \left(\frac{\lambda}{2\pi b}\right)$$

$$= -j \frac{\omega \sqrt{\mu_0 \epsilon_0} \sqrt{\mu_0}}{\sqrt{\epsilon_0}} \left(\frac{\lambda}{2\pi b}\right) = -j\frac{\eta_0}{b}$$

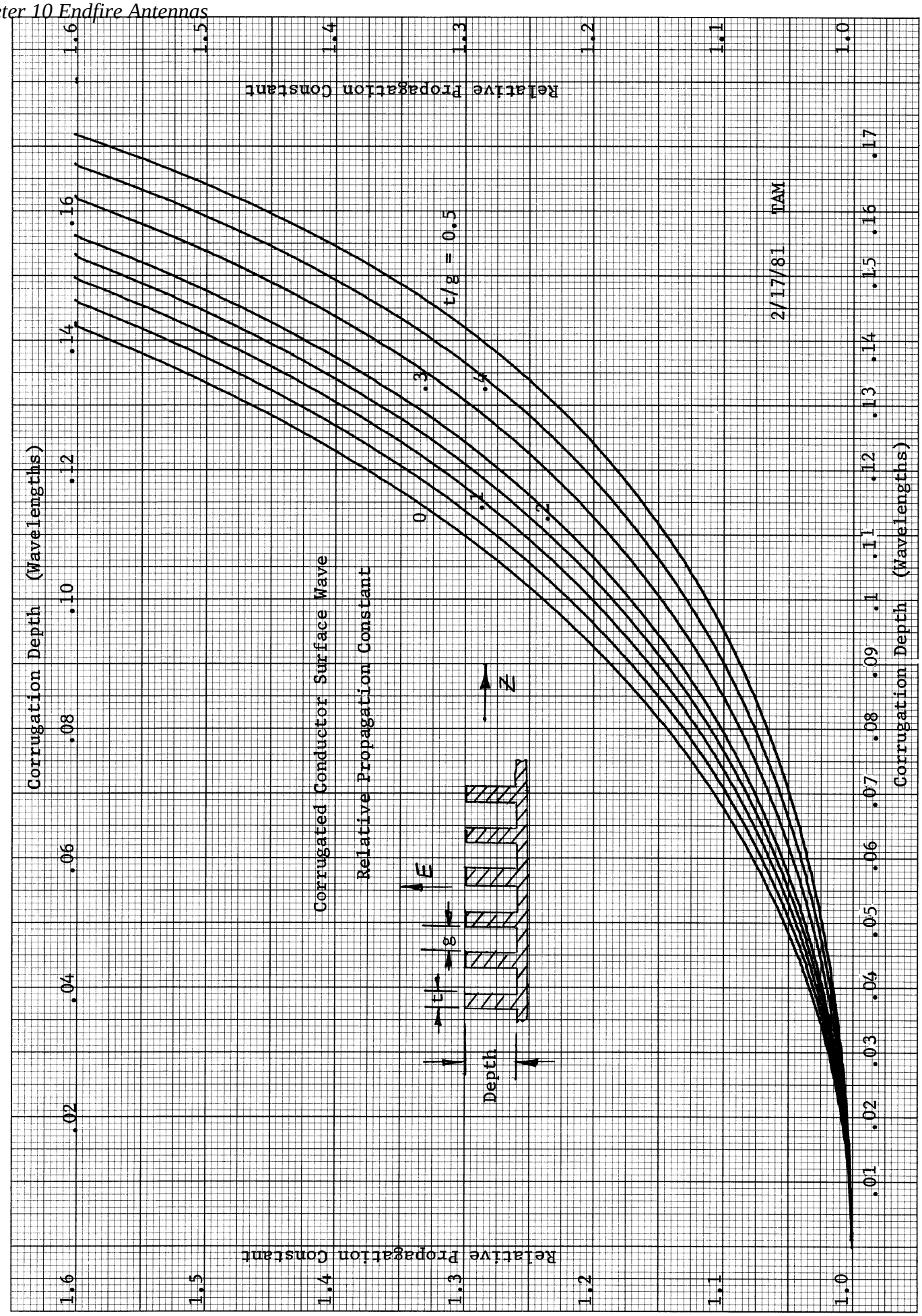

The impedance of the corrugated surface is still given by

$$Z_{-x} = j\eta_0 \tan \beta_0 d$$

This is negative only if $\pi/2 < \beta_0 d < \pi$.

$$b = -\cot \beta_0 d$$

The relative propagation constant is given by

$$P = \sqrt{1 + \cot^2 \beta_0 d}$$

When we average the impedance between the gaps and corrugation thickness, t, the relative propagation constant becomes

$$P = \sqrt{1 + \left(\frac{g+t}{g}\right)^2 \cot^2 \beta_0 d}$$

This is plotted on page 384 for various thickness to gap ratios. The depth of the corrugations must be greater than a quarter wavelength before the surface wave is supported.

PARALLEL STRIPS

Suppose we have a series of parallel conducting strips instead of the corrugated conductor.

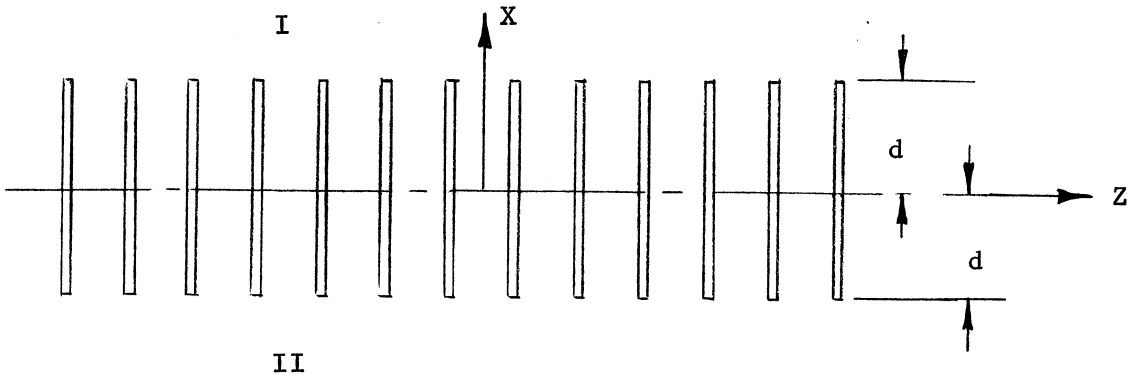

Space has been divided into the regions above and below the parallel plates. There are two possible solutions to this problem.

$$\psi_{II} = (\pm)\, \psi_I\, e^{\frac{4\pi b x}{\lambda}}$$

This structure can only support TM waves whose electric field is perpendicular to the top and bottom planes along the edges of the strips which short out any E_y. The solution in region I is given on page 380 for the corrugated conductor.

$$\psi_I = A_1 e^{-\frac{2\pi b}{\lambda} x} e^{-j\beta_z z}$$

$$E_{x_1} = \frac{2\pi b}{\lambda} \beta_z A_1 e^{-\frac{2\pi b}{\lambda} x} e^{-j\beta_z z}$$

$$E_{z_1} = -\left(\frac{2\pi b}{\lambda}\right)^2 \frac{A_1}{j\omega\epsilon_0} e^{-\frac{2\pi b x}{\lambda}} e^{-j\beta_z z}$$

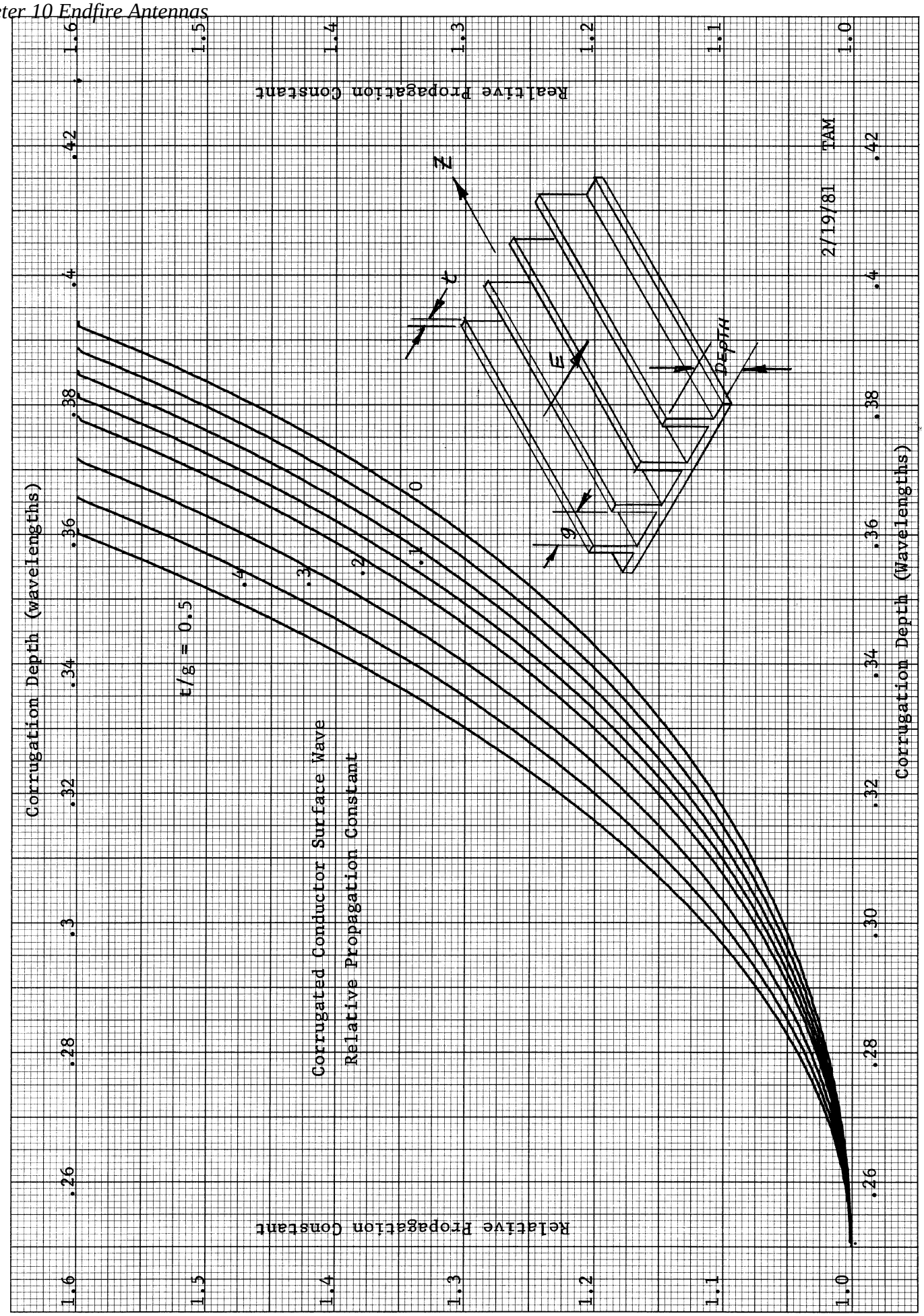

The fields in region II are given as

$$\psi_{II} = (\pm) A_2 e^{+\frac{2\pi b}{\lambda}x} e^{-j\beta_z z}$$

$$E_{x_2} = \left(\frac{-}{+}\right) \frac{2\pi b}{\lambda} \frac{\beta_z A_2}{j\omega\epsilon} e^{\frac{2\pi b}{\lambda}x} e^{-j\beta_z z}$$

$$E_{z_2} = \left(\frac{-}{+}\right)\left(\frac{2\pi b}{\lambda}\right)^2 \frac{A_2}{j\omega\epsilon} e^{\frac{2\pi b}{\lambda}x} e^{-j\beta_z z}$$

Consider the even mode case, i.e. $\psi_I = \psi_{II} e^{\frac{4\pi b}{\lambda}x}$. The electric fields across the gaps are the same at both ends. This gives us a magnetic wall at the center line of the strips. In the circuit model the magnetic wall is a virtual open circuit. The impedance looking into the strips to support this wave is still

$$z_{-x} = j b \eta_0$$

The parallel plate structure gives an impedance per unit length of

$$z_{-x} = -j \eta_0 \cot \beta_0 d$$

from the open circuit. This is negative only if $\pi/2 < \beta_0 d < \pi$.

$$b = -\cot \beta_0 d$$

The relative propagation constant is given by

$$P = \sqrt{1 + \cot^2 \beta_0 d}$$

This is the same as the TE mode case for the corrugated conductor. The solutions curves are given on page 384 using the dimension d given in the figure above which is half the width of the strips. The strips must be greater than a half wavelength long and less than one wavelength plus any integer multiple of wavelengths.

The odd mode case, $\psi_I = -\psi_{II} e^{\frac{4\pi}{d}x}$, has equal and opposite electric fields across the gaps. There will be an electric wall (short circuit) at the center line of the strips. This is exactly the case of the corrugated conductor which is given on page 380. The solution curve is given on page 382 where the depth is taken as half the strip width. The width of the strips must be less than a half wavelength plus any integer multiple of a wavelength.

TE MODES ON PARALLEL STRIPS

If we want to support TE waves on some parallel strips, we must rotate the strips so that they are parallel to the Z axis like the corrugated conductor.

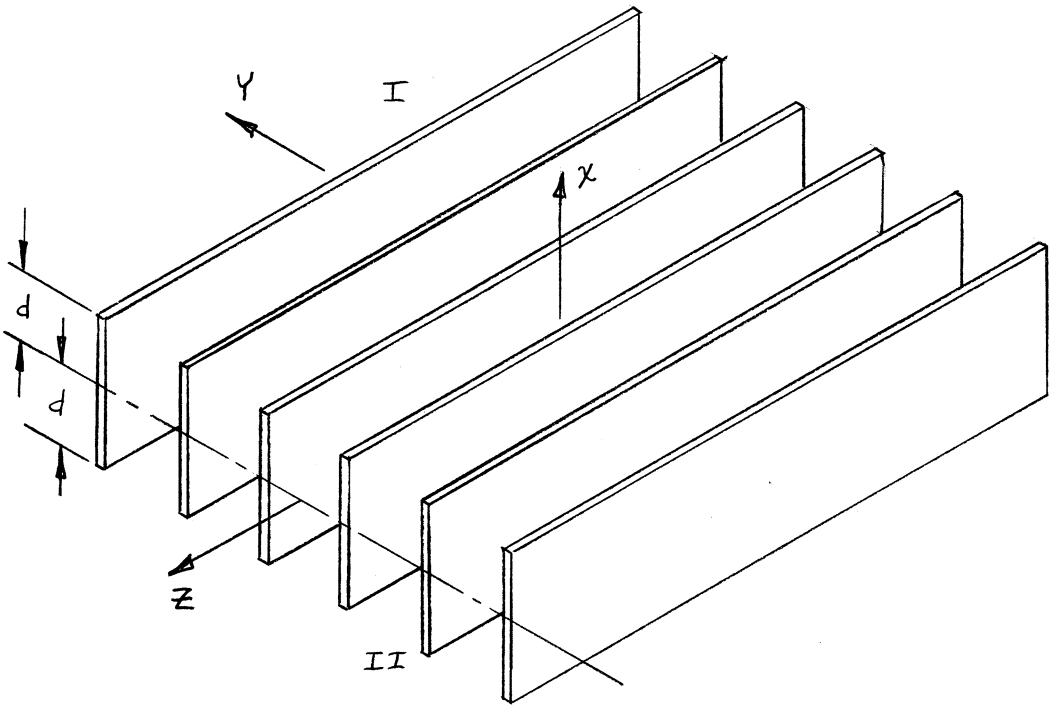

Similiar to the TM mode case, there are two possible solutions

$$\psi_{II} = (\pm)\,\psi_I\, e^{\frac{4\pi d}{\lambda}}$$

The solution in region I is the same as for the corrugated conductor. In region II we will have either the even or odd mode solution.

$$\psi_I = A_1\, e^{-\frac{2\pi b}{\lambda}x}\, e^{-j\beta_z z}$$

$$E_{y1} = -A_1 \frac{2\pi b}{\lambda}\, e^{-\frac{2\pi b}{\lambda}x}\, e^{-j\beta_z z}$$

$$H_{z1} = -\left(\frac{2\pi b}{\lambda}\right)^2 \frac{A_1}{j\omega\mu_0}\, e^{-\frac{2\pi b}{\lambda}x}\, e^{-j\beta_z z}$$

$$\psi_{II} = (\pm)A_1\, e^{\frac{2\pi b}{\lambda}x}\, e^{-j\beta_z z}$$

$$E_{y2} = (\pm)A_1\, e^{\frac{2\pi b}{\lambda}x}\, e^{-j\beta_z z}$$

$$H_{z2} = (\mp)\frac{A_1}{j\omega\mu_0}\, e^{\frac{2\pi b}{\lambda}x}\, e^{-j\beta_z z}$$

Let us take the odd mode of the scalar potential case first. The electric field on both sides of the strips are equal giving a magnetic wall (open circuit) at the plane of the center line of the strips. The impedance looking into the parallel strips to support the mode is

$$Z_{-x} = \frac{-E_y}{H_z} = -j\omega\mu_0\left(\frac{\lambda}{2\pi b}\right) = -j\frac{\eta_0}{b}$$

The impedance of the strips with an open circuit at the center line is

$$z_{-x} = -j\eta_0 \cot \beta_0 d$$

Hence, b = tan(β_0d) which is positive for $d < \lambda/4$. The strips are less than a half wavelength plus any integer multiple of a wavelength. The relative propagation constant is given by

$$P = \sqrt{1 + \tan^2 \beta_0 d}$$

This function is plotted on page 382 where the half strip width is used for the corrugation depth.

The even mode of the scalar potential has a virtual short circuit at the center line plane which gives us the same problem as the corrugated conductor. We can use the solution given on page 381 and the curve on page 384 to find the relative propagation constant.

Excitation of Parallel Strip Slow Wave Guide

We can feed these parallel strip surface wave structures from waveguides similiar to the dielectric slab guide. Once we have identified the similiarity of the modes, we can use the information on page 377 for dielectric slabs to dtermine the feeding waveguide mode.

TM Mode Strips

The TM mode is vertically polarized with respect to the plane of the corrugated edges. It is the same as the TM mode in the dielectric slab. The even mode in the strips corresponds to the even order modes of the dielectric slab. This may be fed from a waveguide in the TE_{02} mode as shown on page 379. The strip width must be greater than a half wavelength. The odd mode in the strips will correspond to the odd mode in the dielectric, therefore it can be fed from a waveguide in the TE_{10} mode as shown on page 379.

TE Mode Strips

The TE mode is horizontally polarized with respect to the plane of the corrugation edges. When we compare the fields on both sides of the series of strips with that on both sides of the TE mode dielectric slabs, we find that the even scalar mode also corresponds to the even order mode in the TE mode dielectric slab. Likewise, the odd modes will match. The odd order mode can be fed from a waveguide in the TE_{10} mode as shown on page 378 for the dielectric slab. The strips are less than a half wavelength wide for the odd mode. The even mode can be fed as shown on the top of page 378 with the waveguide in the TE_{20} mode.

Corrugated Conductors

The corrugated conductor can be placed on a ground plane as shown on page 379 with the dielectric slab. The most used configuration is the TM mode corrugated slab which are placed in the E plane of a horn as shown in the figure. The corrugation must be less than a quarter wavelength deep.

SLAB SURFACE WAVE RESULTS

In order to understand the effects of surface waves on a ground plane, experiments were performed on a grounded dielectric slab fed as shown on the bottom of page 379. A ground plane was placed under the E plane aperture of a small horn which had a 0.095 wavelength thick dielectric slab on it with a dielectric constant of 2.4. We can find the relative propagation constant from the chart on page 372 by using twice the dielectric thickness (grounded slab). The relative propagation constant is 1.065. For every wavelength along the slab the phase increases (0.065)(360) = 23.4 degrees over that which it would in free space.

The surface wave structure will capture some of the energy from the horn aperture, slow it down and radiate it at the end. We can think of a new aperture at the end of the dielectric slab.

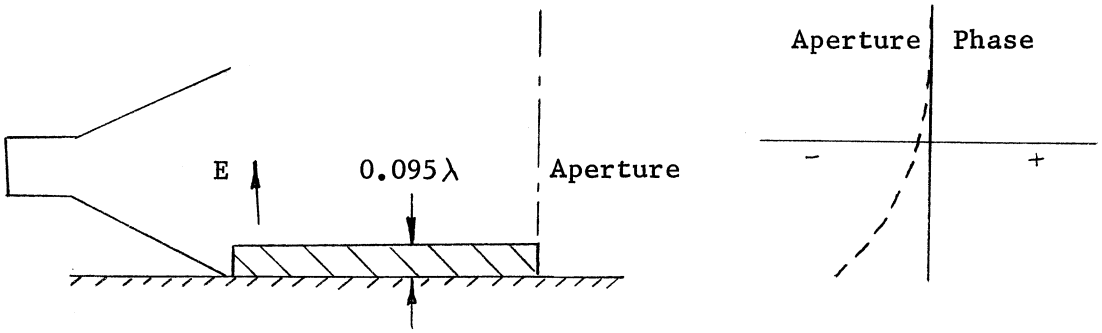

The phase of the signal in the aperture above is the vector combination of the retarded phase energy in the surface wave which is decreasing exponentially from the surface and the free space energy (not bound to the dielectric). The thinner the dielectric slab, the more equal to one is the relative propagation constant and the more the bound fields extend away from the surface (see curve on page 363). On the other hand the slab must be longer and longer to get the same phase shift as the thickness becomes thinner and thinner. The resulting phase will tilt the beam towards the ground plane.

The small horn was placed on a ground plane and the E plane pattern on page 389 was obtained. The beam points up and away from the ground plane. A grounded slab which gave an excess phase shift of 45 degrees was placed in front of the horn and the pattern on page 390 was obtained. The beam has started to bend back toward the ground plane. Then the dielectric slab length was increased until the excess phase shift was 90 degrees. The pattern response is given on page 391. It has a narrowed beam and pointed more towards the ground plane. These surface wave structures can be used to make the wave hug the ground plane instead of pointing up as on page 389. We are using a combination of the direct wave and the surface wave to tilt the beam. If the of the dielectric slab is increased until the excess length is 180 degrees, then the pattern will have a null when the energy in both waves is close to equal.

Let us estimate the ratio of the direct wave to the surface wave by the following argument. The bound surface wave will extend out from the surface and decrease exponentially. The aperture field is assumed to be uniform and the field not in the surface wave will be in the direct wave. We will match the

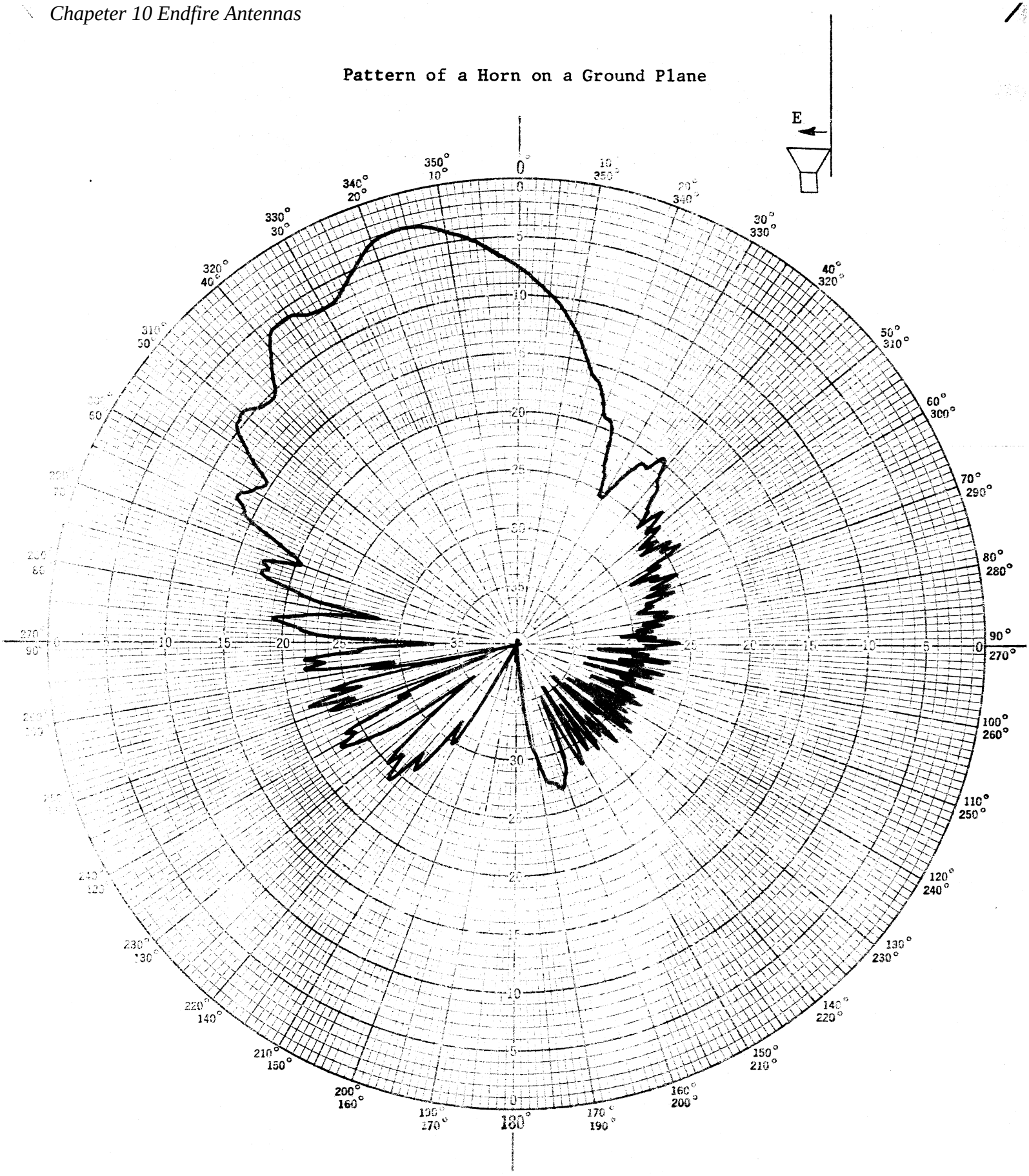

Pattern of a Horn on a Ground Plane with a 45° Excess Phase Shift Surface Wave Slab on the Ground Plane

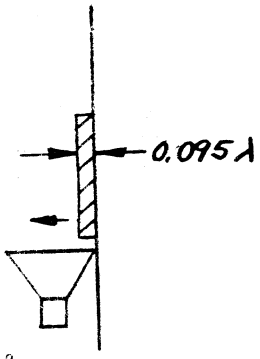

Polar Chart No. 127D
SCIENTIFIC-ATLANTA, INC.
ATLANTA, GEORGIA

Pattern of a Horn on a Ground Plane with a 90° Excess

Phase Shift Surface Wave Slab on the Ground Plane

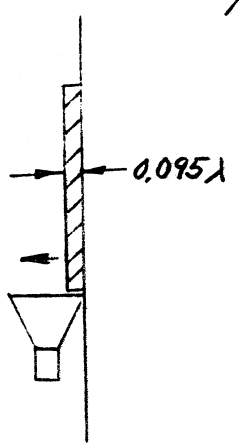

Polar Chart No. 127D
SCIENTIFIC-ATLANTA, INC.
ATLANTA, GEORGIA

the fields in the aperture.

Division of the Field

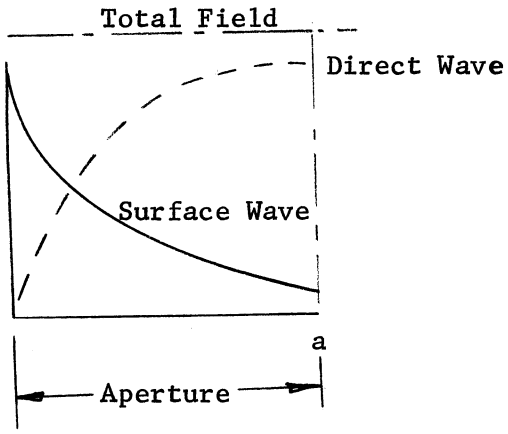

The field in the surface wave will be given by the integral

$$\int_0^a e^{-\alpha x} dx = \frac{1}{\alpha}\left(1 - e^{-\alpha a}\right)$$

$$a = \frac{2\pi}{\lambda}\sqrt{P^2 - 1}$$

The total available field in the aperture is the width of the aperture times the total field which is normalized to one. The portion of the wave in the surface wave is given by:

$$\text{Capture Efficiency} = \frac{\left(1 - e^{-\alpha a}\right)}{\alpha a}$$

$$= \frac{\left(1 - e^{-\frac{2\pi a}{\lambda}\sqrt{P^2 - 1}}\right)}{\frac{2\pi a}{\lambda}\sqrt{P^2 - 1}}$$

This function is plotted on page 393. The assumption has been made that the surface wave device is on the edge of the aperture. When it extends into the aperture, it will capture more of the energy from the aperture.

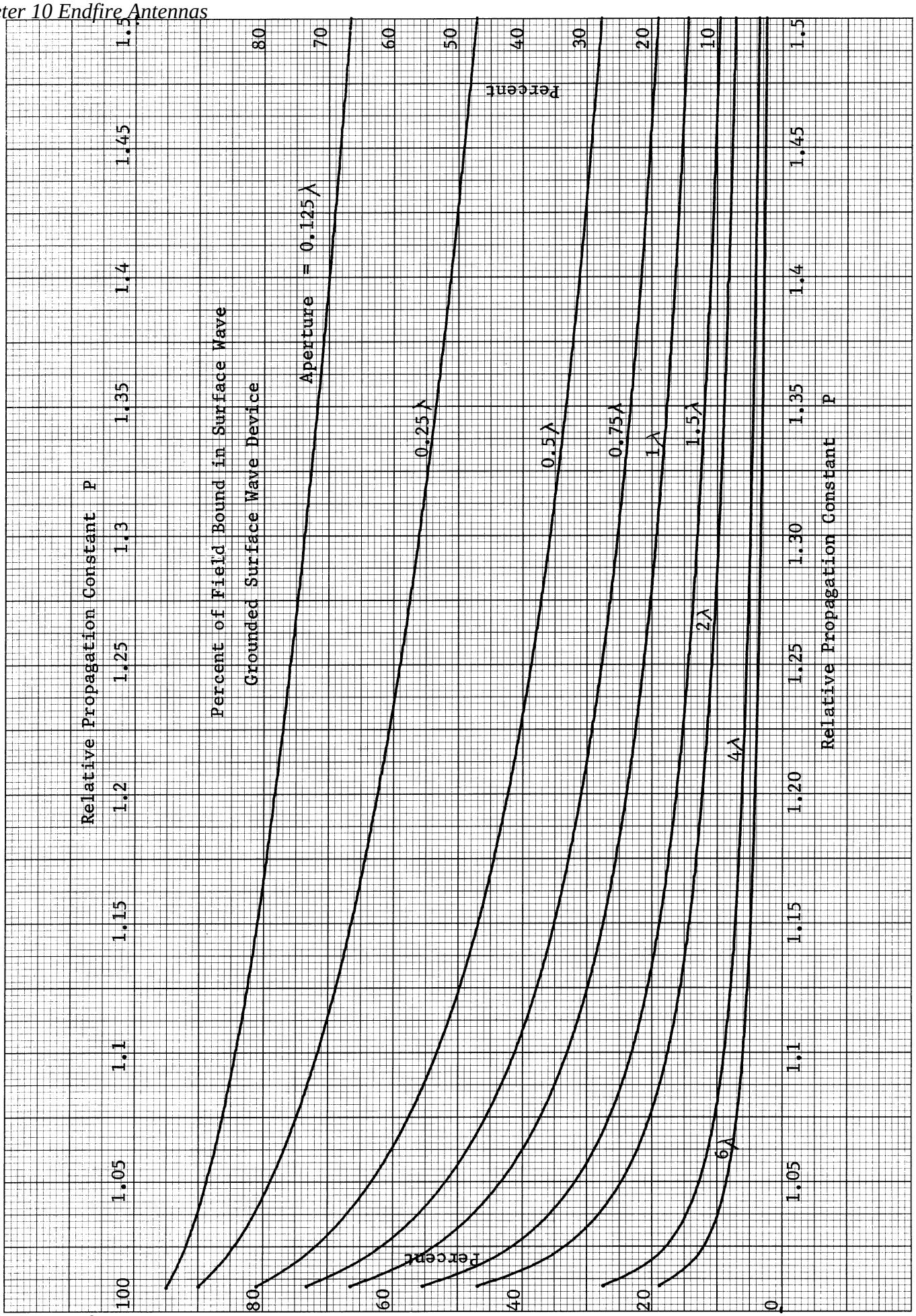

CYLINDRICAL SURFACE WAVE STRUCTURES

We can solve for surface waves on cylindrical structures. This requires a function that decreases exponentially with increasing ρ. On page 257 we introduced the Hankel function $H_n^{(2)}(\beta_\rho \rho)$ which is a traveling wave function similiar to $e^{-j\beta_\rho \rho}$.

For plane waves in rectangular coordinates we made the following substitution:

$$\alpha = -j\beta$$

to obtain an exponentially decreasing function. This substitution gives the modified Bessel function of the second kind in cylindrical coordinates.

$$K_n(\alpha\rho) = \frac{\pi}{2}(-j)^{n+1} H_n^{(2)}(-j\alpha\rho)$$

The function is approximately $\frac{e^{-\alpha\rho}}{\sqrt{\pi\rho}}$ for large arguments.

We will expand the scalar potentials in the two regions I and II to obtain the fields and match the propagation constant and tangential fields across the boundary.

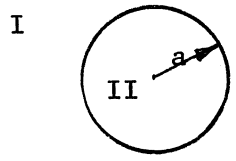

DIELECTRIC CYLINDER

A dielectric cylinder can support surface waves and bind the wave so that it is guided by the dielectric. We will consider TE modes and TM modes on the cylinder which have a finite cut-off frequency and then the hybrid mode which has no low frequency cut off. Remember that below cutoff the surface wave device no longer guides passing waves, but only looks like an obstacle to a passing wave.

TE Modes

A TE mode will have an electric vector potential with only a Z component for a generating function. We will divide the potential into two parts inside and outside the dielectric. The two potential functions are given as:

$$\psi_1 = K_n\left(\frac{2\pi b}{\lambda}\rho\right)\cos n\phi\, e^{-j\beta_z z} \qquad \text{Region I}$$

$$\psi_2 = J_n\left(\frac{2\pi p}{\lambda}\rho\right)\cos n\phi\, e^{-j\beta_z z} \qquad \text{Region II}$$

The modified Bessel function is used in region I so that the fields will die away exponentially from the surface so that there will not be infinite energy

in the wave. In region II the only possible solution is the Bessel function; the Neumann function is excluded because the origin is included. The fields are obtained from the following differential expressions.

$$E_\rho = -\frac{1}{\rho}\frac{\partial \psi}{\partial \phi} \qquad H_\rho = \frac{1}{j\omega\mu}\frac{\partial^2 \psi}{\partial \rho \partial z}$$

$$E_\phi = \frac{\partial \psi}{\partial \rho} \qquad H_\phi = \frac{1}{j\omega\mu}\frac{\partial^2 \psi}{\partial \phi \partial z}$$

$$H_z = \frac{1}{j\omega\mu}(\beta^2 - \beta_z^2)\psi$$

Expanding these equations, we get the following fields in the two regions.

$$E_{\rho_1} = \frac{n}{\rho} K_n\left(\frac{2\pi b}{\lambda}\rho\right) \sin n\phi \; e^{-j\beta_z z} \qquad \text{Region I}$$

$$E_{\rho_2} = \frac{n}{\rho} J_n\left(\frac{2\pi P}{\lambda}\rho\right) \sin n\phi \; e^{-j\beta_z z} \qquad \text{Region II}$$

$$E_{\phi_1} = \frac{2\pi b}{\lambda} K_n'\left(\frac{2\pi b}{\lambda}\rho\right) \cos n\phi \; e^{-j\beta_z z} \qquad \text{Region I}$$

$$E_{\phi_2} = \frac{2\pi P}{\lambda} J_n'\left(\frac{2\pi P}{\lambda}\rho\right) \cos n\phi \; e^{-j\beta_z z} \qquad \text{Region II}$$

$$H_{\rho_1} = \frac{-\beta_z}{\omega\mu_0}\left(\frac{2\pi b}{\lambda}\right) K_n'\left(\frac{2\pi b}{\lambda}\rho\right) \cos n\phi \; e^{-j\beta_z z} \qquad \text{Region I}$$

$$H_{\rho_2} = \frac{-\beta_z}{\omega\mu_1}\left(\frac{2\pi P}{\lambda}\right) J_n'\left(\frac{2\pi P}{\lambda}\rho\right) \cos n\phi \; e^{-j\beta_z z} \qquad \text{Region II}$$

$$H_{\phi_1} = \frac{n\beta_z}{\omega\mu_0} K_n\left(\frac{2\pi b}{\lambda}\rho\right) \sin n\phi \; e^{-j\beta_z z} \qquad \text{Region I}$$

$$H_{\phi_2} = \frac{n\beta_z}{\omega\mu_1} J_n\left(\frac{2\pi P}{\lambda}\rho\right) \sin n\phi \; e^{-j\beta_z z} \qquad \text{Region II}$$

$$H_{z_1} = \frac{-1}{j\omega\mu_0}\left(\frac{2\pi b}{\lambda}\right)^2 K_n\left(\frac{2\pi b}{\lambda}\rho\right) \cos n\phi \; e^{-j\beta_z z} \qquad \text{Region I}$$

$$H_{z_2} = \frac{1}{j\omega\mu_1}\left(\frac{2\pi P}{\lambda}\right)^2 J_n\left(\frac{2\pi P}{\lambda}\rho\right) \cos n\phi \; e^{-j\beta_z z} \qquad \text{Region II}$$

Now we must equate the tangential fields at the boundary between the two regions.

$$E_\phi \qquad \frac{2\pi\rho}{\lambda} J_n'\left(\frac{2\pi\rho a}{\lambda}\right) = \frac{2\pi b}{\lambda} K_n'\left(\frac{2\pi b}{\lambda} a\right)$$

$$H_z \qquad \frac{1}{\mu_1}\left(\frac{2\pi\rho}{\lambda}\right)^2 J_n\left(\frac{2\pi\rho}{\lambda} a\right) = -\frac{1}{\mu_0}\left(\frac{2\pi b}{\lambda}\right)^2 K_n\left(\frac{2\pi b}{\lambda} a\right)$$

When we divide these two equations, we get one of the equations for the two separation constants.

$$\frac{1}{\mu_1}\left(\frac{2\pi\rho}{\lambda}\right)\frac{J_n\left(\frac{2\pi\rho}{\lambda} a\right)}{J_n'\left(\frac{2\pi\rho}{\lambda} a\right)} = -\frac{1}{\mu_0}\left(\frac{2\pi b}{\lambda}\right)\frac{K_n\left(\frac{2\pi b}{\lambda} a\right)}{K_n'\left(\frac{2\pi b}{\lambda} a\right)}$$

We must also have equal H_ϕ components at the boundary which gives us a second equation.

$$\frac{n}{\mu_0} K_n\left(\frac{2\pi b}{\lambda} a\right) = \frac{n}{\mu_1} J_n\left(\frac{2\pi\rho}{\lambda} a\right)$$

The propagation constant in both regions must also be equal which gives us a third equation.

$$\left(\frac{2\pi b}{\lambda}\right)^2 = \omega^2(\epsilon_1\mu_1 - \epsilon_0\mu_0) - \left(\frac{2\pi\rho}{\lambda}\right)^2$$

We have three equations but only two unknowns. These three equations can only be satisfied simultaneously if we restrict the solution to n = 0. This eliminates one of the equations. The fields in the two regions become:

$$E_\rho = 0$$

$$E_{\phi_1} = \frac{2\pi b}{\lambda} K_0'\left(\frac{2\pi b}{\lambda}\rho\right) e^{-j\beta_z z}$$

$$E_{\phi_2} = \frac{2\pi\rho}{\lambda} J_0'\left(\frac{2\pi\rho}{\lambda}\rho\right) e^{-j\beta_z z}$$

$$H_{\rho_1} = \frac{-\beta_z}{\omega\mu_0}\left(\frac{2\pi b}{\lambda}\right) K_0'\left(\frac{2\pi b}{\lambda}\rho\right) e^{-j\beta_z z}$$

$$H_{\rho_2} = \frac{-\beta_z}{\omega\mu_1}\left(\frac{2\pi\rho}{\lambda}\right) J_0\left(\frac{2\pi\rho}{\lambda}\rho\right) e^{-j\beta_z z}$$

$$H_{z_1} = \frac{-1}{j\omega\mu_0}\left(\frac{2\pi b}{\lambda}\right)^2 K_0\left(\frac{2\pi b}{\lambda}\rho\right) e^{-j\beta_z z}$$

$$H_{z_2} = \frac{1}{j\omega\mu_1}\left(\frac{2\pi\rho}{\lambda}\right)^2 J_0\left(\frac{2\pi\rho}{\lambda}\rho\right) e^{-j\beta_z z}$$

When we multiply the two equations by the radius, a, we obtain dimensionless equations for the radial separation constants.

$$\left(\frac{2\pi b}{\lambda}a\right) = \sqrt{(\omega a)^2(\epsilon_1\mu_1 - \epsilon_0\mu_0) - \left(\frac{2\pi\rho}{\lambda}a\right)^2}$$

$$\frac{1}{\mu_1}\left(\frac{2\pi\rho}{\lambda}a\right)\frac{J_0\left(\frac{2\pi\rho}{\lambda}a\right)}{J_0'\left(\frac{2\pi\rho}{\lambda}a\right)} = -\frac{1}{\mu_0}\left(\frac{2\pi ba}{\lambda}\right)\frac{K_0\left(\frac{2\pi b}{\lambda}a\right)}{K_0'\left(\frac{2\pi b}{\lambda}a\right)}$$

We can find the solution to these equations by plotting both of them as a function of the separation constant in the dielectric and identifying the solutions as the intersection of the two curves.

TM Modes

The TM mode solution can be found in a similiar manner as the TE mode. Just like that case, we will only have a solution when n = 0. The TM mode expansion differential expressions are

$$E_\rho = \frac{1}{j\omega\epsilon}\frac{\partial^2\psi}{\partial\rho\partial z} \qquad H_\rho = 0$$

$$E_\phi = 0 \qquad H_\phi = -\frac{\partial\psi}{\partial\rho}$$

$$E_z = \frac{1}{j\omega\epsilon}(\beta^2 - \beta_z^2)\psi$$

The scalar potential for the TM mode has the same form as the TE modes. When we expand the potential, the following equations are obtained.

$$E_{z_1} = \frac{-1}{j\omega\epsilon_0}\left(\frac{2\pi b}{\lambda}\right)^2 K_0\left(\frac{2\pi b}{\lambda}\rho\right) e^{-j\beta_z z}$$

$$E_{z_2} = \frac{1}{j\omega\epsilon_1}\left(\frac{2\pi\rho}{\lambda}\right)^2 J_0\left(\frac{2\pi\rho}{\lambda}\rho\right) e^{-j\beta_z z}$$

$$H_{\phi_1} = -\left(\frac{2\pi b}{\lambda}\right) K_0'\left(\frac{2\pi b}{\lambda}\rho\right) e^{-j\beta_z z}$$

$$H_{\phi_2} = -\left(\frac{2\pi\rho}{\lambda}\right) J_0'\left(\frac{2\pi b}{\lambda}\rho\right) e^{-j\beta_z z}$$

These tangential fields must be equal at the boundary which gives us the following equations.

$$E_z: \quad -\frac{1}{\epsilon_0}\left(\frac{2\pi b}{\lambda}\right)^2 K_0\left(\frac{2\pi b}{\lambda}a\right) = \frac{1}{\epsilon_1}\left(\frac{2\pi p}{\lambda}\right)^2 J_0\left(\frac{2\pi p}{\lambda}a\right)$$

$$H_\phi: \quad \left(\frac{2\pi b}{\lambda}\right) K_0'\left(\frac{2\pi b}{\lambda}a\right) = \left(\frac{2\pi p}{\lambda}\right) J_0'\left(\frac{2\pi p}{\lambda}a\right)$$

If we divide these two equations, we get one of the equations for the separation constants.

$$\frac{1}{\epsilon_1}\left(\frac{2\pi p}{\lambda}\right)\frac{J_0\left(\frac{2\pi p}{\lambda}a\right)}{J_0'\left(\frac{2\pi p}{\lambda}a\right)} = \frac{-1}{\epsilon_0}\left(\frac{2\pi b}{\lambda}\right)\frac{K_0\left(\frac{2\pi b}{\lambda}a\right)}{K_0'\left(\frac{2\pi b}{\lambda}a\right)}$$

This is the same equation as the TE solution except for the interchange of μ and ϵ . The other equation is obtained by equating the propagation constant in both regions. This is the same equation as for the TE solution. We have two equations which can be solved graphically.

These two modes have the same cut off frequency. Cut off is that frequency below which the waves are no longer bound to the dielectric. We define cut off as $\alpha = 0$. The two equations for the separation constants become

$$\frac{2\pi p}{\lambda_c} = \omega\sqrt{\epsilon_0\mu_0}\sqrt{\frac{\epsilon_1\mu_1}{\epsilon_0\mu_0} - 1} = \frac{2\pi}{\lambda_c}\sqrt{\frac{\epsilon_1\mu_1}{\epsilon_0\mu_0} - 1}$$

$$J_0\left(\frac{2\pi p}{\lambda_c}a\right)K'(0) = 0$$

The second equation is zero because the right side is multiplied by the separation constant α . It is zero at the zeros of the Bessel function.

$$\frac{2\pi p}{\lambda_c}a = \chi_{0p}$$

$$\lambda_c = \frac{2\pi a}{\chi_{0p}}\sqrt{\frac{\epsilon_1\mu_1}{\epsilon_0\mu_0} - 1}$$

The waveguide has a finite cutoff frequency which is the same for both modes.

HYBRID MODES

We can find solutions to cylindrical open structures which do not have a low frequency cutoff by using a wave which is neither TE nor TM to any of the coordinates. Divide the fields into TE and TM modes to the Z axis.

$$\left.\begin{aligned} \psi_m' &= A_1 Z_n^{m1}(\beta_{\rho 1}\rho)\cos n\phi\, e^{-j\beta_z z} \\ \psi_e' &= B_1 Z_n^{e1}(\beta_{\rho 1}\rho)\sin n\phi\, e^{-j\beta_z z} \end{aligned}\right\} \quad \text{Region I}$$

$$\left.\begin{aligned} \psi_m^2 &= A_2 Z_n^{m2}(\beta_{\rho 2}\rho)\cos n\phi\, e^{-j\beta_z z} \\ \psi_e^2 &= B_2 Z_n^{e2}(\beta_{\rho 2}\rho)\sin n\phi\, e^{-j\beta_z z} \end{aligned}\right\} \quad \text{Region II}$$

Where $Z_n(\beta_\rho \rho)$ is any linear combination of Bessel functions of order n which satisfy the boundary conditions in each region. We will find the fields by expanding these potentials using the equations on pages 257 and 259.

$$E_\phi = \frac{\partial \psi_e}{\partial \rho} + \frac{1}{j\omega\epsilon\rho}\frac{\partial^2 \psi_m}{\partial \phi \partial z}$$

$$E_{\phi_i} = \left(B_i \beta_{\rho i} Z_n^{ei\prime}(\beta_{\rho i}\rho) + \frac{\beta_z n}{\omega \epsilon_i \rho} A_i Z_n^{mi}(\beta_{\rho i}\rho)\right)\sin n\phi\, e^{-j\beta_z z}$$

$$E_z = \frac{1}{j\omega\epsilon}\left(\frac{\partial^2}{\partial z^2} + \beta^2\right)\psi_m \qquad \beta^2 - \beta_z^2 = \beta_\rho^2$$

$$E_{z_i} = \frac{1}{j\omega\epsilon_i}\beta_{\rho i}^2 A_i Z_n^{mi}(\beta_{\rho i}\rho)\cos n\phi\, e^{-j\beta_z z}$$

$$H_z = \frac{1}{j\omega\mu}\left(\frac{\partial^2}{\partial z^2} + \beta^2\right)\psi_e$$

$$H_{z_i} = \frac{1}{j\omega\mu_i}\beta_{\rho i}^2 B_i Z_n^{ei}(\beta_{\rho i}\rho)\sin n\phi\, e^{-j\beta_z z}$$

$$H_\phi = \frac{1}{j\omega\mu\rho}\frac{\partial^2 \psi_e}{\partial \phi \partial z} - \frac{\partial \psi_m}{\partial \rho}$$

$$H_{\phi_i} = -\left(\frac{\beta_z n}{\omega \mu_i \rho} B_i Z_n^{ei}(\beta_{\rho i}\rho) + A_i \beta_{\rho i} Z_n^{mi\prime}(\beta_{\rho i}\rho)\right)\cos n\phi\, e^{-j\beta_z z}$$

These tangential fields must be equal at the boundary between the two regions. Let us make the following substitutions before equating the fields.

$$F_{ei} = Z_n^{ei}(\beta_{\rho i} a) \qquad F_{mi} = Z_n^{mi}(\beta_{\rho i} a)$$

$$F_{ei}' = Z_n^{ei\prime}(\beta_{\rho i} a) \qquad F_{mi}' = Z_n^{mi\prime}(\beta_{\rho i} a)$$

When we equate the tangential fields, we have the following four equations.

$$E_z: \quad \epsilon_2 \beta_{\rho 1}^2 A_1 F_{m1} - \epsilon_1 \beta_{\rho 2}^2 A_2 F_{m2} = 0$$

$$H_z: \quad \mu_2 \beta_{\rho 1}^2 B_1 F_{e1} - \mu_1 \beta_{\rho 2}^2 B_2 F_{e2} = 0$$

$$E_\phi: \quad A_1 \frac{\beta_z n}{\omega \epsilon_1 a} F_{m1} - \frac{A_2 \beta_z n}{\omega \epsilon_2 a} F_{m2} + B_1 \beta_{\rho 1} F_{e1}' - B_2 \beta_{\rho 2} F_{e2}' = 0$$

$$H_\phi: \quad A_1 \beta_{\rho 1} F_{m1}' - A_2 \beta_{\rho 2} F_{m2}' + \frac{\beta_z n B_1}{\omega \mu_1 a} F_{e1} - \frac{B_2 \beta_z n}{\omega \mu_2 a} F_{e2} = 0$$

The coefficients, A_i and B_i, are nonzero only if the determinant of the coefficients of the equations is zero. This gives us the first equation in the separation constants.

$$\begin{vmatrix} \epsilon_2 \beta_{\rho 1}^2 F_{m1} & \epsilon_1 \beta_{\rho 2}^2 F_{m2} & 0 & 0 \\ 0 & 0 & \mu_2 \beta_{\rho 1}^2 F_{e1} & \mu_1 \beta_{\rho 2}^2 F_{e2} \\ \frac{\beta_z n}{\omega \epsilon_1 a} F_{m1} & \frac{\beta_z n}{\omega \epsilon_2 a} F_{m2} & \beta_{\rho 1} F_{e1}' & \beta_{\rho 2} F_{e2}' \\ \beta_{\rho 1} F_{m1}' & \beta_{\rho 2} F_{m2}' & \frac{\beta_z n}{\omega \mu_1 a} F_{e1} & \frac{\beta_z n}{\omega \mu_2 a} F_{e2} \end{vmatrix} = 0$$

The solution to this determinant gives the following equation in the separation constants.

$$\left[\frac{\mu_r F_{e2}'}{u_2 F_{e2}} + \frac{F_{m1}'}{u_1 F_{m1}} \right] \left[\frac{\epsilon_r F_{m2}'}{u_2 F_{m2}} + \frac{F_{e1}'}{u_1 F_{e1}} \right] - \left[\frac{\beta_z n}{\beta} \frac{u_1^2 + u_2^2}{u_1^2 u_2^2} \right]^2 = 0$$

Where the following substitutions have been made.

$$u_1 = \frac{2\pi b}{\lambda} a \qquad u_2 = \frac{2\pi \rho}{\lambda} a \qquad \frac{\beta_z}{\beta} = \sqrt{1 + b^2}$$

The second equation comes from equating the propagation constant in the two regions.

$$\frac{2\pi b}{\lambda} a = \frac{2\pi}{\lambda} a \sqrt{(\epsilon_r \mu_r - 1) - \rho^2}$$

DIELECTRIC ROD

The dielectric rod will support hybrid modes. The functions that are used in the two regions are

$$F_{e1} = F_{m1} = K_n\left(\frac{2\pi b}{\lambda}\rho\right) \qquad \text{Outside the Rod} \qquad \text{Region I}$$

$$F_{e2} = F_{m2} = J_n\left(\frac{2\pi p}{\lambda}\rho\right) \qquad \text{Inside the Rod} \qquad \text{Region II}$$

When we substitute these into the equation on page 400, we get the following equation for the separation constants.

$$\left[\frac{J_n'(u_2)}{u_2 J_n(u_2)} + \frac{K_n'(u_1)}{u_1 K_n(u_1)}\right]\left[\frac{\epsilon_r J_n'(u_2)}{u_2 J_n(u_2)} + \frac{K_n'(u_1)}{u_1 K_n(u_1)}\right]$$

$$-\left[\frac{\beta_z}{\beta}\frac{n}{}\frac{u_1^2 + u_2^2}{u_1^2 u_2^2}\right]^2 = 0$$

$$u_1 = \frac{2\pi b}{\lambda}a \qquad u_2 = \frac{2\pi p}{\lambda}a \qquad \frac{\beta_z}{\beta} = \sqrt{1+b^2}$$

$$u_1 = \sqrt{\frac{2\pi a}{\lambda}(\epsilon_r - 1) - u_2^2}$$

We can solve these equations graphically. A curve of the relative propagation constant is plotted on page 402. The dielectric rod guide has no low frequency cutoff but from the graph we can see that the rod has little effect on a passing wave if the radius is smaller than 0.15 wavelengths for a dielectric sonstant of 2.

The dielectric rod is used to make an endfire traveling wave antenna. These antennas are called polyrod antennas because they were first made with polystyrene. The rod protrudes from a waveguide feed. The waveguide TE_{11} mode in circular guide will transform into the HE_{11} mode in the rod. The dielectric rod is tapered so that there will be little reflection of the wave at the end.

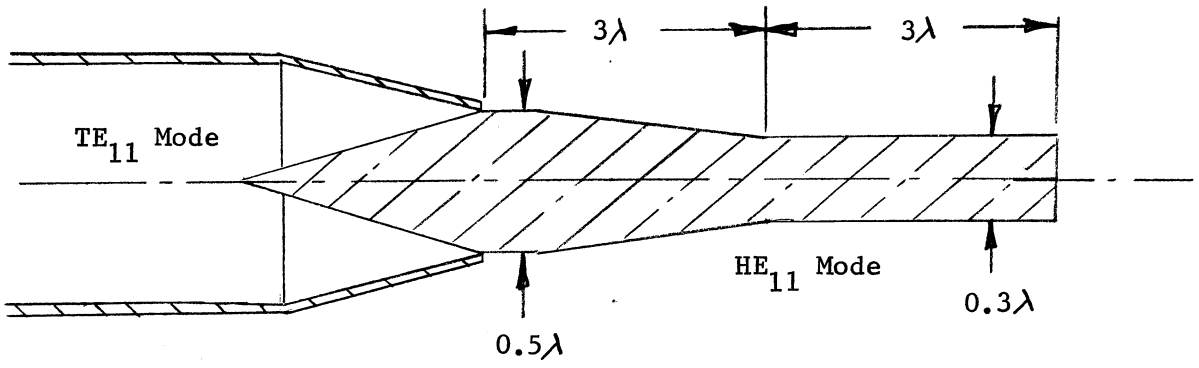

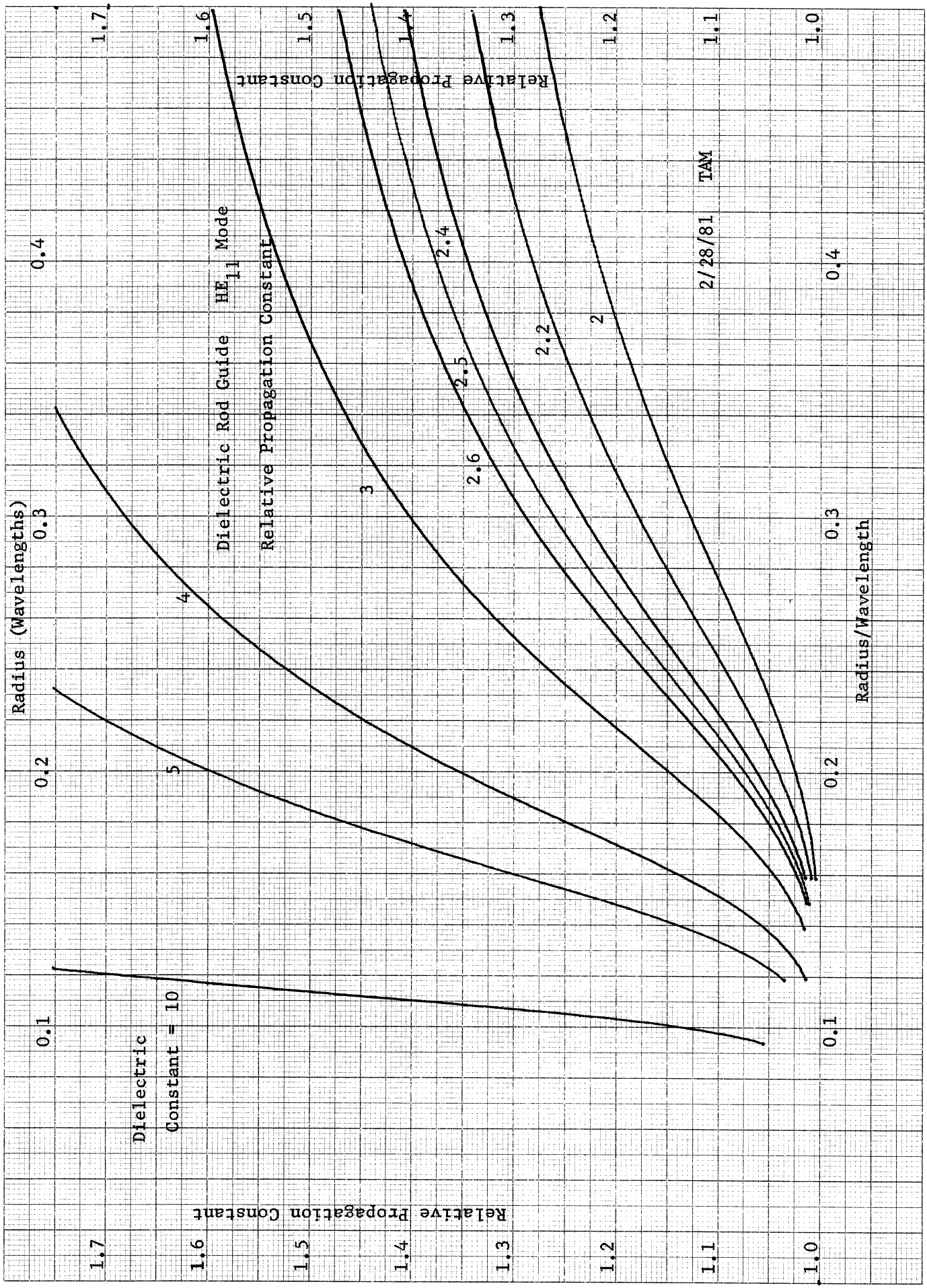

The TE_{11} mode circular guide is tapered at the end into the dielectric as it loads the waveguide. The length of the taper is determined experimentally. It will probably be necessary to insert obstacles in the waveguide to match the transition and will limit the VSWR bandwidth to a few percent. A metal pin may be put through the waveguide and dielectric rod to hold it in place as long as the pin is orthogonal to the electric field in the waveguide.

When the wave emerges from the waveguide section, it is tightly bound to the dielectric guide. The dielectric rod is gently tapered until the wave is only loosely bound to the dielectric rod. When the end of the guide is reached, there will only be a small reflection of the wave. This is an inverted horn.

Since the dielectric rod is tapered, the relative propagation constant varies down the rod. The far field can be found from the integral

$$E = \int_0^L E(z)\, e^{-j\beta z (P(z) - \cos\theta)}\, dz$$

where P(z) is the relative propagation constant function and E(z) is the field level on the rod.

Design: Polyrod antenna 5 wavelengths long in a dielectric constant = 2.5 to satisfy the Hansen and Woodyard criterion. Find the diameter. The required relative propagation constant is given on page 349.

$$P = \frac{1 + 2L}{2L} \qquad L = 5 \qquad P = 1.1$$

From the chart on page 402 this relative propagation constant corresponds to a diameter of 0.428 wavelengths. The pattern response would be half-way between the patterns on pages 355 and 356 for 4 and 6 wavelengths. The diameter of the rod would be tapered to prevent reflections so that this diameter would be the average which is weighted by the propagation constant for each diameter.

RADIAL TRANSMISSION LINES

When we solved the Helmholtz equation in circular coordinates on page 256, we picked the direction of propagation to be in the Z direction. We can also pick ρ as the direction of propagation. The propagation constant in the radial direction is related to the Z separation constant.

$$\beta_\rho^2 = \beta^2 - \beta_z^2$$

We will have standing waves in the Z direction in the radial waveguide. The scalar potential for these guides will be of the form

$$\psi = \cos n\phi \begin{Bmatrix} \cos \beta_z z \\ \sin \beta_z z \end{Bmatrix} \begin{Bmatrix} H_n^{(1)}(\beta_\rho \rho) \\ H_n^{(2)}(\beta_\rho \rho) \end{Bmatrix}$$

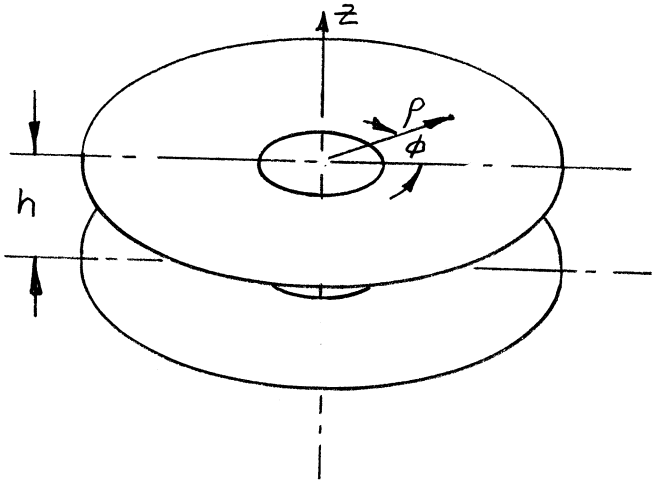

TE Modes

We will expand the fields from the equations on page 257 using the scalar potential given above.

$$E_\rho = \frac{n}{\rho} \sin n\phi \begin{Bmatrix} \cos \beta_z z \\ \sin \beta_z z \end{Bmatrix} \begin{Bmatrix} H_n^{(1)}(\beta_\rho \rho) \\ H_n^{(2)}(\beta_\rho \rho) \end{Bmatrix}$$

$$E_\phi = \beta_\rho \cos n\phi \begin{Bmatrix} \cos \beta_z z \\ \sin \beta_z z \end{Bmatrix} \begin{Bmatrix} H_n^{(1)\prime}(\beta_\rho \rho) \\ H_n^{(2)\prime}(\beta_\rho \rho) \end{Bmatrix}$$

Both these tangential electric fields must be zero at Z = 0 and Z = h. The first condition restricts the solution to the sine term only. The second boundary determines the Z separation constant.

$$\beta_z = \frac{m\pi}{h}$$

The scalar potential function for TE modes is given by

$$\psi_{mn}^{TE} = \cos(n\phi)\sin\left(\frac{m\pi}{h}z\right)\begin{Bmatrix} H_n^{(1)}(\beta_\rho \rho) \\ H_n^{(2)}(\beta_\rho \rho) \end{Bmatrix} \quad \begin{matrix} m = 1, 2, 3, \ldots \\ n = 0, 1, 2, \ldots \end{matrix}$$

The total fields are obtained from the equations on page 257.

$$E_\rho = \frac{n}{\rho}\sin(n\phi)\sin\left(\frac{m\pi}{h}z\right)\begin{Bmatrix} H_n^{(1)}(\beta_\rho \rho) \\ H_n^{(2)}(\beta_\rho \rho) \end{Bmatrix}$$

$$E_\phi = \beta_\rho \cos(n\phi)\sin\left(\frac{m\pi}{h}z\right)\begin{Bmatrix} H_n^{(1)\prime}(\beta_\rho \rho) \\ H_n^{(2)\prime}(\beta_\rho \rho) \end{Bmatrix}$$

$$E_z = 0$$

$$H_\rho = \frac{\beta_\rho}{j\omega\mu}\frac{m\pi}{h}\cos(n\phi)\cos\left(\frac{m\pi}{h}z\right)\begin{Bmatrix} H_n^{(1)\prime}(\beta_\rho \rho) \\ H_n^{(2)\prime}(\beta_\rho \rho) \end{Bmatrix}$$

$$H_\phi = \frac{-n}{j\omega\mu\rho}\frac{m\pi}{h}\sin(n\phi)\cos\left(\frac{m\pi}{h}z\right)\begin{Bmatrix} H_n^{(1)}(\beta_\rho \rho) \\ H_n^{(2)}(\beta_\rho \rho) \end{Bmatrix}$$

$$H_z = \frac{\beta_\rho^2}{j\omega\mu}\cos(n\phi)\sin\left(\frac{m\pi}{h}z\right)\begin{Bmatrix} H_n^{(1)}(\beta_\rho \rho) \\ H_n^{(2)}(\beta_\rho \rho) \end{Bmatrix}$$

Notice that the field is not transverse electric (TE) to the direction of propagation, ρ , but to the Z axis. The wave impedance in the radial direction is given by

$$Z_{+\rho} = \frac{E_\phi}{H_z} = \frac{j\omega\mu}{\beta_\rho}\frac{H_n^{(2)\prime}(\beta_\rho \rho)}{H_n^{(2)}(\beta_\rho \rho)}$$

for positive traveling waves and

$$Z_{-\rho} = \frac{-E_\phi}{H_z} = -\frac{j\omega\mu}{\beta_\rho}\frac{H^{(1)\prime}(\beta_\rho \rho)}{H_n^{(1)}(\beta_\rho \rho)}$$

for negative traveling waves. These impedances are complex conjugates of each other.

Since the constant, m, must be greater than zero, the waves have a cutoff frequency. The cutoff wavelength is given by

$$\frac{2\pi}{\lambda_c} = \frac{m\pi}{h} \qquad \lambda_c = \frac{2h}{m}$$

TM Modes

We can find solutions that are transverse magnetic to the Z coordinate by using the equations on page 259 to expand the fields.

$$E_\rho = \frac{\beta_z \beta_\rho}{j\omega\epsilon} \cos(n\phi) \begin{Bmatrix} -\sin\beta_z z \\ \cos\beta_z z \end{Bmatrix} \begin{Bmatrix} H_n^{(1)\prime}(\beta_\rho \rho) \\ H_n^{(2)\prime}(\beta_\rho \rho) \end{Bmatrix}$$

$$E_\phi = \frac{-n\beta_z}{j\omega\epsilon\rho} \sin(n\phi) \begin{Bmatrix} -\sin\beta_z z \\ \cos\beta_z z \end{Bmatrix} \begin{Bmatrix} H_n^{(1)}(\beta_\rho \rho) \\ H_n^{(2)}(\beta_\rho \rho) \end{Bmatrix}$$

Both these tangential fields must be zero at Z = 0 and Z = h which establishes the function of the scalar potential and the separation constant.

$$\beta_z = \frac{m\pi}{h}$$

$$\psi_{mn}^{TM} = \cos(n\phi)\cos\left(\frac{m\pi}{h} z\right) \begin{Bmatrix} H_n^{(1)}(\beta_\rho \rho) \\ H_n^{(2)}(\beta_\rho \rho) \end{Bmatrix}$$

$$m = 0, 1, 2, \ldots \qquad n = 0, 1, 2, \ldots$$

$$\beta_\rho = \sqrt{\beta^2 - \left(\frac{m\pi}{h}\right)^2}$$

In this case we can have m = 0 which means that the wave does not depend on the Z coordinate. These modes are used with the cylindrical corrugated surfaces becuase they usually have small heights between the corrugations. The fields are found from the equations on page 259.

$$E_\rho = \frac{-m\pi}{h} \frac{\beta_\rho}{j\omega\epsilon} \cos n\phi \sin\left(\frac{m\pi}{h} z\right) \begin{Bmatrix} H_n^{(1)\prime}(\beta_\rho \rho) \\ H_n^{(2)\prime}(\beta_\rho \rho) \end{Bmatrix}$$

$$E_\phi = \frac{m\pi}{h} \frac{n}{j\omega\epsilon\rho} \sin n\phi \sin\left(\frac{m\pi}{h} z\right) \begin{Bmatrix} H_n^{(1)}(\beta_\rho \rho) \\ H_n^{(2)}(\beta_\rho \rho) \end{Bmatrix}$$

$$E_z = \frac{\beta_\rho^2}{j\omega\epsilon} \cos n\phi \cos\left(\frac{m\pi}{h} z\right) \begin{Bmatrix} H_n^{(1)}(\beta_\rho \rho) \\ H_n^{(2)}(\beta_\rho \rho) \end{Bmatrix}$$

$$H_\rho = \frac{-n}{\rho} \sin n\phi \cos\left(\frac{m\pi}{h} z\right) \left\{ \begin{matrix} H_n^{(1)}(\beta_\rho \rho) \\ H_n^{(2)}(\beta_\rho \rho) \end{matrix} \right\}$$

$$H_\phi = -\beta_\rho \cos n\phi \cos\left(\frac{m\pi}{h} z\right) \left\{ \begin{matrix} H_n^{(1)\prime}(\beta_\rho \rho) \\ H_n^{(2)\prime}(\beta_\rho \rho) \end{matrix} \right\}$$

$$H_z = 0$$

Notice that these fields are transverse magnetic to the Z axis and not the radial direction of propagation.

TM_{0n} Modes

For corrugated structures we will only need the TM_{0n} solutions because the distance between the corrugations is much less than a half wavelength required for the first order m mode. The fields reduce to

$$E_\rho = 0 \qquad E_\phi = 0$$

$$E_z = \frac{\beta^2}{j\omega\epsilon} \cos n\phi \left\{ \begin{matrix} H_n^{(1)}(\beta \rho) \\ H_n^{(2)}(\beta \rho) \end{matrix} \right\}$$

$$H_\rho = \frac{-n}{\rho} \sin n\phi \left\{ \begin{matrix} H_n^{(1)}(\beta\rho) \\ H_n^{(2)}(\beta\rho) \end{matrix} \right\}$$

$$H_\phi = -\beta \cos n\phi \left\{ \begin{matrix} H_n^{(1)\prime}(\beta\rho) \\ H_n^{(2)\prime}(\beta\rho) \end{matrix} \right\}$$

The radial propagation constant is now the free space propagation constant.

Take the case n = 0, which corresponds to the axially symmetrical fields of the TM_{01} circular waveguide. It also corresponds to a TEM mode between the plates traveling in the radial direction. Consider the electric field.

$$E_z = \frac{\beta^2}{j\omega\epsilon} \left(C_1 H_0^{(1)}(\beta\rho) + C_2 H_0^{(2)}(\beta\rho) \right)$$

Suppose we have a short at radius a_1 and an outer radius of a_2. We have the additional boundary condition: $E_z(a_1) = 0$.

$$C_2 = -\frac{H_0^{(1)}(\beta a)}{H_0^{(2)}(\beta a)} C_1$$

The electric field becomes

$$E_z = \frac{\beta^2}{j\omega\epsilon} A_1 \left(H_0^{(1)}(\beta\rho) H_0^{(2)}(\beta a) - H_0^{(2)}(\beta\rho) H_0^{(1)}(\beta a) \right)$$

The magnetic field equation becomes

$$H_\phi = -\beta A_1 \left(H_0^{(1)\prime}(\beta\rho)\, H_0^{(2)}(\beta a) - H_0^{(2)\prime}(\beta\rho)\, H_0^{(1)}(\beta a) \right)$$

The radial impedance looking into the guide is given by

$$Z_{-\rho} = \frac{E_z}{H_\phi} = \frac{j\beta}{\omega\epsilon} \frac{H_0^{(1)}(\beta a_2) H_0^{(2)}(\beta a_1) - H_0^{(2)}(\beta a_2) H_0^{(1)}(\beta a_1)}{H_0^{(1)\prime}(\beta a_2) H_0^{(2)}(\beta a_1) - H_0^{(2)\prime}(\beta a_2) H_0^{(1)}(\beta a_1)}$$

We can use the following identities to reduce this equation.

$$H_n^{(1)}(x) = J_n(x) + j N_n(x)$$

$$H_n^{(2)}(x) = J_n(x) - j N_n(x)$$

This will reduce the impedance equation so that it involves Bessel and Neumann functions when expanded. The result of the expansion is given below.

$$Z_{-\rho} = j\eta \frac{J_0(\beta a_2) N_0(\beta a_1) - J_0(\beta a_1) N_0(\beta a_2)}{J_1(\beta a_2) N_0(\beta a_1) - J_0(\beta a_1) N_1(\beta a_2)}$$

Since we knew that we would only be using the radial waveguide as a cavity, we could expand the fields as standing waves in ρ as well.

$$E_z = \frac{\beta^2}{j\omega\epsilon} \left(D_1 J_0(\beta\rho) + D_2 N_0(\beta\rho) \right)$$

$$H_\phi = -\beta \left(D_1 J_0'(\beta\rho) + D_2 N_0'(\beta\rho) \right)$$

When we apply the boundary condition: $E_z = 0$ at $\rho = a_1$, we get the relation

$$D_2 = -D_1 \frac{J_0(\beta a_1)}{N_0(\beta a_1)}$$

We can also use the Bessel function relationships: $J_0' = -J_1$, $N_0' = N_1$

$$E_z = \frac{\beta^2 A_1}{j\omega\epsilon} \left(J_0(\beta\rho) N_0(\beta a_1) - J_0(\beta a_1) N_0(\beta\rho) \right)$$

$$H_\phi = \beta A_1 \left(J_1(\beta\rho) N_0(\beta a_1) - J_0(\beta a_1) N_1(\beta\rho) \right)$$

The radially directed wave impedance becomes

$$Z_{-\rho} = \frac{E_z}{H_\phi} = j\eta \frac{J_0(\beta a_2) N_0(\beta a_1) - J_0(\beta a_1) N_0(\beta a_2)}{J_1(\beta a_2) N_0(\beta a_1) - J_0(\beta a_1) N_1(\beta a_2)}$$

CORRUGATED CYLINDRICAL CONDUCTOR

The circular corrugated conductor can be treated in the same manner as the plane corrugated conductor. The impedance at the interface must be equal. In the figure below the ϕ component of the electric field must be zero. We can pick the TM mode solution given above for the dielectric rod for a solution.

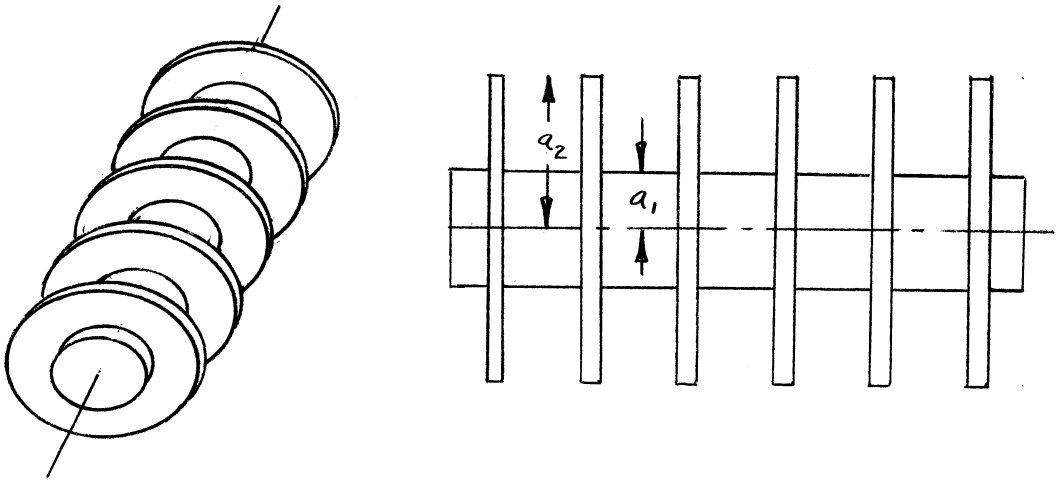

The fields outside the corrugations are given by

$$E_{z_1} = \frac{-A_1}{j\omega\epsilon_0}\left(\frac{2\pi b}{\lambda}\right)^2 K_0\left(\frac{2\pi b}{\lambda}\rho\right) e^{-j\beta_z z}$$

$$H_{\phi_1} = -A_1\left(\frac{2\pi b}{\lambda}\right) K_0\left(\frac{2\pi b}{\lambda}\rho\right) e^{-j\beta_z z}$$

The impedance looking into the corrugated structure to support this wave is given by

$$Z_{-\rho} = \frac{-E_z}{H_\phi} = \frac{-1}{j\omega\epsilon_0}\left(\frac{2\pi b}{\lambda}\right) = j\frac{\eta}{\beta}\left(\frac{2\pi b}{\lambda}\right) = j\eta_0 b$$

This is the same as the plane corrugated conductor. The corrugated surface is a series of short circuited radial transmission lines. The surface must be inductive to support the surface wave. The impedance of the radial transmission line choke is

$$Z_{-\rho} = j\eta\,\frac{J_0(\beta a_2)N_0(\beta a_1) - J_0(\beta a_1)N_0(\beta a_2)}{J_1(\beta a_2)N_0(\beta a_1) - J_0(\beta a_1)N_1(\beta a_2)}$$

Therefore we can find the relative propagation constant given the two radii. A curve of the relative propagation constant for various outer radii is plotted on page 410.

The mode must be fed by an axially symmetrical mode such as the TM_{01} circular waveguide mode or a TEM coaxial mode.

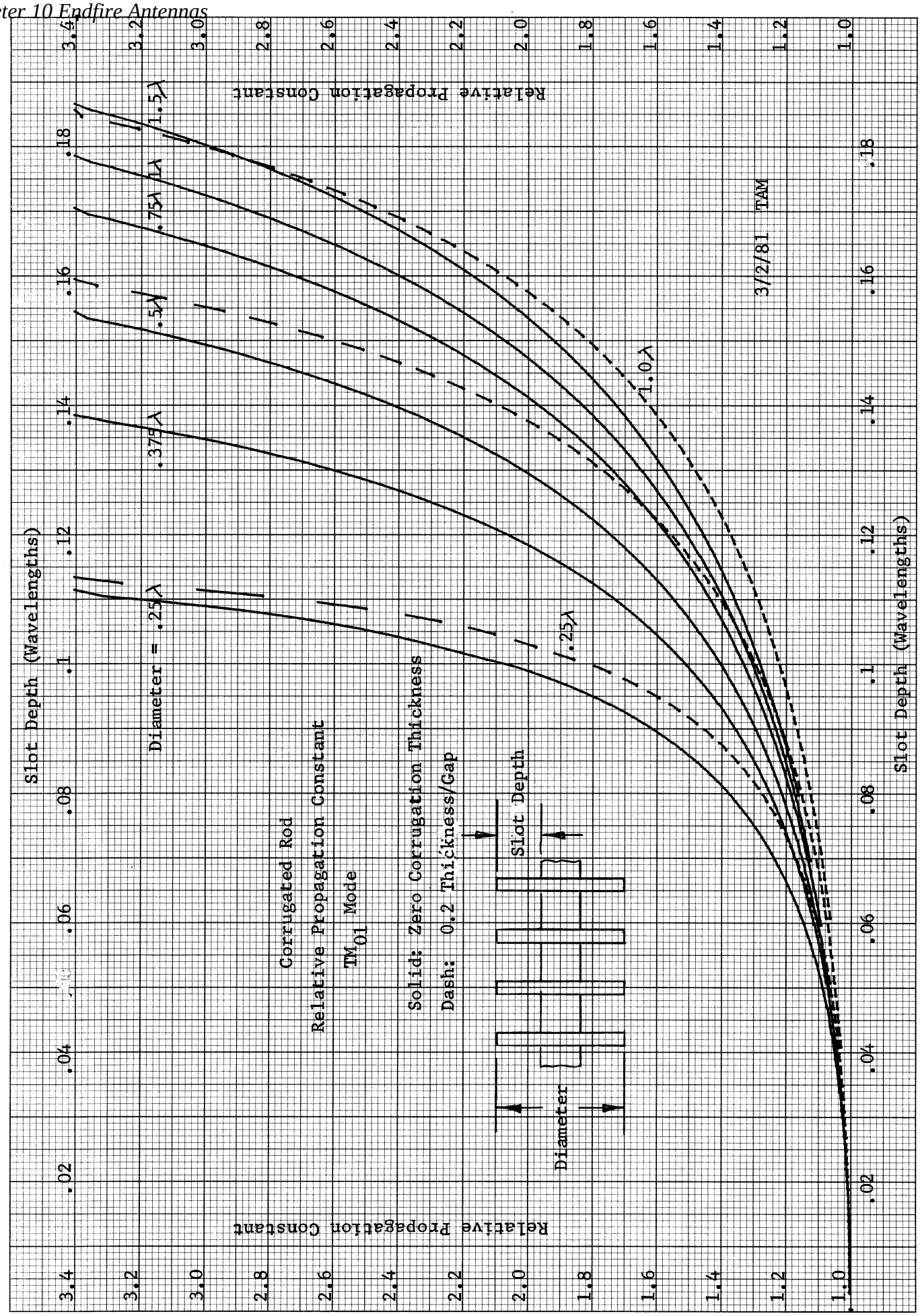

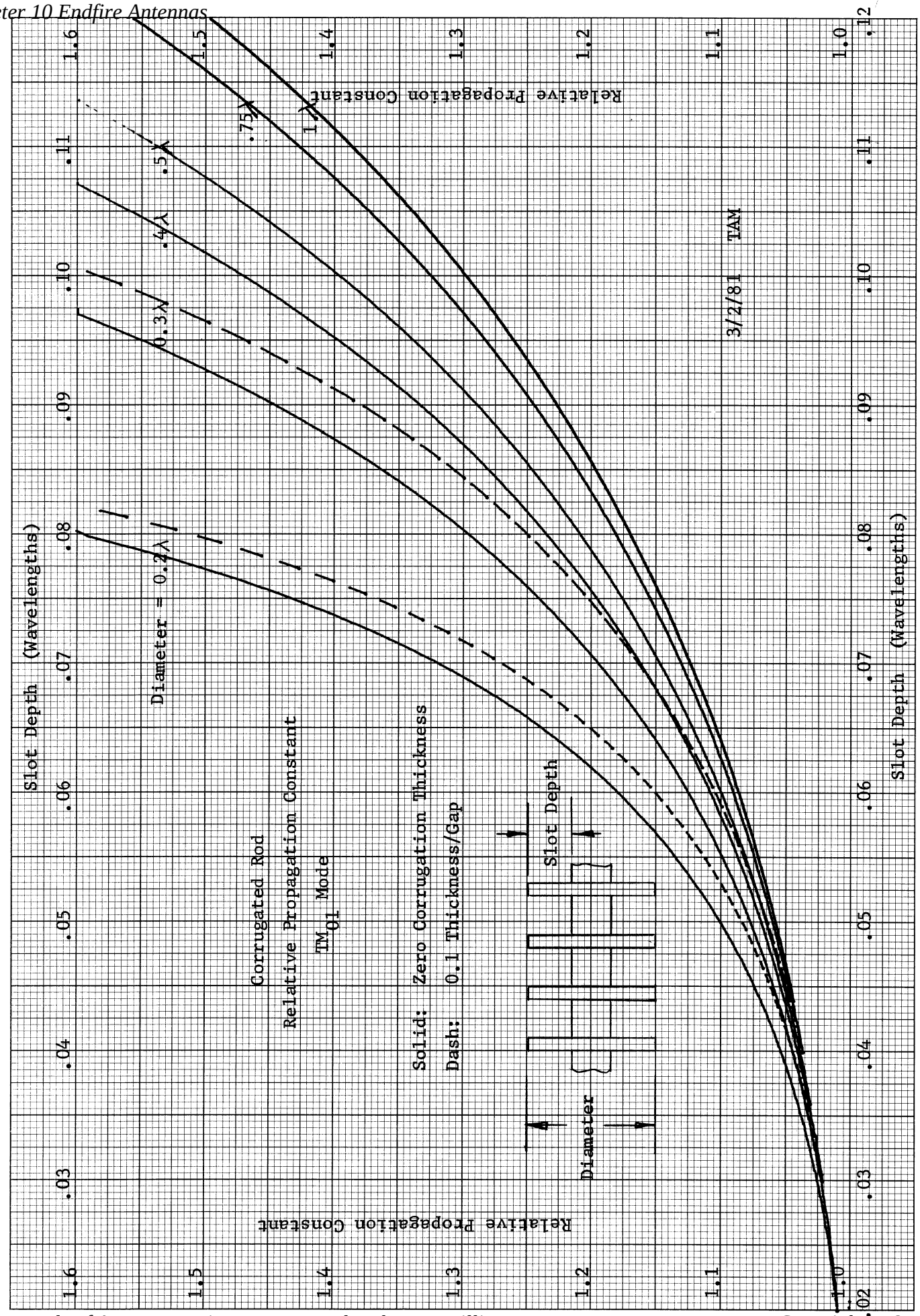

HE_{11} MODE ON CORRUGATED CYLINDRICAL CONDUCTOR

We will derive a hybrid mode on the corrugated cylindrical conductor. The assumptions are that there are many corrugations per wavelength along the conductor and that the corrugations will short out any ϕ component of the electric field on the surface of the corrugations. The fields are derived from a sum of Z directed electric and magnetic vector potentials.

$$\psi_{e_1} = B_1 K_n\left(\frac{2\pi b}{\lambda}\rho\right) \sin n\phi \, e^{-j\beta_z z}$$

$$\psi_{m_1} = A_1 K_n\left(\frac{2\pi b}{\lambda}\rho\right) \cos n\phi \, e^{-j\beta_z z}$$

The ϕ component of the electric field is a sum of terms.

$$E_\phi = \frac{\partial \psi_e}{\partial \rho} + \frac{1}{j\omega\epsilon\rho}\frac{\partial^2 \psi_m}{\partial \phi \partial z}$$

Expanding this expression we get

$$E_{\phi_1} = \left(B_1 \frac{2\pi b}{\lambda} K_n'\left(\frac{2\pi b}{\lambda}\rho\right) + \frac{A_1 \beta_z n}{\omega\epsilon\rho} K_n\left(\frac{2\pi b}{\lambda}\rho\right)\right) \sin n\phi \, e^{-j\beta_z z}$$

This electric field will be zero at $\rho = a_2$ which gives us a relation between the magnitudes of the scalar potentials.

$$B_1 = -\frac{A_1 \beta_z n}{\omega\epsilon a_2}\left(\frac{\lambda}{2\pi b}\right)\frac{K_n\left(\frac{2\pi b}{\lambda}a_2\right)}{K_n'\left(\frac{2\pi b}{\lambda}a_2\right)}$$

We need to find the impedance of the wave looking into the corrugated surface. This requires the Z component of the electric field and the ϕ component of the magnetic field.

$$E_z = \frac{1}{j\omega\epsilon}\left(\frac{\partial^2}{\partial z^2} + \beta^2\right)\psi_m \qquad \beta^2 - \beta_z^2 = \beta_\rho^2 = -\left(\frac{2\pi b}{\lambda}\right)^2$$

$$E_z = \frac{-A_1}{j\omega\epsilon}\left(\frac{2\pi b}{\lambda}\right)^2 K_n\left(\frac{2\pi b}{\lambda}\rho\right) \cos n\phi \, e^{-j\beta_z z}$$

$$H_\phi = \frac{1}{j\omega\mu\rho}\frac{\partial^2 \psi_e}{\partial \phi \partial z} - \frac{\partial \psi_m}{\partial \rho}$$

$$H_\phi = -\left(\frac{B_1 \beta_z n}{\omega\mu\rho} K_n\left(\frac{2\pi b}{\lambda}\rho\right) + A_1\left(\frac{2\pi b}{\lambda}\right) K_n'\left(\frac{2\pi b}{\lambda}\rho\right)\right) \cos n\phi \, e^{-j\beta_z z}$$

When we substitute in the restriction on the ϕ component of the electric field, the ϕ component of the magnetic field becomes

$$H_\phi = A_1 \left(\frac{\beta_z^2 n^2}{\omega^2 \epsilon \mu a \rho} \left(\frac{\lambda}{2\pi b} \right) \frac{k_n\left(\frac{2\pi b}{\lambda} a_2\right)}{k_n'\left(\frac{2\pi b}{\lambda} a_2\right)} k_n\left(\frac{2\pi b}{\lambda}\rho\right) - \frac{2\pi b}{\lambda} k_n'\left(\frac{2\pi b}{\lambda}\rho\right) \right) \cos n\phi \, e^{-j\beta_z z}$$

The impedance looking into the corrugations to support this wave will be the ρ component of the wave impedance.

$$Z_{-\rho} = \frac{E_z}{H_\phi}$$

$$Z_{-\rho} = \frac{\frac{-1}{j\omega\epsilon}\left(\frac{2\pi b}{\lambda}\right)^2 k_n\left(\frac{2\pi b}{\lambda} a_2\right)}{\frac{\beta_z^2 n^2}{\beta^2 a_2^2}\left(\frac{\lambda}{2\pi b}\right)\frac{k_n\left(\frac{2\pi b}{\lambda} a_2\right)}{k_n'\left(\frac{2\pi b}{\lambda} a_2\right)} k_n\left(\frac{2\pi b}{\lambda} a_2\right) - \frac{2\pi b}{\lambda} k_n'\left(\frac{2\pi b}{\lambda} a_2\right)}$$

With a few substitutions this expression reduces to

$$Z_{-\rho} = \frac{j\eta b \left(\frac{2\pi b}{\lambda} a_2\right)^2 k_n\left(\frac{2\pi b}{\lambda} a_2\right) k_n'\left(\frac{2\pi b}{\lambda} a_2\right)}{n^2(1+b^2) K_n^2\left(\frac{2\pi b}{\lambda} a_2\right) - \left(\frac{2\pi b}{\lambda} a_2\right)^2 K_n'^2\left(\frac{2\pi b}{\lambda} a_2\right)}$$

The corrugated surface is a series of short circuited radial transmission lines. The wave impedance of the radial line choke transmission line is

$$Z_{-\rho} = j\eta \frac{J_0(\beta a_1) N_0(\beta a_2) - J_0(\beta a_2) N_0(\beta a_1)}{J_1(\beta a_2) N_0(\beta a_1) - J_0(\beta a_1) N_1(\beta a_2)}$$

Equating these two equations for the radial wave impedance, we obtain the characteristic equation of this mode which can be solved for the attenuation constant.

$$\frac{b\left(\frac{2\pi b}{\lambda} a_2\right)^2 K_1\left(\frac{2\pi b}{\lambda} a_2\right) K_1'\left(\frac{2\pi b}{\lambda} a_2\right)}{(1+b^2) K_1^2\left(\frac{2\pi b}{\lambda} a_2\right) - \left(\frac{2\pi b}{\lambda} a_2\right)^2 K_1'^2\left(\frac{2\pi b}{\lambda} a_2\right)}$$

$$= \frac{J_0(\beta a_1) N_0(\beta a_2) - J_0(\beta a_2) N_0(\beta a_1)}{J_1(\beta a_2) N_0(\beta a_1) - J_0(\beta a_1) N_1(\beta a_2)}$$

On pages 414 and 415 are curves of the relative propagation constant of the corrugated rod excited in the HE_{11} hybrid mode. These curves are similiar to the curves on pages 410 and 411. The propagation constant increases slower than the TM_{01} case which means this mode requires deeper slots to achieve the same relative propagation constant. The second plot shows the effect of varying the ratio of the thickness of the corrugations to the gaps.

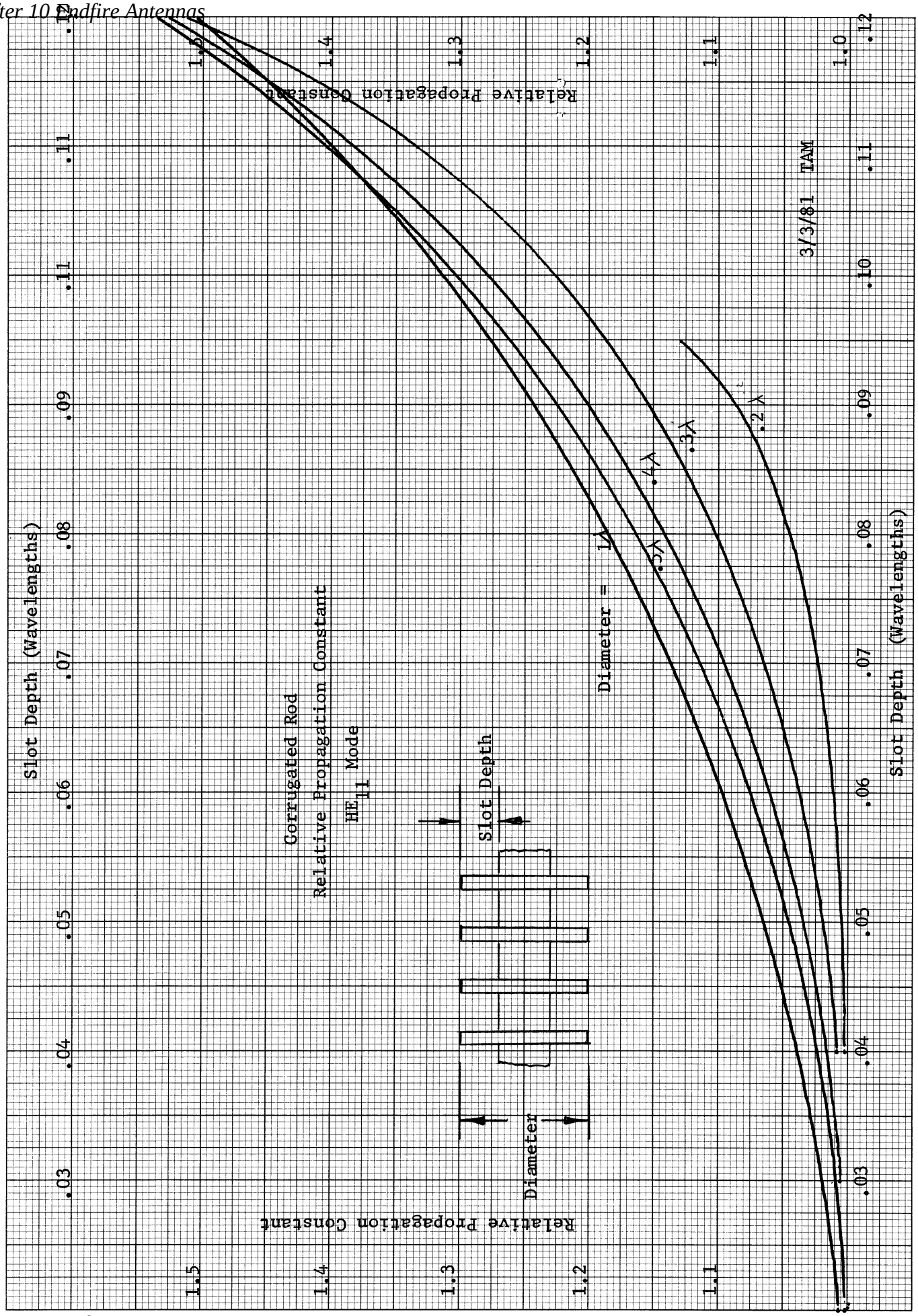

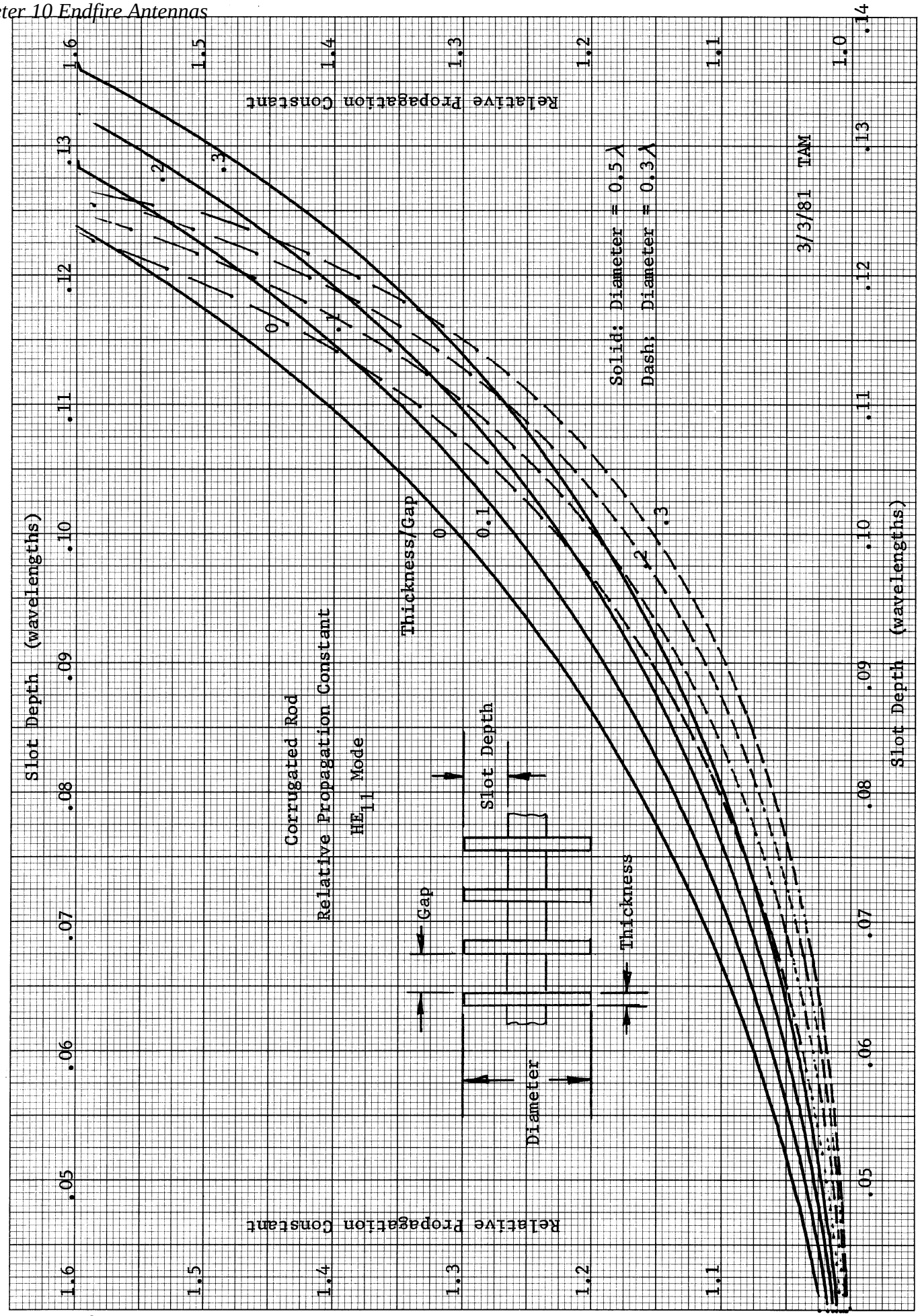

46 1320

10 X 10 TO ½ INCH 7 X 10 INCHES
KEUFFEL & ESSER CO. MADE IN U.S.A.

An antenna using a corrugated rod has been called a cigar antenna when excited in the HE_{11} hybrid mode (linear polarization). We have assumed that the corrugations are closely spaced in wavelengths which allowed a solution by matching the impedance at the edges of the corrugations. This can be done if we assume that the ϕ component of the electric field is zero at the corrugations; the same assumption is made for corrugated horns. If there is a ϕ component of the electric field at the corrugation edges, then it must be supported by a TE_{11} mode in the radial cavities. This mode is cutoff. The antenna has been made with the gaps up to but less than a half wavelength. As long as the gaps are less than a half wavelength, the structure will be a slow wave structure. In general as the gap size grows, we can expect that the relative propagation constant will approach one. This effect can be counteracted by increasing the slot depth.

A method of solving the problem of widely spaced disks on the cigar antenna is to use a periodic structures analysis. In this analysis the electric

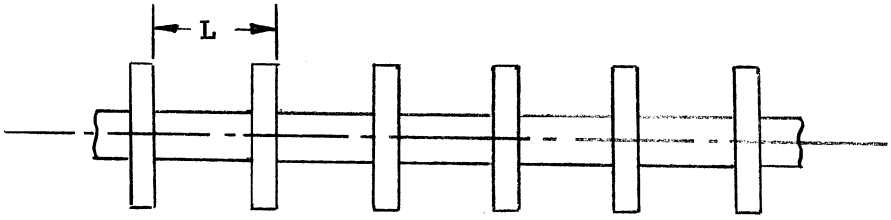

field is expanded in terms of space harmonics of the periodic length, L.

$$E_\phi = e^{-j\beta z} \sum_{n=-\infty}^{\infty} a_n e^{-j\left(\frac{2\pi n}{L}\right)z}$$

An electric field is assumed in the gaps and the coefficients of the infinite series are found by using a Fourier series approach. The characteristic equation for the separation constant would include the infinite series in the space harmonics. By assuming the corrugations are close, we have set $a_n = 0$ in the infinite series for all n. It is suggested that an empirical approach will yield a design for widely spaced disks when we start with the design curves realizing that the depth of the slots will have to be increased.

FEEDING CYLINDRICAL SLOW WAVE STRUCTURES

These structures may be fed by mounting them in front of a horn which is excited in the proper mode to excite the slow wave cylinder. The TE_{11} mode in circular waveguide or the TE_{10} mode in rectangular waveguide will excite the HE_{11} hybrid mode on the cylinder. A flared coax where the center conductor is connected to the corrugated rod will excite the TM_{01} mode.

In these cases the total pattern will be a combination of the traveling wave endfire structure and the fields of the horn aperture which are not bound to the slow wave. The efficiency of exciting the slow wave will be a function of the aperture size and the external attenuation constant. For narrow bandwidth applications the structure can be excited with a feed dipole or resonant loop with a reflector. In this case the slow wave structure becomes the directors of a Yagi antenna.

HELICAL ANTENNA

The helical antenna was developed by J. D. Kraus in the late 1940's. It is an endfire antenna when the circumference of the antenna is around one wavelength with circular polarization. H. A. Wheeler in 1947 published results for helical antennas of small diameter called the normal mode which also gives circular polarization over a limited frequency range. The axial mode helical antenna (endfire) gives good pattern responses over the range of cicumferences from about .78 wavelengths to about 1.33 wavelengths for helices of a few turns (less than 15). The antenna will work over a smaller bandwidth for more turns. Since the antenna will work over a 1.7 to 1 bandwidth and is able to give very good circularity, it has become a very useful antenna.

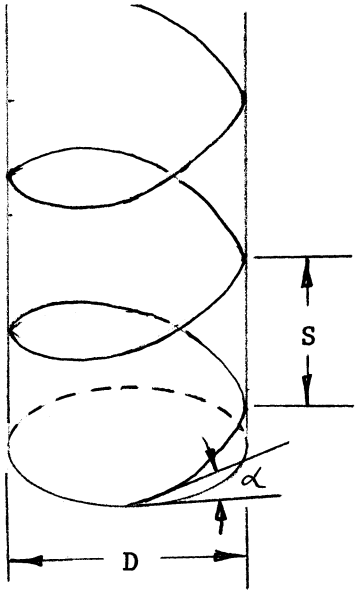

The figure above is that of a right hand helix showing some of the parameters of a helical antenna. We will use the circumference: $C = \pi D$. The length of each turn is given by the following diagram. α is the pitch angle; S is the spacing between turns; L is the length of the wire; and D is the diameter.

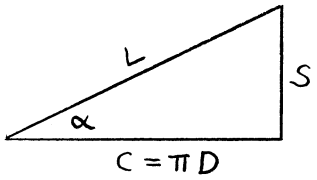

The length of the turn is given by $L = \sqrt{S^2 + C^2} = \pi D / \cos \alpha$

HELICAL MODES

The antenna can be understood by considering the modes of the helical transmission line. When the diameter of the helix is small comparied to a wavelength, the wave traveling on the wire of the helix is called the T_o mode. It travels along the wire at about the free space velocity.

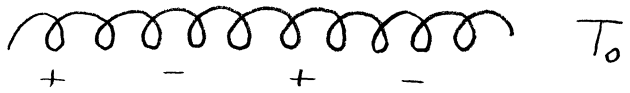

The equal phase points of the waves occur on separate turns. In this mode the helix radiates in the normal mode. The normal mode radiates at 90 degrees from the axis of the helix. This mode is the primary mode used in the traveling wave tube to couple energy from an electron beam. Energy is coupled into the wave from the beam when the velocity of the wave in the axial direction is close to the electron drift velocity. Since the wave travels along the wire at about the free space, the axial velocity of the wave is the velocity of the wave on the wire times the sine of the pitch of the helix. This is a slow wave structure in the axial direction.

The second mode occurs when the circumference of the helix approaches one wavelength, T_1 mode. This mode will have a distribution $e^{j\phi}$ or $e^{-j\phi}$

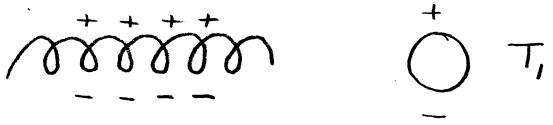

The whole variation of phase occurs on every turn. The axial mode or endfire mode is due to this mode. The velocity of the wave on the wire reduces to less than the free space velocity and increases with circumference. The velocity increases in a fashion so that the phase between turns closely approximates the Hansen and Woodyard criterion for increased directivity from an endfire array.

The third mode on the helix will have an $e^{\pm j2\phi}$ variation around the helix which we can see best from the end view of the helix. The velocity of this

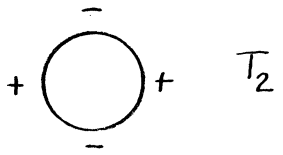

wave along the wire of the helix is even slower than the T_1 mode, less than half for a circumference of one wavelength. As the diameter of the helix increases the energy is coupled into the higher order modes.

In general we can express any current distribution on the helix as a linear combination of the general modes

$$e^{\pm jm\phi}$$

where m is an integer. Using these modes we can explain the radiation from a helical antenna.

NORMAL MODE

When the helix is small, the antenna looks like a combination of loops with short linear elements between them. The pattern of the small loop and the short dipole are the same. There is a null on the axis of the helix. Since

the loop and the linear elements have different polarizations, it is possible to pick a combination of sizes to give circular polarization in the normal direction. This is true when the spacing and diameter are related by

$$\pi D = \sqrt{2S\lambda}$$

As we can see, this is a frequency dependent relationship. This is inherently a narrow bandwidth antenna. The current on the helix is a standing wave pattern of two traveling waves in the T_0 mode. We can expect an input impedance variation similiar to the dipole or loop. The normal mode helix has failed to become a practical antenna.

AXIAL MODE

The axial mode is radiation from the T_1 mode on the helix. There are components of the other modes on the helix which must be present to satisfy the boundary conditions. The presence of these modes can be seen in the patterns. This antenna is part of the general class of slow wave endfire antennas. Not only is the current on the wire a slow wave but the diameter is picked so that the wave is a slow wave in the axial direction. It appears that the slow wave naturally fits the Hansen and Woodyard criterion for increased directivity from an endfire antenna over a large variation of parameters.

Instead of analyzing the structure as a continuous endfire array, it is convenient to consider the antenna as a discrete array. Each element is one turn of the helix. The antenna is the following linear array.

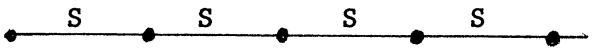

Where S is the spacing between turns. We will analyze the array of isotropic elements and then multiply by the pattern of a single element to obtain the pattern of the helical wire antenna. All this assumes that the T_1 mode is uniform along the helix which appears to be a good assumption. From page 105 or 348 the pattern of the isotropic array is given by

$$E = E_o \frac{\sin(N\psi/2)}{\psi/2}$$

where $\psi = \beta S \cos\theta + \delta$; S is the spacing between turns, θ is the angle from the axis of the helix, δ is the equal phase shift between elements, and N is the number of turns. This expression is limited to integer number of turns but we would not expect the pattern to change much for non integer number of turns from near by patterns of integer number of turns.

For circumferences from 0.78 wavelengths to about 1.33 wavelengths the antenna will satisfy the Hansen and Woodyard criterion for a few turns (less than about 2 wavelengths long). Based on these experimental results with helices, we can find the wave velocity on the wire. The distance along the wire between turns is found from the diagram on page 417.

$$L = \sqrt{S^2 + C^2} = C/\cos\alpha$$

Since the circumference is about one wavelength, the phase change on one turn will exceed 2π . The phase shift in the axial direction is determined by the Hansen and Woodyard criterion.

$$-\delta = \beta s + \frac{\pi}{N}$$

Since we are going around the wire, we will add 2π to this to get the phase along the wire

$$\beta p L = \beta s + 2\pi + \frac{\pi}{N}$$

$$PL/\lambda = S/\lambda + 1 + \frac{1}{2N}$$

Where P is the relative propagation constant.

$$PC_\lambda/\cos\alpha = C_\lambda \tan(\alpha) + (2N+1)/2N$$

$$P = \sin\alpha + ((2N+1)/2N)\cos\alpha/C_\lambda$$

C_λ is the circumference in wavelengths. As N, the number of turns, becomes large, P approaches a constant which is the relative propagation constant of the infinitely long helix. Because P is not the same as the infinite helix in the T_1 mode, there must be a combination of modes which increases P for shorter helices. When the circumference of the helix increases, more energy is coupled into the T_2 mode. This limits the upper end of the range of allowable values of C_λ .[2] As the number of turns is increased, the upper limit shrinks toward the lower limit. The lower end is established by the smallest circumference which will support the T_1 mode.

The polarization of the helix pattern is determined by the pattern of a single turn; the isotropic array does not determine anything about polarization. Consider the T_1 mode on a one wavelength in circumference loop when looking from above.

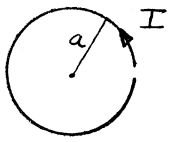

The traveling current wave is $I_0 e^{-j\beta P \phi a}$

Since the loop is approximately one wavelength around, we see a current wave rotating on the loop at the rotation rate of the radian frequency. When we discussed a circularly polarized wave, we found that the wave polarization rotated with the radian frequency. From these statements we can see that the T_1 mode on the helix radiates a circularly polarized wave since the current rotates its direction at the radian frequency. The sense of polarization is the same as the screw of the helix. When looking down on a helix which is transmitting, the polarization is right hand circular if the traveling wave current is traveling counter clockwise on the helix.

If the helical wire follows the increased directivity criterion, then the boresight axial ratio will decrease with increasing number of turns. This assumes that there is only the T_1 mode on the helix. The axial ratio is given by

$$\text{Axial Ratio} = (2N + 1)/2N$$

When the velocity along the wire varies away from the increased directivity criterion, then the axial ratio will increase for increased P. Axial ratio equals one (0 dB) for P = 1. The axial ratio will increase when the T_2 mode is generated, This mode radiates a four lobed pattern which disturbs the pattern polarization on boresight. If the helix has more than 10 turns, the boresight axial ratio will depend on the feed region and the tip region.

For an example consider a 5 turn helix with a circumference of 0.9 wavelengths and a pitch angle of 13 degrees. On page 422 is the pattern of a single turn of the helical antenna. The solid curve is the right hand circular polarization component and the dashed is the left hand component. Note that the cross polarization component is down by about 26.3 dB from the co-polarization component at boresight. The pattern of the full 5 turn helix is plotted on page 423. It has the same boresight cross polarization response as the single turn. We can compare this pattern to the pattern on page 424 of a traveling wave endfire antenna the same length and axial relative propagation constant. The pattern response of the single turn has reduced the sidelobe level and the beamwidth compared to the isotropic element pattern. It would be a more direct comparison of pattern multiplication if the helix turn did not represent such a large proportion of the full length of the helix.

The directivity of the helical wire antenna can be found by integrating the pattern. In order to properly integrate the pattern, the energy in both the co-pol. and cross pol. components must be added together. When this is done a composite pattern which is suitable for directivity integrations can be found. Using this pattern the helical wire antenna can be treated as a continuous endfire antenna. It was found that the directivity is proportional to the axial length of the antenna and only slightly on the circumference of the antenna for those which will support primarily the T_1 mode only. A curve of the directivity versus length is plotted on page 425. This curve shows that it requires a very long helix to obtain large gains which is true of all traveling wave endfire antennas. The very long helices require special considerations to get a reasonable design and achieve the predicted directivities. Similiarly a curve of the beamwidth versus length is plotted on page 426. This curve is based on the composite pattern of the right and left hand components and will predict slightly larger beamwidths for short helices.

Feeding a Helical Antenna

The axial mode helical wire antenna is usually fed from the center pin of a connector mounted to a ground plane. The pattern does not depend on the ground plane to achieve a good F/B. The pattern on page 423 does not include effects of a ground plane. The ground plane is required to achieve

Single Turn of a Helical Wire Antenna of 5 Turns

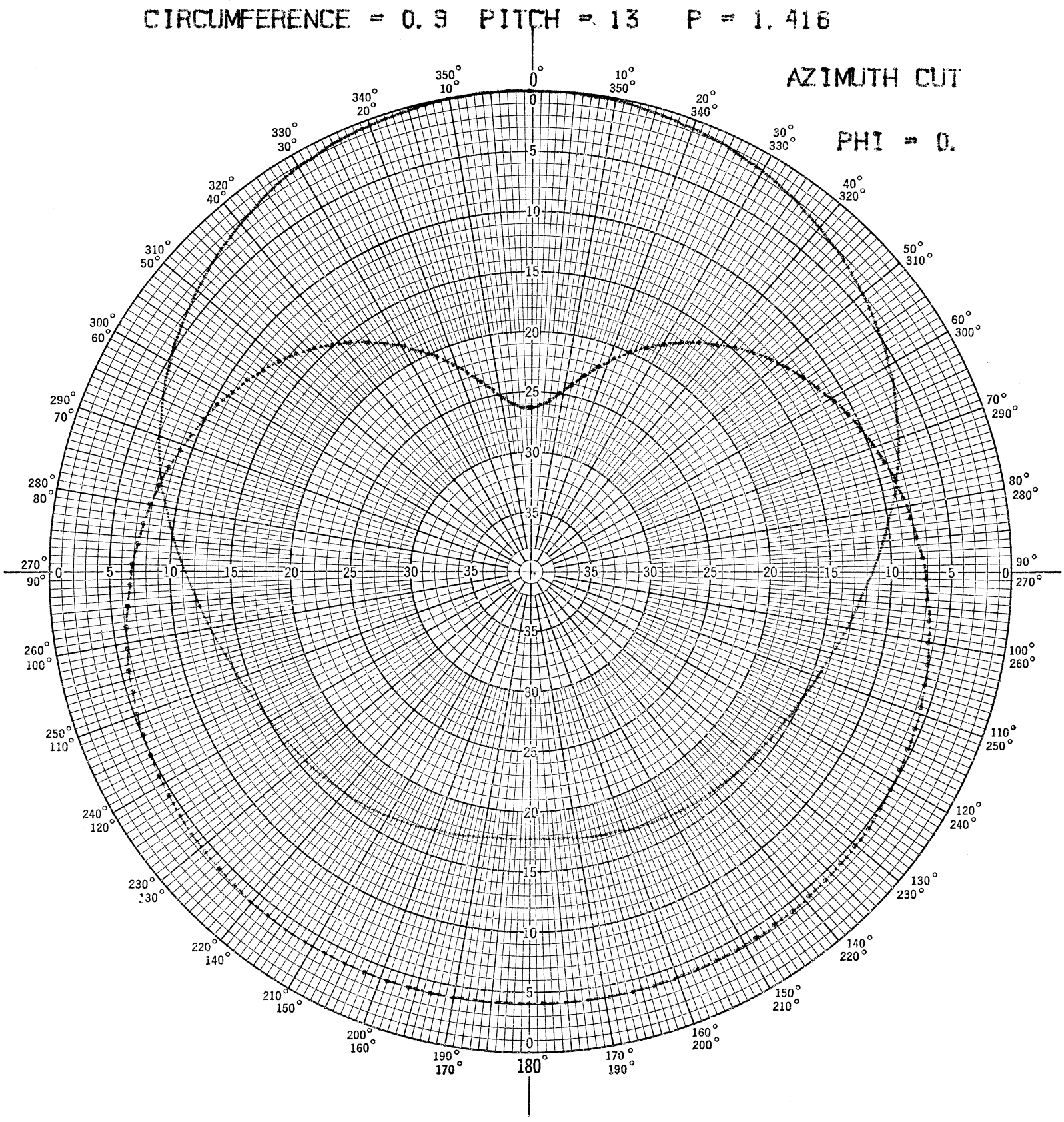

Polar Chart No. 127D
SCIENTIFIC-ATLANTA, INC.
ATLANTA, GEORGIA

5 Turn Helical Wire Antenna in Axial Mode

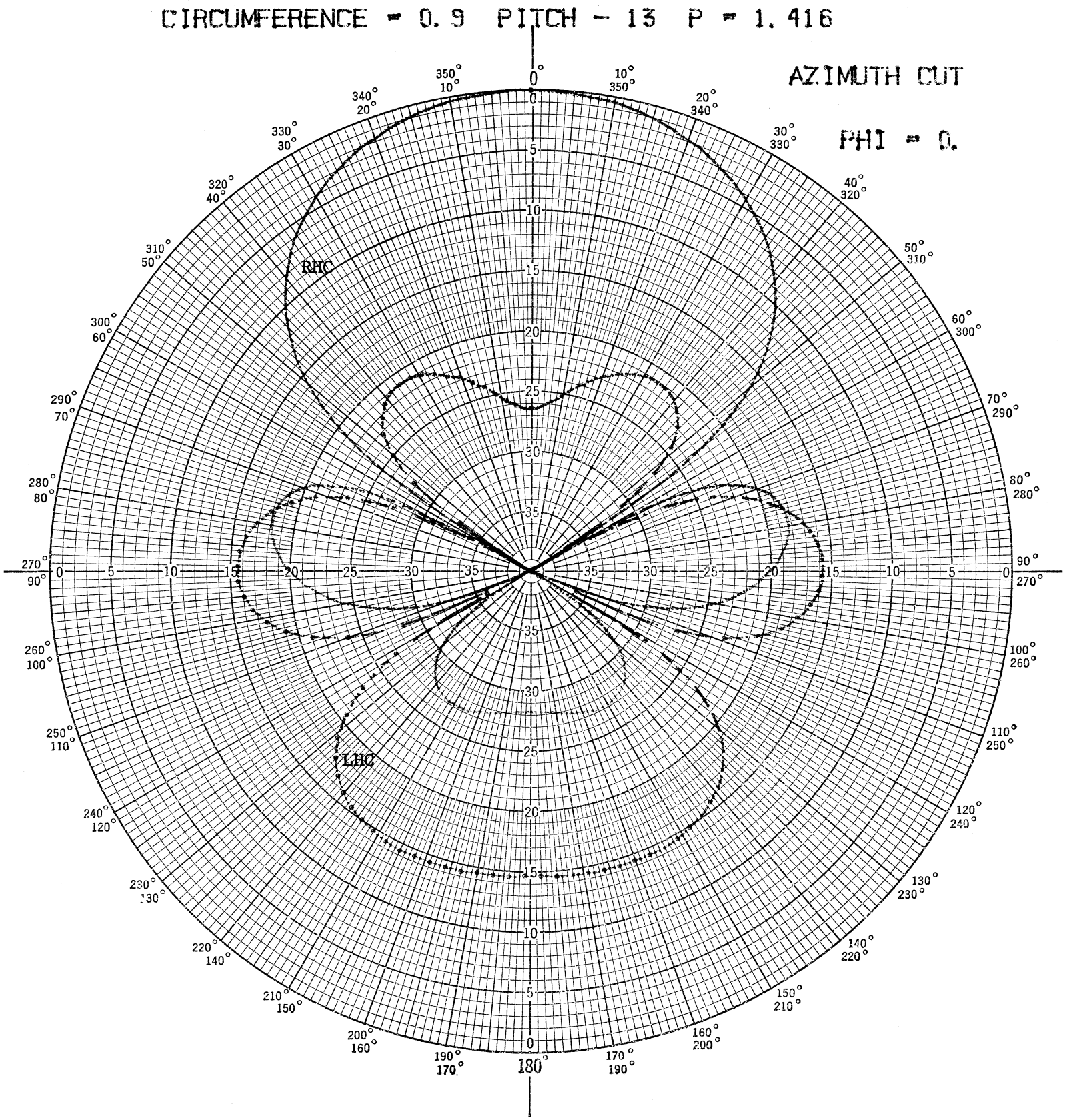

Polar Chart No. 127D
SCIENTIFIC-ATLANTA, INC.
ATLANTA, GEORGIA

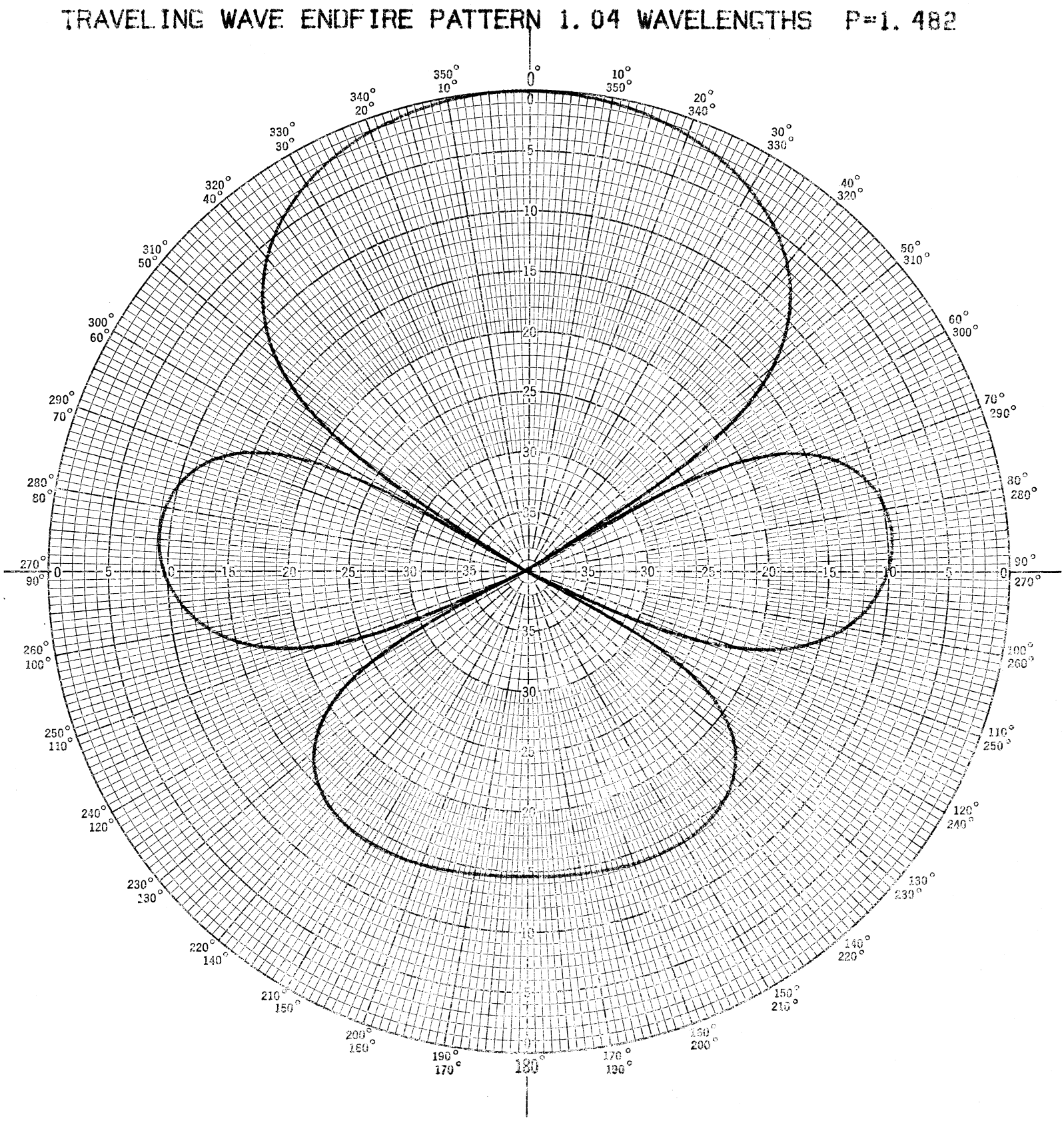

Polar Chart No. 127D
SCIENTIFIC-ATLANTA, INC.
ATLANTA, GEORGIA

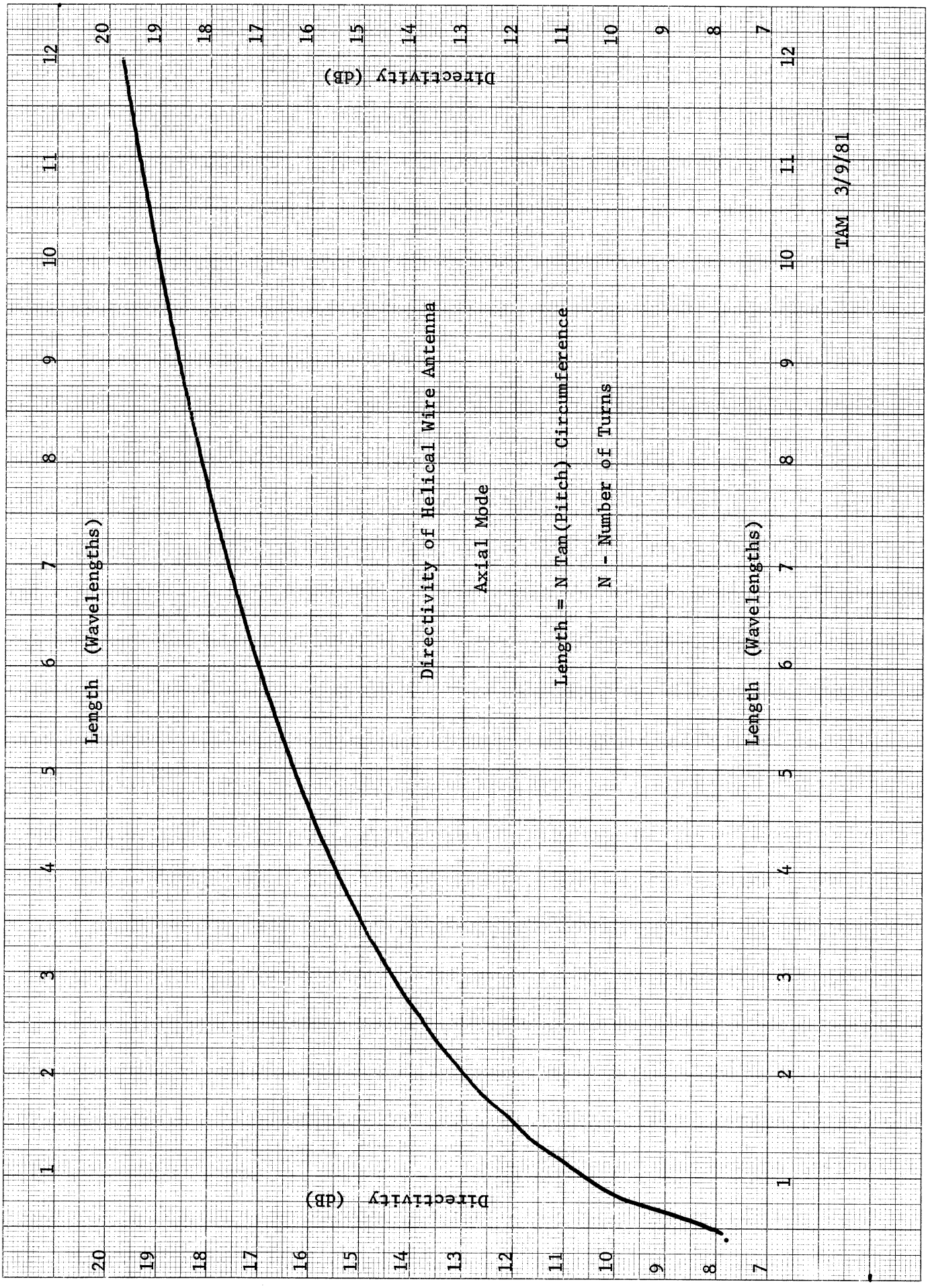

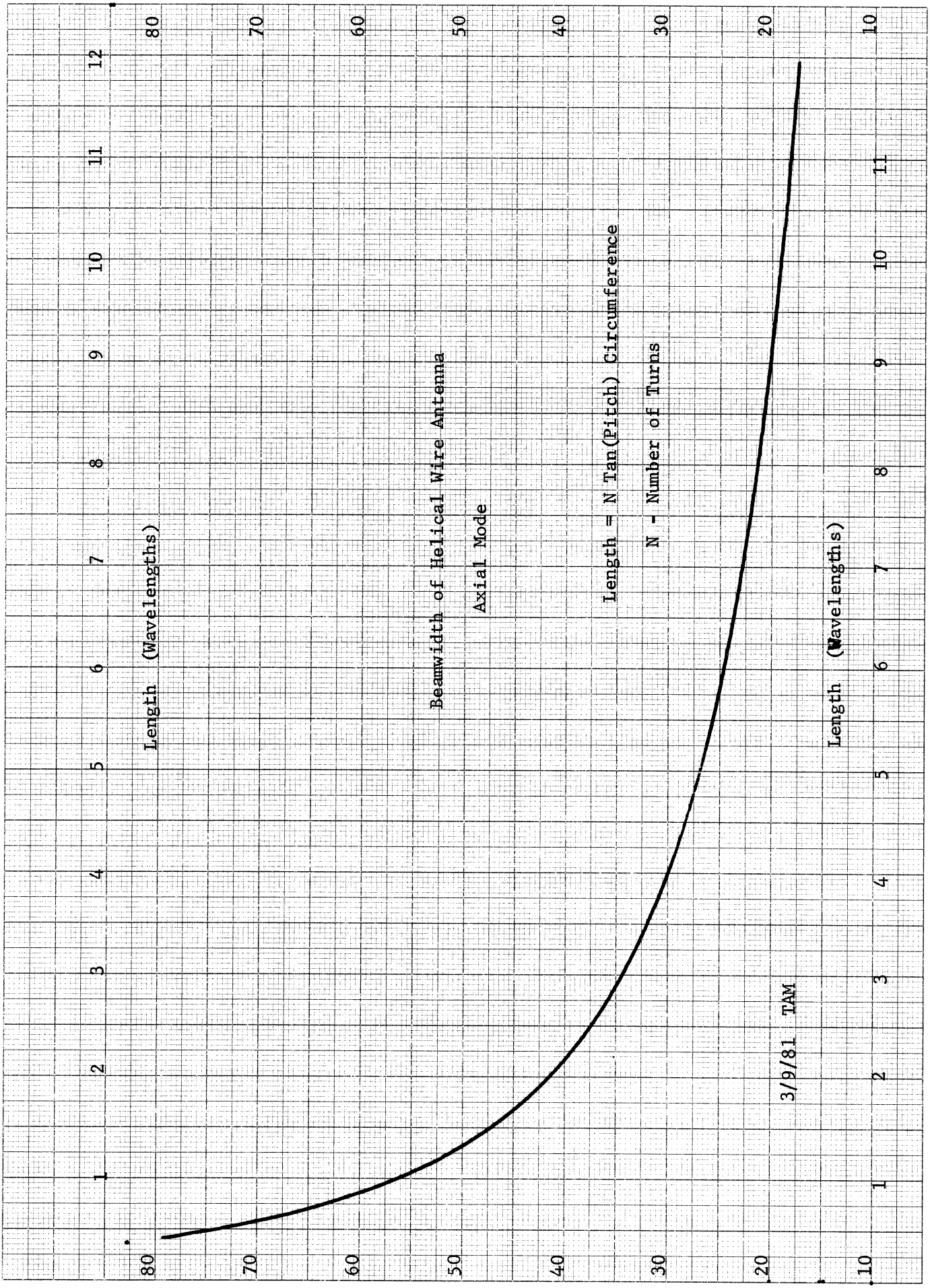

the transition between the coaxial line and the helix. It has been found that a ground plane a half wavelength in diameter is sufficient to achieve a good transition. The ground plane will reduce the backlobe of the antenna, but it can also effect the boresight axial ratio. Kraus gives the following formula for the impedance of the helix.

$$R = 141\ C/\lambda$$

This value is changed in the presence of the ground plane and the manner of feeding. It is usually less than the predicted value. Some designers have tapered the last turn of the helix down close to the ground plane so that the wire and ground plane will be a tapered transformer to better match the antenna.

Another method of feeding the helix is to use a helical coax. The coax is wound in a helix and the outer shield of the coax is split and tapered down similiar to the split tapered balun, pp. 149, to transform into the helical wire antenna. This reduces the axial ratio because modes other than the T_1 mode are not generated at the feed.

The helical antenna may be grounded and fed with a gamma match as well. A feed like this will reduce the possible bandwidth but in some applications it is desireable to have a grounded antenna. This will prevent static charge buildup and reduce the effects of lightning strokes nearby.

It is necessary to have modes other than the T_1 mode to satisfy the boundary conditions at the input and the end of the helix. The currents on the helix will be approximately as shown below.

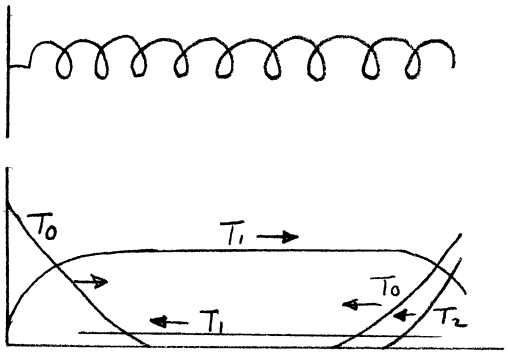

At the feed the T_0 mode will be generated as well as the T_1 mode. The energy in this mode will be coupled into the T_1 mode in a few turns. The T_0 mode will radiate normal to the helix and give a larger pattern response around $\theta = 90$ degrees. At the end of the antenna the current in the T_1 mode will be coupled into the T_0 and T_2 with some energy being reflected in the T_1 mode. The energy in the T_2 mode and the reflected T_1 mode energy can be reduced by tapering slightly the last few turns of the helix. This will improve the boresight axial ratio since the reflected T_1 mode will radiate in the opposite sense of circular polarization.

LONG HELICAL ANTENNAS

The helical antenna is usually limited in length to less than 2 wavelengths for wideband designs. As long as the antenna is less than this length, it will have good pattern responses over the 1.7:1 bandwidth. There are applications where it would be nice to have higher gains and the circular polarization of the helix. It appears that there is no inherent limitation on the length of the helix. But to achieve higher gains it is necessary to limit the bandwidth. The low frequency limitation on the bandwidth is determined by the smallest diameter needed to support the T_1 mode on an infinite helix. The upper end of the band is determined by the coupling of the energy into the T_2 mode. When the number of turns is increased, the upper bound approaches the lower bound.

In order to test these ideas about the long helix an antenna was built with the following parameters.

Diameter: 0.68 inches

No. of Turns: 50

Pitch 14^o

Frequency 5 GHz $C_\lambda = 0.9$

The antenna was wound on a Lexan tube to give it support which we will see had a slight effect on the velocity of the wave on the wire. This antenna was about 10 wavelengths long which from the graph on page 425 gives an estimated directivity of 19 dB. On page 429 is a pattern of the theoretical pattern of the helix when it is assumed that the relative propagation constant on the wire is that given for increased directivity. The 3 dB beamwidth is about 18^o which compares well with the graph of beamwidth on page 426. The helix was mounted on a ground plane and fed directly from a coax connector center pin.

When this antenna was measured, it appeared that the common wisdom about long helices was correct. It has been stated that it is not possible to build long helical wire antennas to achieve high directivities. The pattern of the antenna as built is on page 430. This pattern was taken with a rotating linear source so that the axial ratio and the pattern response can be obtained from the same graph. The antenna has a somewhat smaller beamwidth than the predicted pattern, but the boresight axial ratio is quite good. The first sidelobe is about 4 dB higher and is closer to boresight by a few degrees than the theoretical pattern. Finally the other sidelobes do not continue to diminish in amplitude as the theoretical pattern response does diminish. There is quite a bit of energy in these sidelobes around $\theta = 90$ degrees. This pattern does not have the predicted directivity.

Since the antenna had close to the predicted beamwidth and good boresight axial ratio, it was felt that the antenna was radiating in the T_1 mode. The bad response could be due to the T_0 mode that is generated at the transition from the coax to the helix. A method of testing this idea was to place a circular cup around the first few turns to limit the radiation of the T_0 mode which would die away after these few turns. This cup improved the far out sidelobe response without any effect on the boresight response. It was shielding the radiation from the T_0 mode on the first few turns.

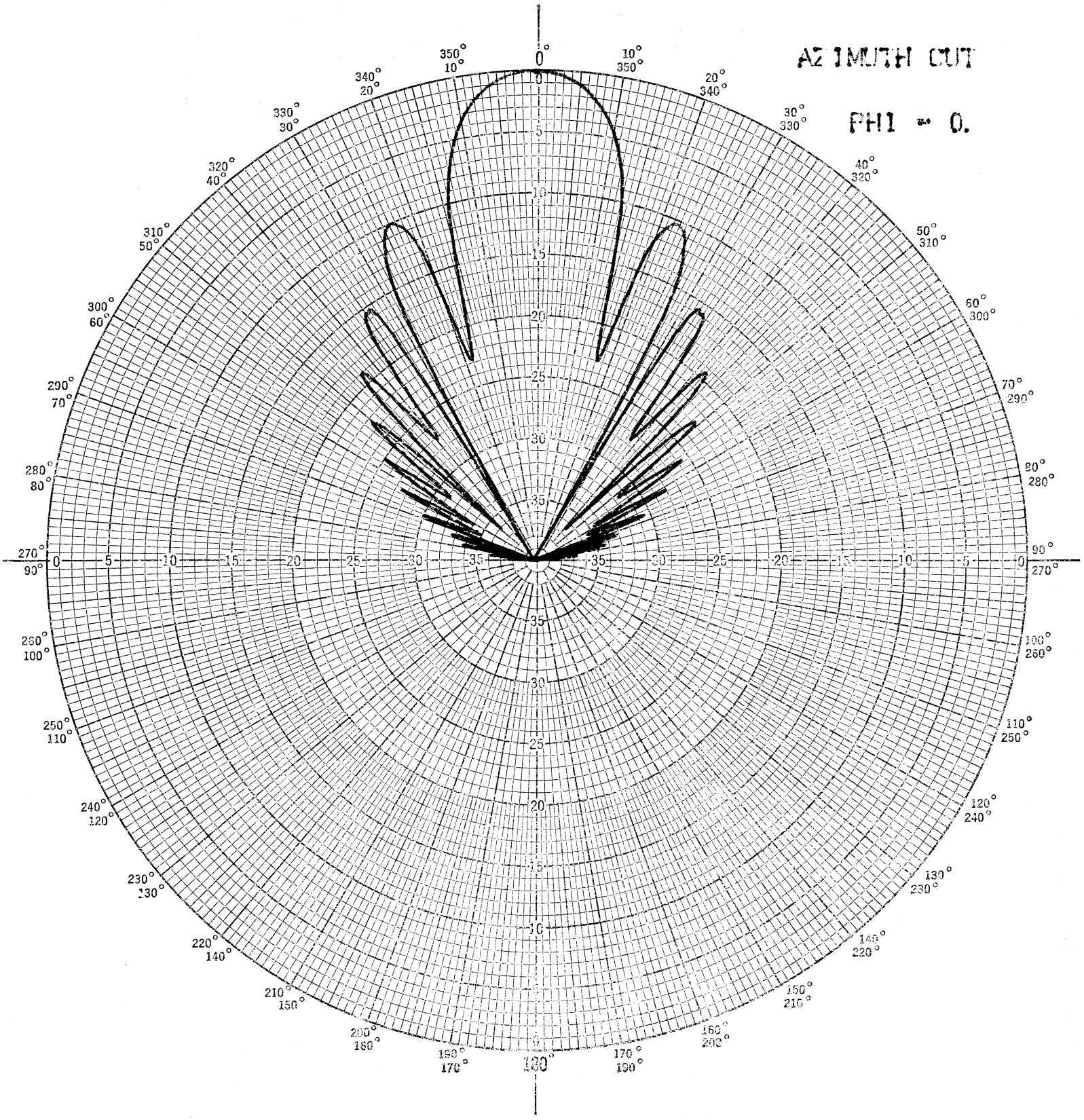

Polar Chart No. 127D
SCIENTIFIC-ATLANTA, INC.
ATLANTA, GEORGIA

50 Turn Helical Wire Antenna Diameter 0.68 inches

Pitch Angle 14°

Frequency 5 GHz $C_\lambda = 0.9$

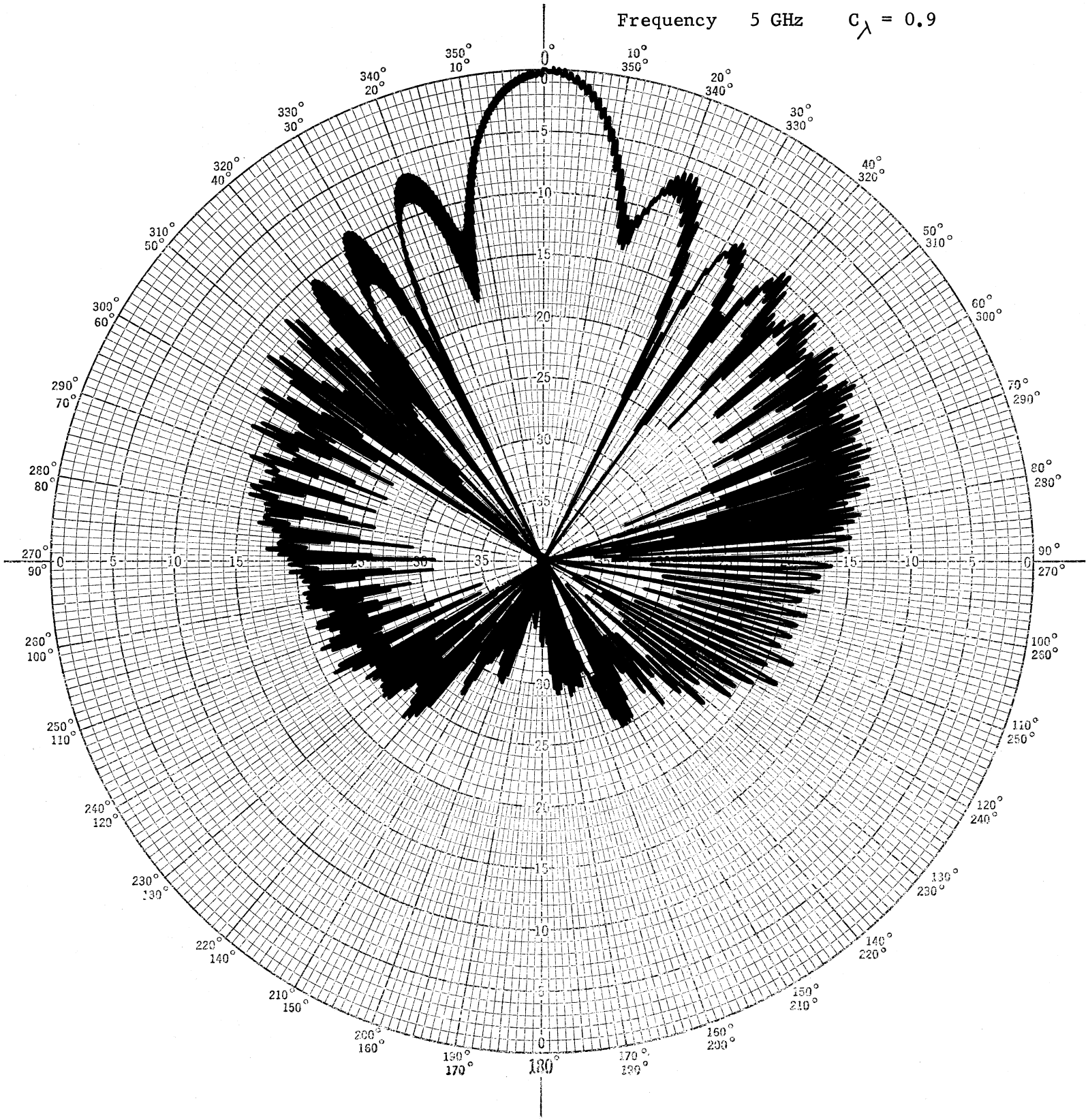

Polar Chart No. 127D
SCIENTIFIC-ATLANTA, INC.
ATLANTA, GEORGIA

After some experimentation, the following circular cup at the base on the helix covering the first few turns was found to give the best pattern response at 5 GHz.

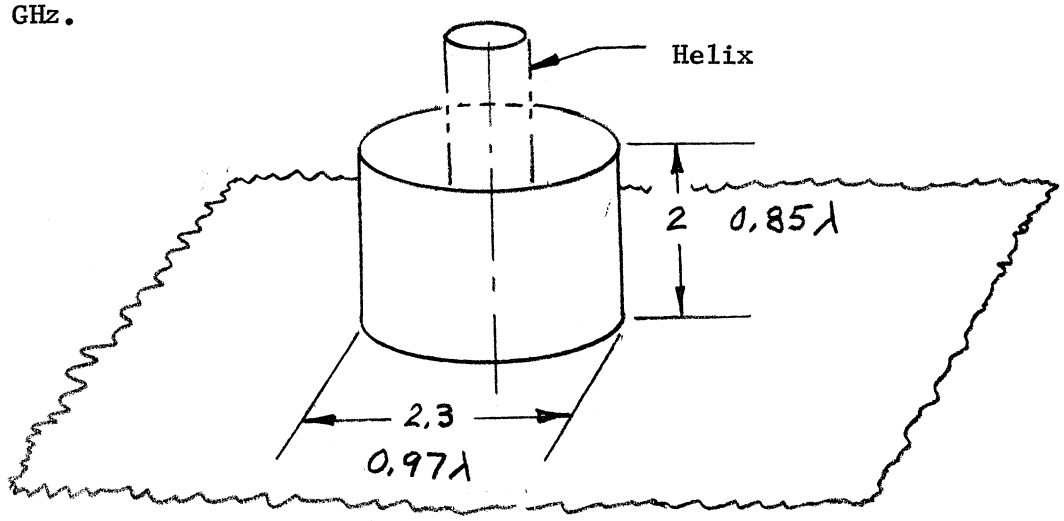

The pattern response of the antenna is given on page 432 with the above cup at the base of the helix. The far out sidelobe response has improved greatly from the initial response of the antenna (pp. 430). The directivity was measured by integrating the pattern and accounting for the energy in both the right hand and left hand circular components. The directivity is 18.8 dB.

The antenna still has higher than predicted sidelobes and slightly narrower beamwidth. It is felt that the dielectric tube that the helix was supported on may have changed the velocity of the wave on the wire. On page 433 is a pattern of the 50 turn helical antenna where the relative proagation constant has been increased by 0.2%. The sidelobes have increased by about 2.5 dB from the previous theoretical pattern and the beamwidth has narrowed slightly. Although the dielectric tube has changed the velocity of the wave on the wire by only a very little, the pattern sidelobes have changed rapidly. It would appear from this pattern that the relative propagation constant has changed by about 0.25% by the presence of the dielectric tube. On a shorter helical antenna this small change in the wave velocity would not be detected.

The bandwidth of the antenna has decreased to about 10%, but this is what is expected for long helical antennas. The pattern degrades rapidly as the frequency is increased and gradually for decreasing frequencies. The antenna works best at 5 GHz because the circular cup was adjusted to give the best pattern response at that frequency.

The conclusion is that long helical wire antennas can be built, but the bandwidth will be limited. The second point is that the bandwidth shrinks down to the low frequency limit which says the circumference should be 0.8 to 0.9 wavelengths.

50 Turn Helical Wire Antenna with Circular Cup at the Base

Diameter 0.68 inches Pitch angle 14° 5 GHz

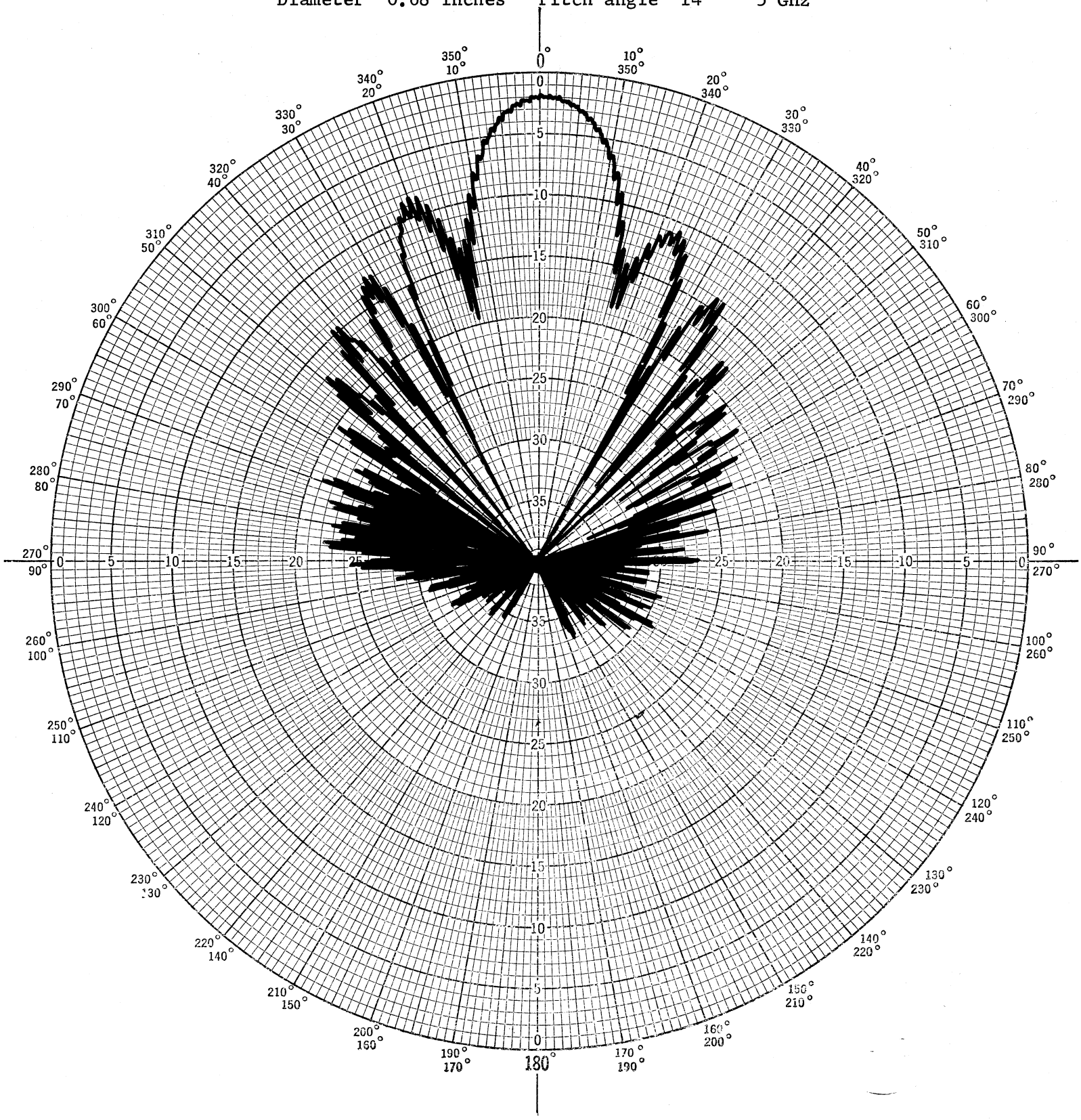

Polar Chart No. 127D
SCIENTIFIC-ATLANTA, INC.
ATLANTA, GEORGIA

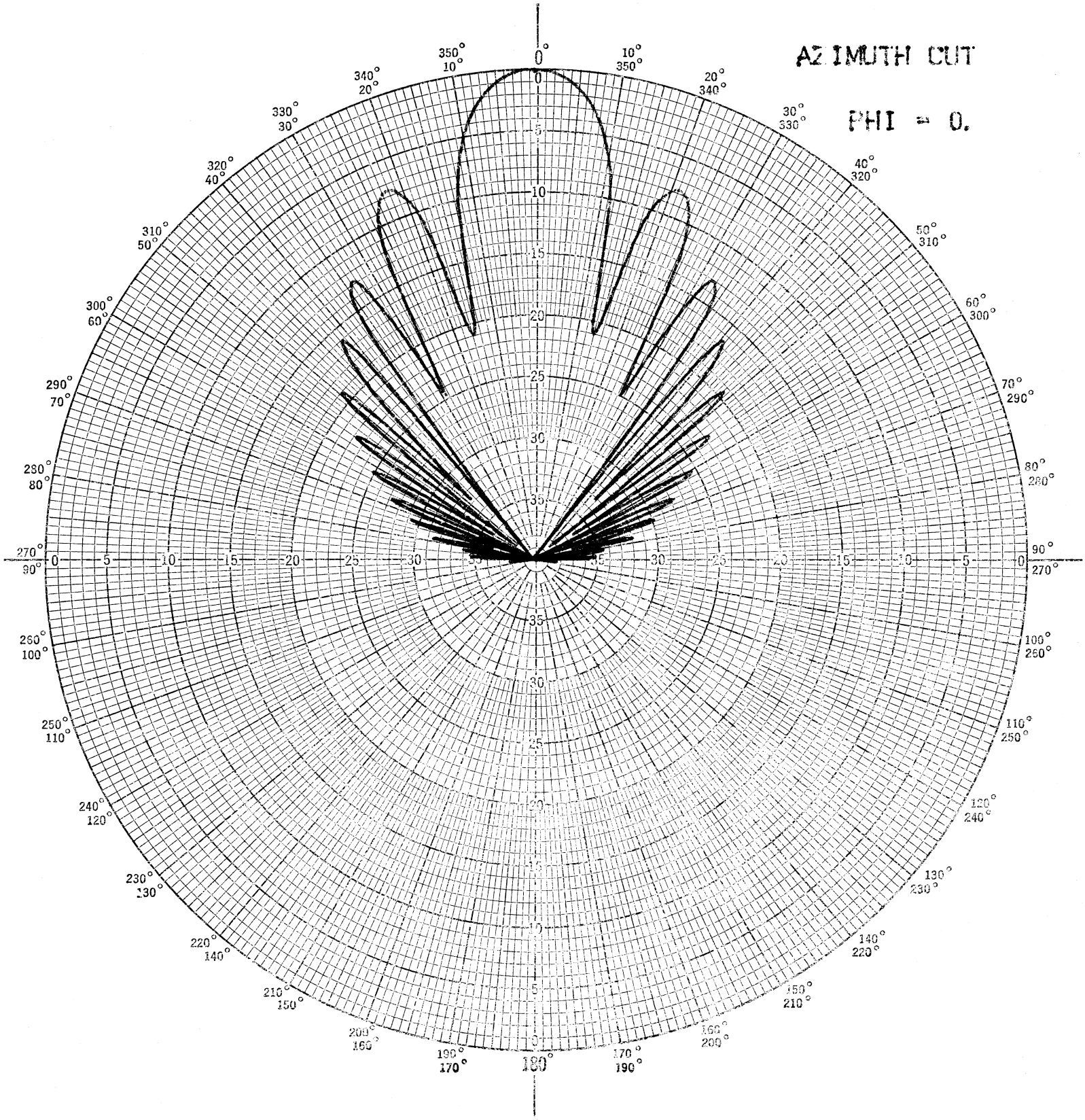

Polar Chart No. 127D
SCIENTIFIC-ATLANTA, INC.
ATLANTA, GEORGIA

